Mathematical model of a pulsating combustor

Craigen, J. G.

MATHEMATICAL MODEL OF A PULSATING COMBUSTOR

BY

J.G.Craigen B.Sc.

Thesis submitted for the degree of
Doctor of Philosophy in the
University of Durham

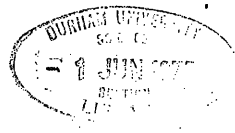

Department of Engineering Science
The University
Durham

April 1975

A B S T R A C T

A pulsating combustor producing longitudinal acoustic oscillations was constructed and a mathematical model of the system developed. The combustor was a closed - open tube, combustion taking place at the closed end into which were fed air and propane. The two lowest modes of longitudinal acoustic vibration were obtained. The fundamental occurring at low fuel flowrate up to a maximum flowrate corresponding to an energy input of 12Kw, at which either the fundamental or first harmonic occurred and above which only the first harmonic was obtained up to the maximum flowrate of the system corresponding to an energy input of 20 Kw.

The analysis of the system used the conservation equations of mass, momentum and energy from these suitably formed equations could be derived which were solved by the method of characteristics. The combustion model was governed by a simple overall-reaction rate equation. Plug flow was assumed with perfect radial mixing and no axial mixing, conduction or diffusion. The convective heat transfer coefficients were evaluated by means of the quasi-steady-state theory.

The mathematical model predicted the gas temperature gradient and the distribution of pressure and velocity standing waves. Owing to the use of a much simplified combustion model, it was not possible to predict the acoustic energy required to determine the amplitude and frequency of oscillation. The amplitude was found to be highly dependent on the fuel injection system, Air/Fuel ratio and mode of oscillation.

The practical results confirmed the higher rates of heat transfer associated with pulsating flow.

ACKNOWLEDGEMENTS

I would like to acknowledge the guidance and encouragement given by my supervisor, Dr. P.H. Clarke, throughout this investigation.

Thanks are due also to Mr. 'Sam' Beale and Dr. S.L. Hirst for many long discussions.

I wish to thank the technical staff of the Department of Engineering Science, especially Mr. L. Fleet, for his assistance with the experimental work.

I would like to thank Anne Sowerby for typing the thesis.

I am indebted to Union Carbide Limited for providing the financial support for the research.

TABLE OF CONTENTS

NOMENCLATURE

Symbol		Units
A	Cross-sectional area of combustor	m^2
A_s	Surface area	m^2
c	Velocity of sound	m/s
$\bar{c}$	Time-independent velocity of sound	m/s
c_a	Speed of sound after isentropic change of state to reference pressure	m/s
c_f	Mass fuel concentration/unit volume	Kg/m^3
c_p	Specific heat at constant pressure	KJ/Kg K
d	Diameter of thermocouple wire	m
D	Diameter of combustor	m
E	Activation energy	KJ/Kg-mol
F	Frequency of acoustic oscillation	1/S
H	Calorific value of propane	KJ/Kg
h	Heat transfer coefficient	KW/m^2 K
K	Frequency factor	m^3/KgS
K_T	Thermal conductivity	KW/mK
L	Length of combustor	m
L_a	Acoustic length	m
m	Mixture mass flowrate	Kg/S
M_f	Propane flowrate	Fm^3/h
M	Rate of change of sound for linear variation	1/S
n	Integer n=1,2,3	
N	Velocity of sound at X=0	m/s
N_u	Nusselt number	1
P	Pressure	N/m^2
$\hat{P}$	Pressure amplitude	N/m^2
$\hat{P}_a$	Pressure amplitude X=0	N/m^2
P_a	Atmospheric pressure	N/m^2
P_r	Prandtl Number	1
q	Energy transfer/unit mass/unit time	KW/Kg

Symbol		Units
Q	Energy transfer/Unit time	Kw
R	Gas constant	KJ/KgK
R_e	Electrical resistivity	ohm-cm
R_n	Reynolds Number	1
R_u	Universal gas constant	KJ/Kg-mol K
r	Inner radius of combustor	m
r_f	Reaction rate	Kg/m^3S
S	Specific entropy	KJ/KgK
t	Time	S
t_p	Period of oscillation	S
T	Gas temperature	K
$\hat{T}$	Gas temperature amplitude	K
T_a	Time-independent axial gas temperature	K
T_w	Time-independent wall temperature	K
$\bar{T}$	Time-independent mean gas temperature	K
u	Particle velocity	m/s
$\hat{u}$	Particle velocity amplitude	m/s
w	Angular frequency	1/s
X_{CH}	Mass fraction of propane	1
X_{O_2}	Mass fraction of oxygen	1
x	Co-ordinate direction	m
γ	Ratio of specific heats	1
ε	Flame emissivity	1
η_E	Effectiveness of the heat exchanger	1
θ	Fuel to air ratio	1
λ	Wavelength	m
μ	Dynamic Viscosity	Kg/ms
ρ	Density	Kg/m^3
ρ_a	Density at atmospheric pressure	Kg/m^3
σ	Stefan-Boltzmann constant	$J/m^2S\ K^4$

CHAPTER 1

1.0 Introduction

1.0 Introduction

Rayleigh (23) was the first to advance a hypothesis regarding the driving of oscillations by a periodic heat release in a gaseous medium. This hypothesis states that for a heat-driven oscillation to occur, there must be a varying rate of heat release having a component in phase with the varying component of the pressure. Although the validity of this hypothesis has been questioned where large pressure amplitude and energy inputs are involved, it serves well as an initial criterion of whether or not oscillations will occur. Putman (5) has suggested the following mathematical formulation of the above criterion

$$\oint q P \, dt > 0$$

where q is the instantaneous heat release rate, P the oscillating component of the pressure and t the time.

The treatment of flames in enclosures has received a great deal of attention under the general heading of combustion instability. In their review of instability phenomena Barrere and Williams (24) defined the three main forms of instability, these have been summarised as :

1) Instabilities that are specific to the geometry and acoustic character of the combustion chamber, (combustion chamber instability).

2) Instabilities involving interaction of the dynamics of the combustion process and the components of the system, (system instability).

3) Instability involving only the reactants (Intrinsic instability).

An increasing interest is being shown in practical applications of combustion driven acoustic oscillations mainly due to the higher combustion intensity and heat transfer rates associated with such a process, leading to the possibility of constructing compact, high efficiency combustion units.

Combustion - driven acoustic oscillations can be classified into three basic types :

a) Longitudinal

The gases move back and forth along the axis of the chamber (referred to as organ-pipe oscillations).

b) Radial

The gases oscillate between the axis of the chamber and the wall.

c) Tangential

The gases oscillate around the perimeter of the chamber.

In addition combined modes are possible.

This investigation is only concerned with the longitudinal type. Such oscillations are produced if the combustion is designed so that a periodic heat release is obtained at a point corresponding to a pressure antinode. If this varying heat release is in phase with the pressure oscillation the pressure amplitude can be driven to high values (The Rayleigh Criterion). The frequency of oscillation being related to the length of the combustor and the velocity of sound in the combustion gases. The aim of this investigation was to construct such a combustor as shown in Figure (1·1) and to develop a mathematical model of the system.

The combustor was of the organ - pipe type with the inlet end acoustically closed and the outlet end fully open. Combustion taking place at the closed end where air and propane were fed. Such an acoustic system if fed with a broadband noise, in this case the flame, can select and amplify certain narrow frequency bands characterised by various acoustic modes of the system. As acoustic modes can couple with and be driven by a varying heat release rate from the flame, the condition having to satisfy the Rayleigh criterion. The varying heat release rate can be affe cted by many factors such as, a regular variation of pressure, changing in mixing pattern or vortex shedding from a flame holder. A more detailed discussion of such mechanisms being given in references (24-27).

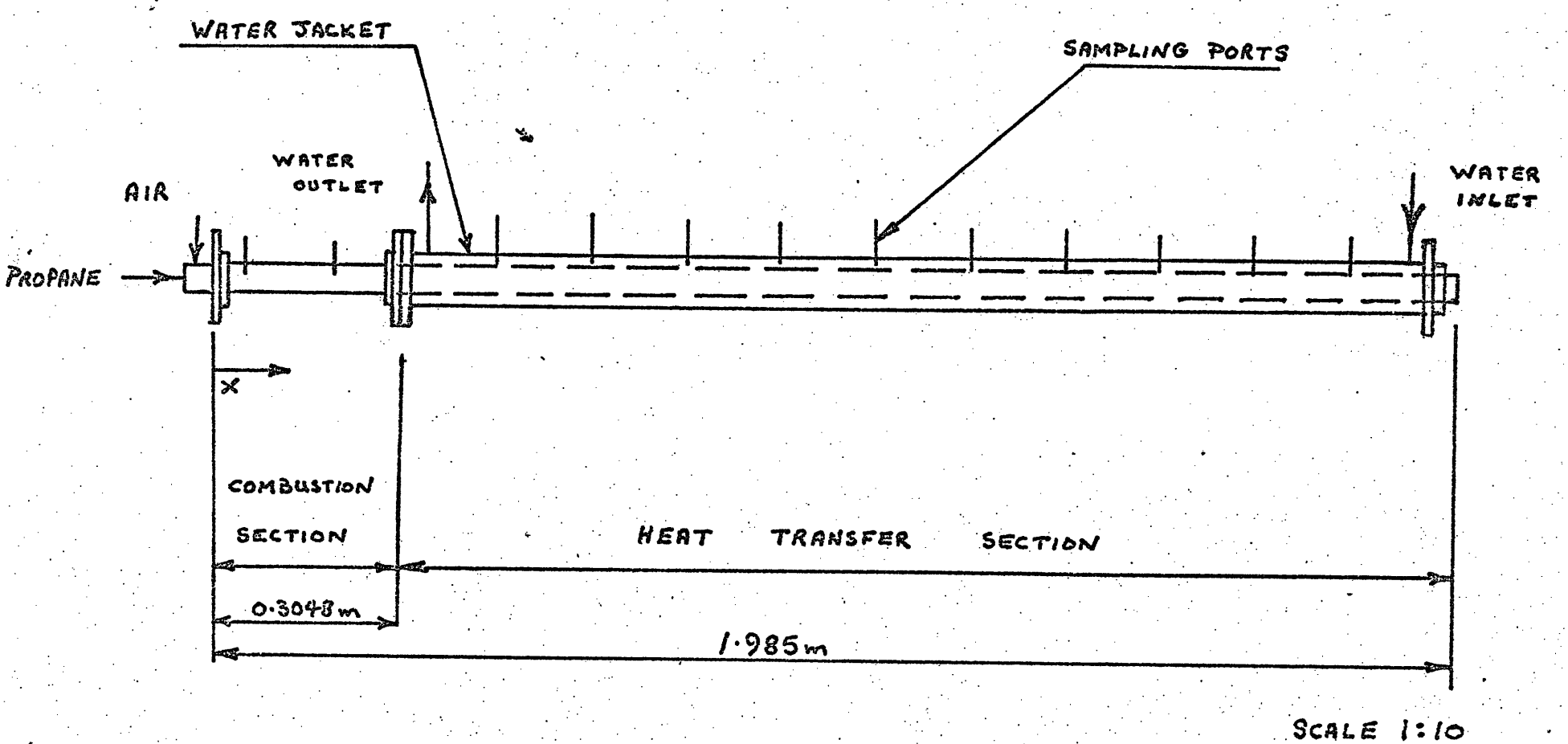

THE ORGAN PIPE PULSATING COMBUSTOR. Figure(1·1)

CHAPTER 2

Previous Work

2.1 Historical Background of Pulsating Combustion

2.2 Analytical Approaches

2.3 Numerical Solution of the Equations

2.0 Previous Work

There has been a vast amount of experimental work on pulse combustion. However, theoretical studies except of the most rudimentary kind are largely lacking. The reason is mainly due to the working complexity of such combustors which when combined with the unknowns cause the mathematics to become formidable.

2.1 Historical Background of Pulsating Combustion

The first reported work on combustion-driven oscillations was made by Byron Higgins in 1777, when he enclosed a hydrogen diffusion flame in a large tube open at both ends. He found oscillations occurred for certain lengths of the fuel supply. No major work in the field, though, was carried out until the beginning of the 20th century and this work is recorded in a number of German, Swiss and French patents dating from 1900 to 1910. General interest appears to have been lacking and the study of pulse combustion again drifted into oblivion until 1930, when Schmidt in Germany and Reynst in Germany and France revived the phenomenon of pulsating combustion and its practical applications. From these basic ideas, designs have been produced for the use of pulsating combustors in aeronautical engines, domestic heating and grain dryers. The field has been reviewed recently by Putman (1) and Beale (2) with specific applications being dealt with in references (3 - 6).

2.2. Analytical Approaches

It is convenient to divide the analysis into two main areas :-

2.2.1 The Gas Dynamics of the System

The physcial laws which primarily govern the process in question are those of mass, momentum and energy conservation, these, when coupled with the relations describing the thermodynamic properties of the gas form a set of quasi-linear hyperbolic partial differential equations. This type of equation is obtained whenever the problem is associated with wave propagation and so has received considerable attention.

If it is assumed that the flow is a steady one with small perturbations superimposed then the equations become linear. The solution of the linear equations has been highly developed in the study of the theory of sound. As the equation is linear, the complete solution of a problem may be obtained by superimposing the solutions of a number of simple cases, thus the actual pressure variation may be expressed as a fourier serier and the partial solutions for each term superimposed. Much of the development of this theory was due to Rayleigh (23) whose text book is still a standard work on the subject, Putman (5) and Raushenbakh (6) having applied this method to pulsating combustion problems.

The fundamental problem of finite waves followed the early development of the theory of sound. Poisson and Earnshaw first extended the theory of sound to the case of finite amptitude disturbances propagating in one direction. Riemann introduced the method of characteristics by presenting the theory in a form suitable for calculating the propagation of waves of finite amplitude proceeding in both directions.

During World War II a considerable impetus was given to this subject from two sources. First, there was considerable interest in explosions and their resultant pressure waves. Wartime research in this direction by the group working with Courant and Friedrichs has been summarised in their book (7). This work contains a general mathematical treatment of the method of characteristics but a good text with emphasis on a variety of engineering systems is given by Abbott (8).

A second source of interest in waves of finite amplitude was the wartime German development of the Schmidt tube which was developed to power the V1 flying bomb. For this purpose the method of characteristics was developed using numerical integration. This method having been developed and applied to one-dimensional nonsteady flow problems by many workers (7 - 16) and is the basis of the method employed by this investigation.

An alternative approach to the problem is to use a finite difference method based on the fundamental hyperbolic equations. Methods of this type have been known since the work of Courant and Friedrichs but seems to have been neglected until the development of the digital computer. The main obje ction to this approach being the appearance of unrealistic features in the solution of the equations such as improbable peaks in pressure profiles and sometimes the fluid velocity being given the wrong sign.

2.2.2 General Aspects of the Combustion

The primary problem in modelling any practical combustion system is to simultaneously account for mixing and chemical reaction. At present, no accurate formulation considering both exists, but three major theories are at present being developed. One method employs the calculations of turbulent flame speed based on the turbulent parameters of the flow and the chemical reaction rate introduced by the use of the laminar flame speed. A second approach uses a microvolume burning concept by identifying eddies of size and lifetime dependent on the turbulence parameters, these eddies are assumed to burn either from the surface at the laminar flame speed or homogenously throughout the volume, but perhaps the most suitable approach for this investigation is based upon reaction rate theory and is the method adopted. This method assumes the turbulence level to be so high that mixing is instantaneous, thus the mixing rate is so fast compared to the reaction rate that mixing can be neglected and the performance can be determined by reaction rate alone.

The combustion model assumes a plug flow reactor which is a continuous series of infinitesimally stirred reactors through which the flow passes. A more comprehensive review of the above techniques is given in reference (17).

Early workers in this field (18) attempted a reaction rate equation based upon a single step. The application of computer techniques has facilitated the treatment of multistep reactions and recently (17) a nine-step mechanism has been treated. For the present investigation a simple one-step model is proposed since there is still insufficient knowledge to be able to propound a proven Kinetic scheme.

The investigation assumes heat transfer in the combustion section to be mainly by convection and radiation, and in the heat transfer section by convection alone.

At the present time, no complete analytical solution of predicting conve ctive heat transfer coefficients in unsteady turbulent flow exists. However, a simple semi-empirical approach, the quasi-steady state theory, has been used by several workers (19 - 21) to describe the effe cts on heat transfer rates. This treatment is based on the assumption that the heat transfer coefficient at any instant can be calculated from the instantaneous value of the velocity by means of the appropriate steady state relationship. Convection heat transfer coefficients for turbulent flow in pipes have been correlated by the following expression :-

$$h = 0.02 \left(\frac{\rho u D}{\mu} \right)^{0.8} \frac{K_T}{D} \qquad \text{2.1}$$

The main fault in such an analysis is due to the thermal capacity of the fluid causing a phase lag between driving temperatures difference and resulting flux at the surface which has been observed experimentally by Overbye., who noted that temperature difference and transfer rate did not pass through zero simultaneously as reported by Annand. (20).

The workers who have used this analysis have shown the method to be adequate and have achieved good correlation between predicted and experimental values .

Theoretical considerations relating to radiant transfer is even less advanced and from present knowledge on the subject it is apparent the best that can be done is to determine empirically an average radiation factor as expressed by the following equation.

$$\frac{Q}{A_s} = \varepsilon \sigma (T^4 - T_w^4) \qquad \text{2.2}$$

This expression is admittedly much over simplified, but due to the lack of data on the subject no more elaborate treatment seems useful.

2.3 Numerical Solution of the Equations

Numerical procedures for solving the hyperbolic equations of unsteady compressible flow are of two basic kinds characteristic methods and fixed-grid or finite-difference methods.

The method of characteristics focuses attention on the fact that, in processes governed by hyperbolic equations, disturbances to the fluid are transmitted only in discrete directions. These directions form a network of lines, known as characteristics which cover the domain of integration. For unsteady one-dimensional flow, they comprise three sets of lines on the distance - time plane , the lines of a particular set do not intersect, but the lines of one set intersect the lines of another. When the flow is isentropic, it is necessary to consider only two of the sets of characteristics as the third set is made redundant.

The main objection to characteristic methods is that the locations of intersections of the characteristics often fail to correspond with those at which boundary condition information is available or flow predictions are required.

With fixed - grid methods the great advantage is that their grid points are predetermined. When the grid has been chosen, a set of algebraic equations are formed which connect the values of the flow variables for a

particular grid point with the values for neighbouring points on the distance time plane . These are the finite difference equations. However, when they are applied to the prediction of flow phenomena, unrealistic features sometimes appear in the solutions, thus, improbable peaks may appear in the pressure profiles and sometimes the fluid velocity may be given the wrong sign. Numerous ways have been tried to eliminate this behaviour, but none are entirely free from undesirable features. So it seems that the characteristics form the only natural co-ordinate set for the equations, and also fixed-grid systems tend to lose some of the information that the characteristics convey, and to replace it with spurious information of their own.

The method which forms the basis of the present investigation is basically the one suggested by Hartree (22) and developed by Benson (10), this method combines the best features of both the characteristics and fixed - grid methods, for it uses a fixed grid, but the relations between the dependent variables at adjacent grid points are firmly based on the information that is conveyed only along the direction of the characteristics.

CHAPTER 3

Theory

3.0 Theory

In formulating a mathematical model of the combustor the following assumptions are made :-

1) The flow is one-dimensional and flow across boundaries may be considered as quasi-steady.

2) Longitudinal mixing and heat transfer are negligible.

3) The fluid is considered to behave as a perfect gas at each point in the duct, with variation in fluid properties due to large axial temperature gradients being taken into account.

4) In the absence of reliable heat transfer data for unsteady flow, the heat transfer coefficients in any given pipe element at a certain instant are taken as those for fully developed steady flow at the Reynolds number then prevailing in that element.

5) Second-order effects caused by friction and variation in gas composition are considered negligible.

6) The inside wall temperatures are assumed known for all points along the length of the combustor and are regarded as steady ie changes due to transient variations in heat transfer are neglected.

7) The combustion model assumes the turbulence level is so high that the mixing is instantaneous, thus the mixing rate is so fast compared to the rea ction rate that mixing can be neglected.

8) Pressure and velocity are continuous with time, ie there are no shocks in the flow

3.1 Fundamental Differential Equations

Consider a one-dimensional frictionless flow in a constant area duct with heat transfer taking place. The conservation equations of mass, momentum and energy take the form given by equations (3.1 - 3.3).

The flow of mass, momentum and energy into and out of a pipe element dx at time dt is shown in Figure (3.1)

Continuity of Mass

$$-A \frac{\partial}{\partial x}(u\rho)\,dx = A\,dx \frac{\partial \rho}{\partial t}$$

expanding gives

$$\frac{\partial \rho}{\partial t} + \rho \frac{\partial u}{\partial x} + u \frac{\partial \rho}{\partial x} = 0 \qquad \text{3.1}$$

Momentum equation

$$-A \frac{\partial P}{\partial x} dx = \frac{\partial}{\partial t}(A \rho u\, dx) + \frac{\partial}{\partial x}(A u^2 \rho)\, dx$$

expanding gives

$$\frac{\partial P}{\partial x} + \rho \frac{\partial u}{\partial t} + \rho u \frac{\partial u}{\partial x} + u\left[\frac{\partial \rho}{\partial t} + \rho \frac{\partial u}{\partial x} + u \frac{\partial \rho}{\partial x}\right] = 0$$

from (3.1) $\left[\quad\right] = 0$

Hence

$$\frac{\partial u}{\partial t} + u \frac{\partial u}{\partial x} + \frac{1}{\rho} \frac{\partial P}{\partial x} = 0 \qquad \text{3.2}$$

Conservation of Energy

$$q \rho A\, dx = \frac{\partial}{\partial t}\left((\rho A\, dx)\left(\frac{u^2}{2} + \frac{1}{\gamma - 1}\frac{P}{\rho}\right)\right) + \frac{\partial}{\partial x}\left((\rho u A)\left(\frac{u^2}{2} + \frac{\gamma}{\gamma - 1}\frac{P}{\rho}\right)\right) dx$$

3.3

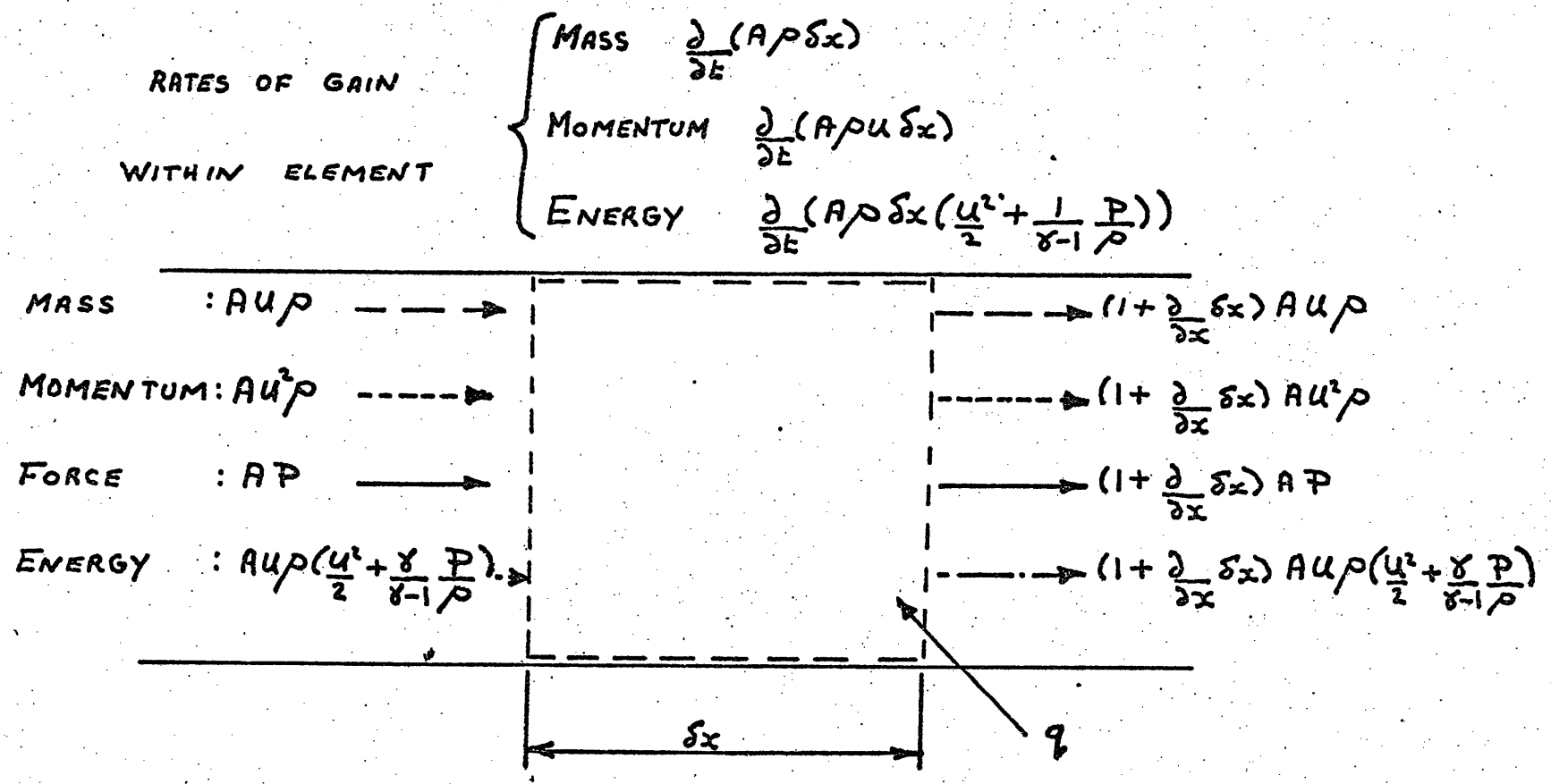

Fig.(3.1) INSTANTANEOUS CONDITIONS IN A PIPE ELEMENT

3.2 Basic Principle of Method of Characteristics

An analytical solution of equations (3.1 - 3.3) being impossible, a step by step integration is adopted, the solution thus comprising P, U and C. Given the values of P. U and C at a certain initial time, the task is to find their values at all locations at any later time. The integration procedure depends on the existence at each point in the X, t plane of three (characteristic) directions (dt/dx). If in any of these directions, a small step is taken with resulting increments dP, du and dc, then the partial equations (3.1 - 3.3) reduce to a total differential relationship (the compatibility relationship) between dP, du, dc and dt Had the chosen dx, dt caused a step in a direction other than one of the three characteristics, such a relationship would have been unobtainable.

3.2.1 Characteristics Equations

The differential equations (3.1), (3 .2) and(3.3), although they express the physical laws correctly are not in a form which brings out the dominant effect of the three characteristics directions, the equations therefore have to be transformed to produce this effect. They have to be expressed in the form,

$$\frac{d\phi}{dt} = \frac{\partial \phi}{\partial t} + m \frac{\partial \phi}{\partial x}$$

Consider figure (3.1a), if a function ϕ varies along a curve 'm' and if ϕ is a function of x and t then :

$$d\phi = \frac{\partial \phi}{\partial t} dt + \frac{\partial \phi}{\partial x} dx$$

and along m

$$\left(\frac{d\phi}{dt}\right)_m = \frac{\partial \phi}{\partial t} + \frac{\partial \phi}{\partial x} \frac{dx}{dt}$$

or

$$\left(\frac{d\phi}{dt}\right)_m = \frac{\partial \phi}{\partial t} + m\frac{\partial \phi}{\partial x}$$

where $m = dx/dt$, the slope of the curve at any point along the curve,

Under these conditions the curve is a characteristic curve

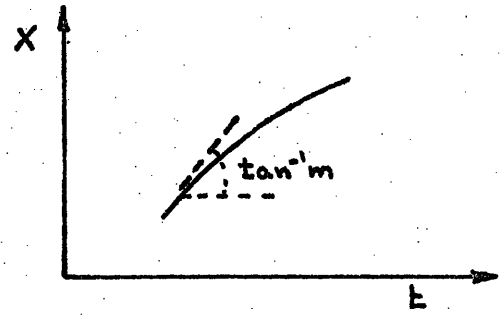

Fig 3.1a

In general along a characteristic curve :

$$\frac{dx}{dt} = m$$

and

$$\left(\frac{d\phi}{dt}\right)_m = \frac{\partial \phi}{\partial t} + m\frac{\partial \phi}{\partial x}$$

The characteristic equations are obtained by combining the equations of conservation in the following manner.

Using equation (3.1) and (3.2) the energy equation can be expressed in the form

$$\left(\frac{\partial P}{\partial t} + u\frac{\partial P}{\partial x}\right) - c^2\left(\frac{\partial e}{\partial t} + u\frac{\partial e}{\partial x}\right) - (\gamma-1)\rho q = 0 \qquad \text{——— } 3.4$$

Combining equations (3.1), (3.2) and(3.4) in the following manner.

equation (3.4) $+c^2$ (equation (3.1)) + ρc (equations (3 .2)) :-

$$\left(\frac{\partial P}{\partial t} + (u+c)\frac{\partial P}{\partial x}\right) + \rho c\left(\frac{\partial u}{\partial t} + (u+c)\frac{\partial u}{\partial x}\right) - (\gamma-1)\rho q = 0 \qquad \text{——— } 3.5$$

equation (3.4) + C^2 (equation (3.1)) - ρC (equation (3.2)) :-

$$\left(\frac{\partial P}{\partial t} + (u-c)\frac{\partial P}{\partial x}\right) - \rho c\left(\frac{\partial u}{\partial t} + (u-c)\frac{\partial u}{\partial x}\right) - (\gamma-1)\rho q = 0 \qquad \text{3.6}$$

along a characteristic $\frac{dx}{dt} = u+c$ the compatability conditions, from equation (3.5) is :

$$\frac{dP}{dt} + \rho c \frac{du}{dt} - (\gamma-1)\rho q = 0 \qquad \text{3.7}$$

along a characteristic $\frac{dx}{dt} = u-c$ the compatability condition, from equation (3.6)

$$\frac{dP}{dt} - \rho c \frac{du}{dt} - (\gamma-1)\rho q = 0 \qquad \text{3.8}$$

along a characteristic $\frac{dx}{dt} = u$ the compatability condition, from equation (3.4)

$$\frac{dP}{dt} - C^2 \frac{d\rho}{dt} - (\gamma-1)\rho q = 0 \qquad \text{3.9}$$

The lines having slopes of 1/(U+C) and 1/(U-C) are the loci of pressure waves moving relative to the fluid at speeds of C and -C, and are called wave characteristics. The line of slope 1/(U) is the locus of a fluid element and is called the path line characteristic.

As a fluid element moves along a duct, its energy content may vary as a result of combustion and other phenomena. These energy changes take place with changes of the entropy of the particles. As the entropy is no longer constant throughout the flow field it must be introduced in some suitable form.

Consider the second law of thermodynamics as applied to a perfect gas in the form:

$$dS = C_p \frac{dT}{T} - R\frac{dP}{P}$$

then along an isobar $dS = C_p \frac{dT}{T}$

Hence $S_2 - S_1 = C_p \log_e \frac{T_2}{T_1}$

Referring to figure (3.2), if the isobar is defined at some reference pressure P_a and C_a is the speed of sound on the isobar then :

$$S_2 - S_1 = S_{2a} - S_{1a} = 2C_p \log_e \frac{C_{2a}}{C_{1a}}$$

Thus a change in the speed of sound C_a represents a change in the entropy level.

The following identities apply for a perfect gas undergoing an isentropic process.

$$\frac{P}{P_a} = \left(\frac{C}{C_a}\right)^{\frac{2\gamma}{\gamma-1}} , \quad \frac{\rho}{\rho_a} = \left(\frac{P}{P_a}\right)^{\frac{1}{\gamma}} , \quad \frac{\gamma P}{\rho} = C^2$$

hence

$$\frac{dP}{P} = \frac{2\gamma}{\gamma-1}\frac{dC}{C} - \frac{2\gamma}{\gamma-1}\frac{dC_a}{C_a}$$

$$\frac{d\rho}{\rho} = \frac{d\rho_a}{\rho_a} + \frac{1}{\gamma}\frac{dP}{P}$$

$$\frac{d\rho_a}{\rho_a} = -2\frac{dC_a}{C_a}$$

therefore

$$\frac{d\rho}{\rho} = -2\frac{dC_a}{C_a} + \frac{2}{\gamma-1}\frac{dC}{C} - \frac{2}{\gamma-1}\frac{dC_a}{C_a}$$

multiplying by γP and substituting C^2 for $\frac{\gamma P}{\rho}$ gives :

$$dP - C^2 d\rho = 2\rho C^2 \frac{dC_a}{C_a}$$

from (3.9)

$$2\rho C^2 \frac{dC_a}{C_a} = (\gamma-1)\rho q\, dt$$

therefore

$$dC_a = \frac{C_a}{2C^2}\, q(\gamma-1)\, dt \qquad \text{——————} \quad 3.10$$

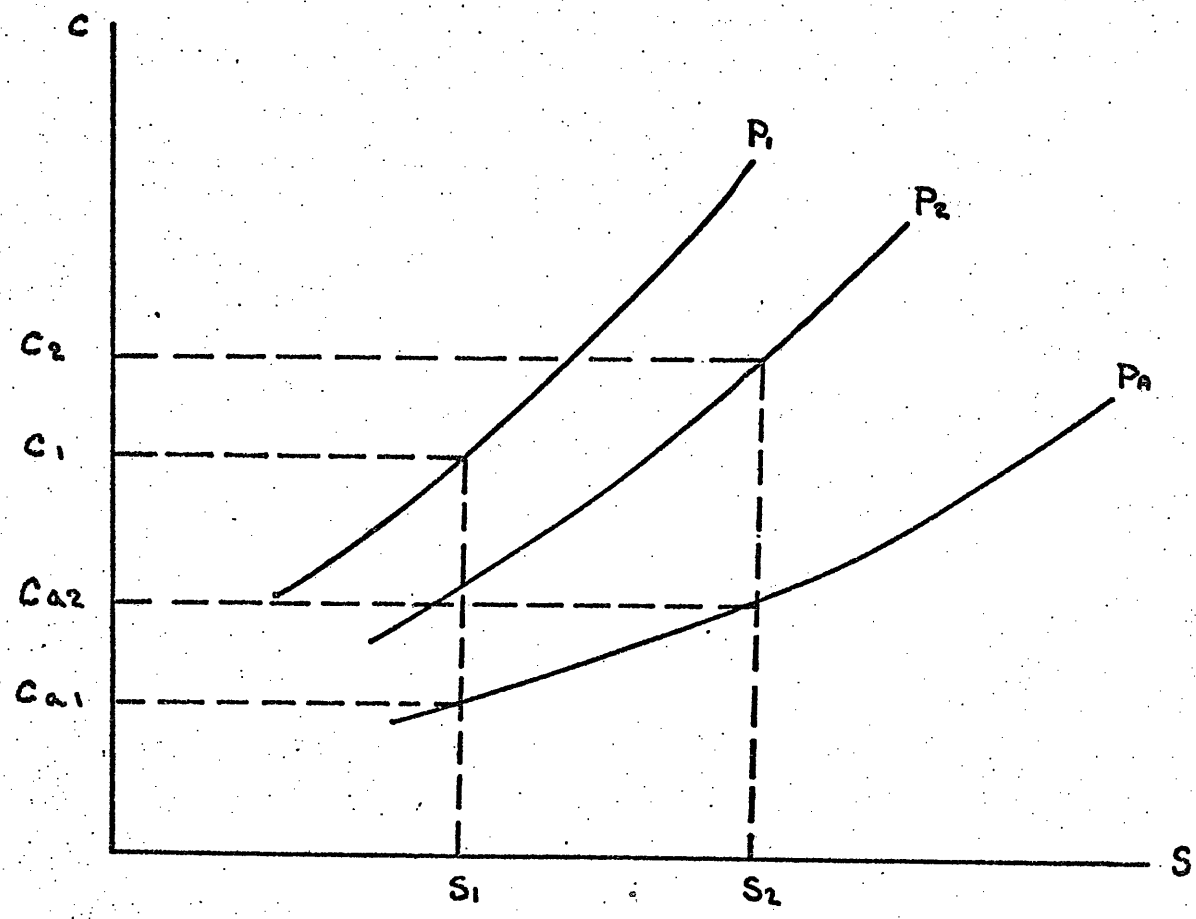

ENTROPY DIAGRAM Fig. (3·2)

3.2.2 Determination of q

If a path line is followed in the combustor it may be considered as representing the motion of a infinitesimal layer of gas, the rate at which energy is being transferred per unit mass in this layer is given by q and it is for this quantity that some assumption must be made.

The mathematical model of the combustor has two distinct sections, the combustion and heat transfer sections figure (1.1). The determination of q in the combustion section depends on the energy released by combustion and the energy lossed due to heat transfer by convection and radiation, the details of which are given in section (3.3).

The determination of q in the heat transfer section assumes no combustion takes place in the section and that heat transfer is by convection alone. In evaluating q the assumption that the heat transfer coefficient at any instant can be calculated from the instantaeous value of the velocity by means of the appropriate steady state relationship, q is given by

$$q = 4h(T_w - T)/\rho D \qquad \text{——————} \quad 3.11$$

where h is given by equation (2.1)

3.3 Combustion Model

At the present time, the rate of heat release of a burning gas mixture as a function of flow conditions is not well known. None of the combustion models proposed to date enables accurate quantative estimates to be made, the most promising are those based upon reaction rate theory, upon which the model of this investigation is based.

The primary problem in modelling any practical combustion system is to simultaneously account for mixing and chemical reaction. At present, no accurate formuation considering both exists. The reaction rate theory assumes that the turbulence level is so high that mixing is essentially instantaneous, thus mixing is so fast compared to the reaction rate that mixing can be neglected.

The law of mass action may be expressed by :

$$-\frac{d[C_F]}{dt} = A[XCH]^B[XO2]^C e^{-E/R_uT}$$

where the parameters A, B, C and E are defined empirically.

This expression may only be applied in a meaningful way to elementary reaction steps corresponding to actual reaction mechanism. However, most combustion reactions are extremely complex, and most likely include chain initiating, chain carrying, chain branching and chain breaking steps. The precise details of which are most complex. For this reason, the only feasible approach to the problem of determining the reaction mechanism of a technical combustion system is to measure the dependence of the overall reaction rate on the concentrations of the species involved.

Most chemical reactions are bi-molecular and proceed as the result of reactions following binary collisions. In complex combustion processes, second order kinetics have been used successfully by considering that one of the bi-molecular processess involved in the reaction constitutes the rate determining step.

It is convenient in determining the overall reaction rates in a combustion process to consider the rates of consumption of original fuel and oxygen on the basis of a second order reaction.

Thus for the reaction

$$\text{Fuel} + \text{Oxygen} \xrightarrow[\text{Reaction}]{\text{2nd order}} \text{Products}$$

The fuel consumption rate in such a process may then be described by the Arrhenius expression

$$\dot{r}_F = K\rho^2 X_{CH}^{3/2} X_{O2}^{1/2} e^{-E/R_uT} \qquad 3.12$$

as used by Chen (31) which assumes a negligible reverse reaction

The combustion model is based on a plug flow reactor which is a continuous series of infinitesimally stirred reactors, that is a reactor with perfect radial mixing and negligible axial mixing, conduction and diffusion. It assumes the reaction rate can be calculated from the instantaneous value of gas properties by means of equation (3.12) Heat transfer from the combustion zone is accounted for by radiation and convection assuming the combustion wall temperature is known and radiates as a black body.

Then $$q = \frac{r_F H}{\rho} + \frac{4h(T_w - T)}{\rho D} + \frac{4\varepsilon\sigma(T_w^4 - T^4)}{\rho D} \qquad 3.13$$

and $$- d(XCH) = \frac{\pi D^2 r_F \, dx}{4m}$$

with

$$XCH = \frac{\theta}{(1+\theta)} \qquad \text{at } x = 0$$

By stoichiometry, assuming reaction to CO_2 and H_2O only

$$XO2 = \frac{(0.233 - 3.63(\theta - (1+\theta)\, XCH))}{(1+\theta)}$$

In engineering combustion analysis based upon reaction rate theory, it is usual to assume a constant value of activation energy. Walburn (32) has shown it to be a variable quantity for propane, and suggest that the activation energy varies almost exponentially with temperature through the reaction zone. From observed species distribution through the reaction zone it has been deduced that the combustion of the hydrocarbon proceeds as follows : Initially the hydrocarbon breaks down via chain branching reactions into radicals which are then oxidized to carbon monoxide and hydrogen.

Subsequently, these two constituents are further oxidized to carbon dioxide and water vapour respectively. The rate of decomposition of the hydrocarbon is greater than the oxidation of carbon monoxide or hydrogen, resulting in the continuing increase in these species concentration.

Fast chain branching reactions associated with the decomposition of hydrocarbons are recognised as having low activation energies, while slow carbon monoxide oxidation reaction has high activation energy. Hence the variation in activation energy. As the predominating flame reaction changes from a fast chain branching hydrocarbon reaction to the slower oxidation reactions of carbon monoxide and hydrogen, the activation energy increases progressively from a low to a high value.

It is worth noting that the basic equation

$$B = A_o e^{-\frac{E}{R_u T}} \qquad \text{3.13b}$$

assumes a similar form if E is assumed to change linearly with temperature.

ie $E = MT + N$

then equation (3.13b) becomes

$$B = A_o e^{-(MT+N)/R_u T}$$

hence $$B = A_1 e^{-N/R_u T}$$

where $$A_1 = A_o e^{-M/R_u}$$

Thus the basic equation does in fact assume a linear variation in activation energy.

The values of K and E were chosen such that they gave the 'best fit' (temperature wise) between calculated and experimental values.

The quoted measured values of E for propane and air mixture ranges from 21000KJ/Kg-mol -168000 KJ/Kg-mol, the value of E which gave the 'best fit curve' for this investigation was 43000 KJ/Kg-mol. The values of K quoted in the literature range from 3.0×10^5 m^3/Kgs - 4.8×10^9 m^3/Kgs the value of K used in this investigation was 3.125×10^5 m^3/Kgs.

The combustion model assumed that the ignition temperature occurred at X = 0 and was varied between 600^0 K - 800^0 K so 'best fit' curves could be obtained while accommodating the use of only one value for E and K for all test conditions. In all calculations ϵ was taken to be 0.2.

3.4 Boundary Conditions

Given the values of the dependent variables at all locations at a certain initial time, it is necessary to find their values at all locations at any later time. Knowledge of the initial values is not enough, information must also be supplied about the conditions that are enforced at the two ends of the duct at all later times.

The boundary conditions for this investigation are a closed end at the inlet and an open end at the outlet considering each in term:-

Inlet Boundary Condition

The inlet is assumed acoustically closed the value of U is equal to the mean velocity. The value of C_a is assumed known and corresponds to the inlet condition of a path line characteristic. It is assumed the inlet of the duct corresponds with the pressure plane of recovery after the sudden enlargement i.e. the plane where the pressure is uniform and the flow one-dimensional.

Outlet Boundary Conditions

In the problem considered only subsonic flow is assumed to occur, and neglecting the inertia of the fluid outside the duct exit, the state

of the gas at the plane of the open end can be assumed to be that of the surroundings. For the open end condition two conditions can occur they are :

(Out flow)

In this case only one condition is required. As long as the flow velocity at the exit remains subsonic, and the gas in the external region is at rest, the pressure at the end of the duct can be assumed equal to the external pressure. The outlet velo city can then be calculated from equation (3.7) and C_a can be calculated from equation (3.10)

(Inflow)

In this investigation due to the presence of a standing wave for which the open end is a pressure node, it can still be assumed the pressure at the open end to be the same as the external region, however, the entropy of the gas entering the du ct from the external region has to be calculated. When the flow enters the duct from an external reservoir, it must be accelerated from rest to the entrance velocity. Making the assumption that the flow in the vicinity at the end of the duct can be treated as quasi-steady. The state of the gas in the external region represents the stagnation condition (denoted by subscript o) for the flow at the inlet section to the duct, and assuming the inflow to be isentropic. Applying the energy equation in the form,

$$u^2 + \frac{2C^2}{\gamma-1} = \frac{2C_o^2}{\gamma-1} \qquad \text{——————} \quad 3.14$$

from which C can be calculated as u can be obtained from equation (3.7)

3.5 Operating Frequency

Hanby (28) has reported an accuracy of 5% in predicting frequency by using the mean square root gas temperature as a basis for computing the speed of sound in the basic equation;

$$F = (2n-1)\frac{C}{4L}$$

for $n = 1, 2, 3$

Hirst (29) - see Appendix I has recently considered a closed/open pipe of acoustic length 2.0 m assuming a linear rise in velocity of sound for a temperature rise of 1000° C, with a sinusoidal pressure oscillation of angular frequency W generated at X = 0.

Considering the same problem but using a less rigorous approach :

The period of oscillation is related to the standing wavelength and velocity of sound by the equation.

$$t_p = \frac{\lambda}{C}$$

For the fundamental mode of vibration the period of oscillation is given by :

$$t_p = \frac{4L}{C}$$

ie a pressure pulse must travel the length of the tube four times before the cycle is repeated, for reflection at the closed end takes place without change of phase , and so two reflections at the open-end are necessary before the reflected pulse is restored to the initial phase.

with $C = MX + N$

then $$t_p = \int_0^{4L} \frac{dx}{(MX+N)}$$

$\therefore$ $$t_p = \frac{4}{M} \log_e \left(\frac{ML}{N} + 1\right)$$

for higher harmonics

$$t_p = \frac{4}{(2n-1)M} \log_e\left(\frac{ML}{N} + 1\right)$$

for $n = 1,2,3$

The frequency of oscillation being given by :

$$f = \frac{1}{t_p}$$

The following table shows the comparison of the above theory to the basic sound theory and the one proposed by Hirst.

	Fundamental	1st Harmonic	2nd Harmonic
Basic Sound Theory	65.2	195.6	325.9
Predicted	62.5	187.5	312.5
Hirsts	71.9 *	191.2	314.9

(* possible error)

To be able to predict the operating frequency in this manner, it would be necessary to know the temperature gradient. This investigation used the measured frequencies for all predicted results.

3.6 Numercial Solution

The mathematical model of the combustor is divided into two sections, the combustion section and the heat transfer section.

The numerical solution for the combustion section is more elaborate than for the heat transfer section, due to the chemical reactions occurring in the combustion section. It is necessary to preserve the identity of path lines in the combustion section as the mass fractions of propane and oxygen vary along each path line figure (5·8), and so a non-mesh method has to be employed for the path line characteristic.

The numerical method used in the heat transfer section is described first followed by the description of the non-mesh method for the path lines in the combustion zone.

3.6.1 Numerical solution in the heat transfer section

The geometrical relationship between the points which have to be considered during a forward step in time are shown in figure (3.3) Figure (3.3a) concerns a point in the central part of the grid, while figure (3.3b), figure (3.3c) and figure (3.3d) represents points near a boundary.

For a central grid point figure (3.3a), the task is to calculate values of P, U and Ca at point 'P' , given the values of these variables at points T,V and W. First, the characteristic lines RP, AP and SP are located, having slopes 1/(U+C) , 1/(U) and 1/(U-C) respectively. Then the values of P,U and Ca for the points R, A and S are obtained from those at T, V and W by interpolation. Finally the variables P and U at point P are found by combining equations (3.7) and (3.8) in Finite difference form and the value of Ca at point P is found by applying equation (3.10)

For the boundaries, the procedure is modified by the fact some of the information implied by the above relations is replaced by information derived from boundary conditions. Consider outflow to the right figure (3.3d) instead of knowledge transmitted by the SP characteristic, the value of P is known and U can be calculated from equation (3.7) Similar relationships can be formed for the other boundary conditions.

a) Calculations of the variables at R, A and S

The slope of the characteristics through R, A and S are respectively 1/(U+C), 1/(U) and 1/(U-C), but the U and C values are different for each point, and they vary along the length of the lines that lead to P. Many methods can be derived of varying accuracy and complexity for the evaluation of appropriate mean values of U andC, the one that is adopted in the program is to use the value of U and C at position V.

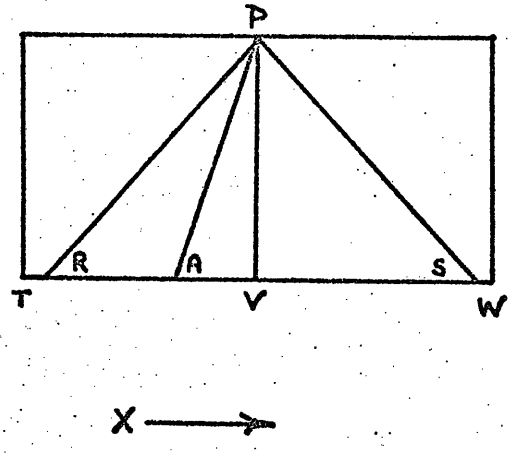

CENTRAL REGION

(a)

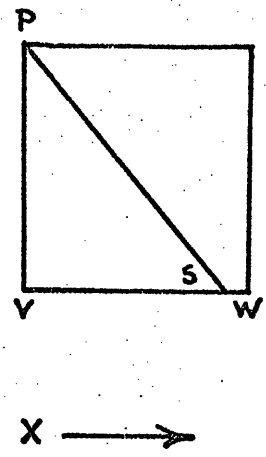

INFLOW AT THE INLET BOUNDARY

(b)

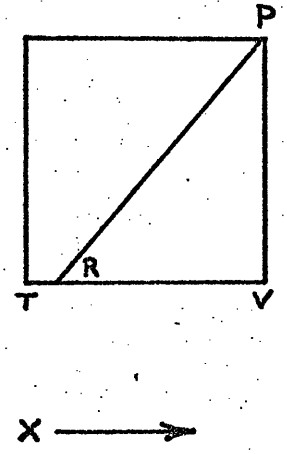

INFLOW AT THE OUTLET BOUNDARY

(c)

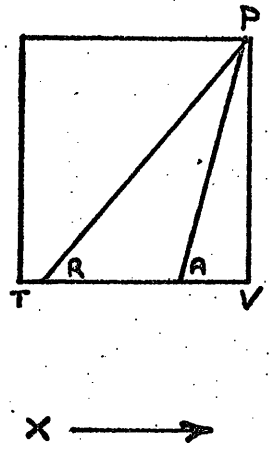

OUTFLOW AT THE OUTLET BOUNDARY

(d)

Figure. (3-3)

The corresponding X co-ordinates of the points R. A and S are thus :

$$X_R = X_v - (u+c)\,dt$$

$$X_A = X_v - (u)\,dt$$

$$X_S = X_v - (u-c)\,dt$$

dt had to be chosen so that none of the ends of the characteristics R, A and S lie outside the range TW, this is dealt with more fully in Appendix I.

It is also assumed that dt is sufficiently small that parts of the characteristics between R and P between S and P and between A and P are straight lines.

With location of the points determined, the values of the variables there can be fixed by interpolation. Linear interpolation is used in the program, because it is the simplest and because more complex procedures appear to have no advantage. The formulae are :

$$F_R = F_v + (F_T - F_v)(X_R - X_v)/(X_T - X_v)$$

$$F_S = F_v + (F_w - F_v)(X_S - X_v)/(X_w - X_v)$$

If the velocity of the particle is positive A will be to the left of V, then :

$$F_A = F_v + (F_T - F_v)(X_A - X_v)/(X_T - X_v)$$

If the velocity of the particle is negative A will lie to the right of V, then :

$$F_A = F_v + (F_w - F_v)(X_A - X_v)/(X_w - X_v)$$

where F denotes any property of the fluid.

b) Calculating Ca, P and U at a Central Grid point at the time $t+dt$

To find the value of the flow variables at the point P, which has the same X value as V but at a later time considering the three characteristic equations : (3.7), (3.8) and (3.10).

The value of q in equation (3.10) is the value the path line has at A given by equation(3.11) . All grid point values of q assume the value their respective path line characteristics had at point A. Therefore, all path line calculations for time step dt must be carried out first.

The value of q in equation (3.8) is the arithmetic mean value of the values at V and W. The value of q in equation (3.7) is the arithmetic mean value of the values at T and V.

The values of ρ and C are the values they have at V.

The compatability equations in Finite difference form for equation (3.7) and (3.8) are :

$$(P_p-P_R)+\rho c(u_p-u_R)-(\gamma-1)\rho dt\,(q_v+q_T)/2 = 0$$

$$(P_p-P_s)-\rho c(u_p-u_s)-(\gamma-1)\rho dt\,(q_v+q_w)/2 = 0$$

$$\therefore\ u_p=\frac{1}{2}\left(\left((P_R-P_s)+(\gamma-1)\rho dt\,(q_T-q_w)/2\right)/\rho c+u_R+u_s\right)$$

and

$$P_p=P_R-\rho c(u_p-u_R)+(\gamma-1)\rho dt\,(q_v+q_T)/2$$

Thus the velocity at p becomes the arithmetic mean of the values at R and S, plus a contribution from the difference between the pressures at those two points plus the heat transfer effect.

Likewise the pressure at P can be shown to be the arithmetic mean of the pressure at R and S, plus a contribution from the difference between the velocities at those points plus the effect of heat transfer.

The value of C_a at P is found by finding the value of C_a at A and applying equation (3.10)

$$C_{a_P} = C_{a_A} + dC_a$$

hence $$C_{a_P} = C_{a_A} + \frac{C_{a_A}}{2C_A^2} q_A(\gamma-1)\,dt$$

c) The calculation of p, u and Ca at the boundary grid points at time $t+dt$

Inlet boundary

If the inlet is considered an acoustically closed end, the value of u at P is given by the mean velocity. Then the value of p at P is given by equation (3.8) in finite - difference form :

$$P_P = P_S + \rho c(u_P - u_S) + (\gamma-1)\rho q\,dt$$

The value of q is assumed to be composed of two distinct parts, a mean value which determines the change in mean values of fluid properties due to energy transfers and the second part, an unsteady component a small fraction of the mean q value causing the fluctuations in flow conditions ie pressure amplitude. Many attempts have been made to predict the pressure amplitude of oscillation, it has been suggested by Bhaduri (30) that the pressure amplitude may be calculated by assuming, that the energy of the wave is proportional to the thermal input rate. This investigation found that the amplitude was dependent on fuel injection system, air/fuel ratio and mode of oscillation, suggesting Bhaduri assumption to be unsatisfactory as Hanby (28) has suggested

This investigation then has to rely on the measured pressure amplitude at the inlet and uses a steady flow value for the mean value of q

It is proposed to represent P_p the pressure at the inlet boundary by the equation :

$$P_p = P_a + \hat{P} \sin(wt) + (\gamma-1) \rho q_m dt$$

where P_a is the atmospheric pressure, $\hat{P}\sin(wt)$ represents the measured pressure amplitude at the inlet, and the term $(\gamma-1)\rho q_m dt$ represents the increase in mean pressure due to combustion.

C_a assumes the value it had in steady state calculations when obtaining the 'best fit' curves for the measured axial temperature gradients in the combustion zone for non-pulsating conditions.

Outflow through a fully open end.

The end of the path line characteristic A figure (3.3d) lies within the duct. The value of Ca at P can be calculated from equation (3.10). The pressure at the duct outlet can be taken to equal the external pressure. The value of u at p may be calculated from equation (3.7)

$$U_p = U_R - \left((P_p - P_R) - (\gamma-1) \rho (q_v + q_T)/2 \, dt \right) / \rho C$$

Inflow through a fully open end figure (3.3c)

When fluid enters the duct from an external region, it is assumed the stagnation condition at the end of the duct is the same as that of the external region, and assuming the inflow to be isentropic. The energy equation can be expressed, from equation (3.14) by :

$$U_p^2 + \frac{2}{\gamma-1} C_p^2 = \frac{2}{\gamma-1} C_o^2$$

The pressure at P may still be assumed to be equal to the external pressure due to the formation of a pressure node at the open end.

3.6.2 Calculating, Ca at a central grid point in the Combustion Zone

A non-grid method had to be used for path line characteristics in the combustion zone as it was necessary to preserve the identity of each path line due to the complexity of burning.

Referring to figure (3·4), a search is made to find the nearest path line on either side of the grid point (J+1) in this case XK1 and XK2.

The velocity and pressure at these points can be found by linear interpolation ie for XK1

$$U_{K1} = U_J + (U_{J+1} - U_J)(XK1 - XJ)/\Delta x$$

Since the slope of the path line is $\frac{dt}{dx} = \frac{1}{u}$ its new position after an interval of time dt , is (assuming the path line is straight over the short interval dt).

$$XK\grave{1} = XK1 + U_{K1}\, dt$$

from the path line compatibility equation (3.10)

$$C\grave{a}_{K1} = C_{aK1} + dC_{aK1}$$
$$= C_{aK1} + \frac{C_{aK1}}{2C_{K1}}\, q\,(\gamma-1)\, dt$$

where q is given by equation (3.13).

It is necessary when calculating the wave characteristics to know the q value at grid points, this is done in the combustion zone by interpolating between the points XK1 and XK2. The basic information which must be stored for a path line is its position, its entropy level in terms of C_a and the mass fraction of unburnt fuel.

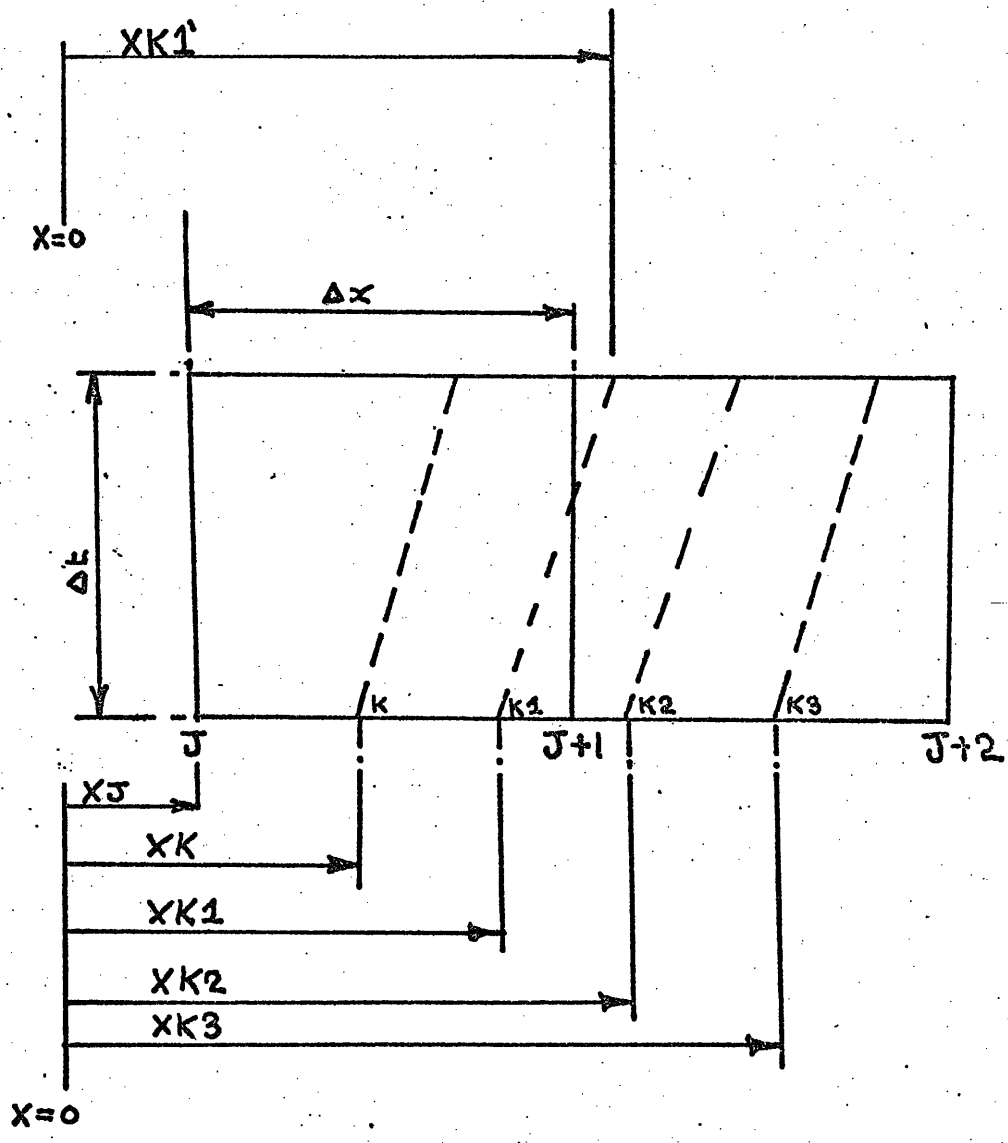

PATH LINES AND GRID POINTS FOR NON-MESH METHOD

Fig. (3.4)

Combustion was considered complete when XCH = 0.003 which corresponded to $X \simeq 0.3$ m for all test conditions considered by the investigation, this giving a combustion efficiency of 95%.

3.7 Computer Program

The computer program was written in Fortram IV and was executed on an IBM 360 computer. The organisation of the program is shown in figure (3·5)

In working with the program great difficulty was found in choosing the correct number of path line characteristics for the combustion section of the program. However, it was found that a good approximation could be had, if the mean velocity for the path line characteristic direction was used instead of the instantaneous velocity. This approximation greatly reduced the difficulty and computer time was saved due to a reduction in the number of path line characteristics required. A typical comparison of results from the two methods is shown in figure (5·6) and figure (5·7), a further comparison being given in the test results for tests 3a and 3b. The comparison shows that a reduction of temperature oscillations in the combustion section is obtained, when using the mean velocities for calculation of path line characteristi c s, this producing a change in the distribtuion of standing waves as shown in the results for tests 3a and 3b.

All predicted results for tests 1 - 5 (section 5·2) used the instantaneous velocity for pathline calculations.

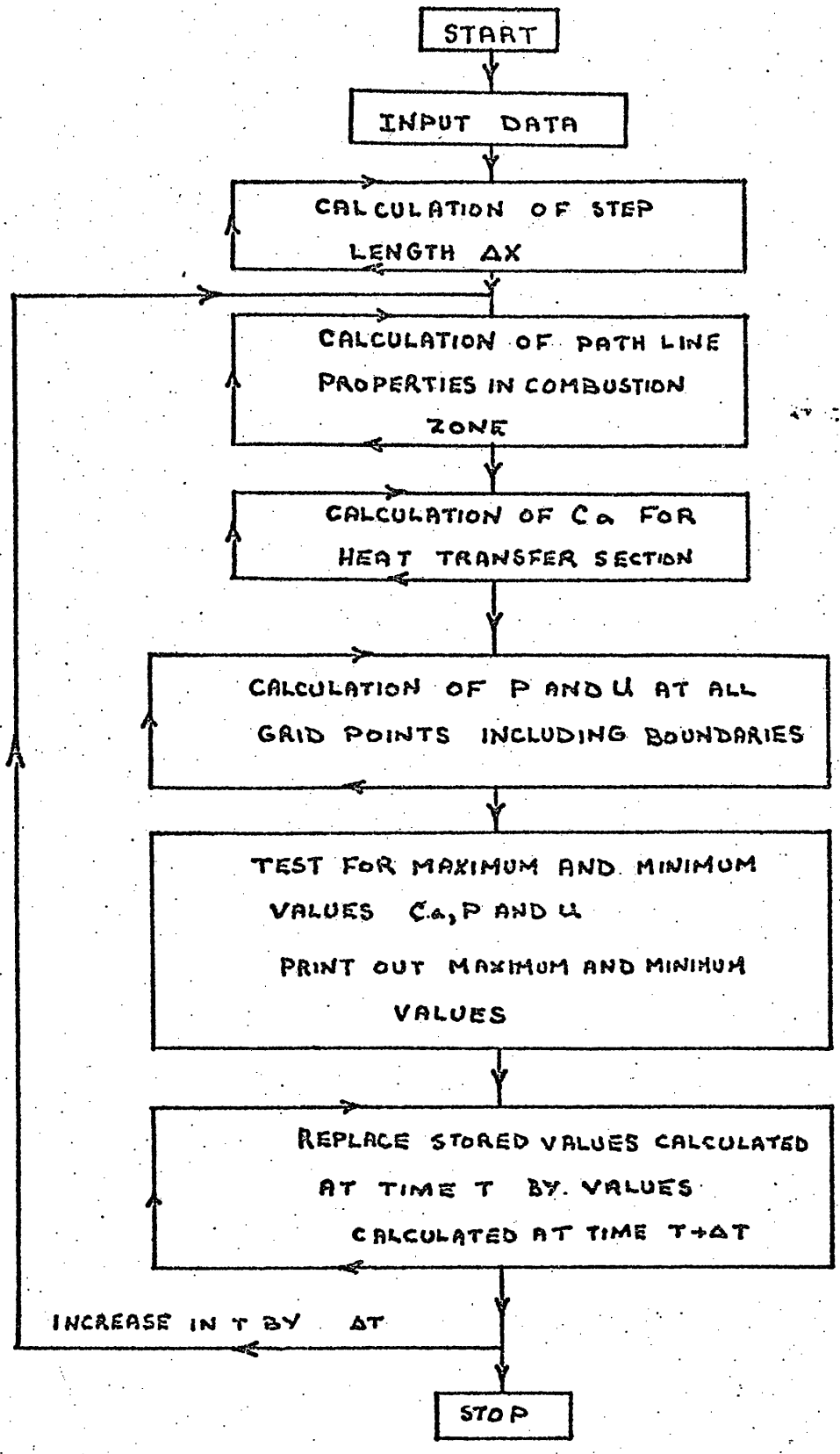

GENERAL ORGANIZATION OF MATHEMATICAL MODEL Fig (3·5)

CHAPTER 4

4.0 Experimental Method

The aim of the experimental work was to construct a pulsating combustor of simple design which would facilitate mathematical ayalysis, and allow measurement of the variables thought to affect the combustion oscillations.

4.1 Experimental Apparatus

The combustor is shown in Figure (4.1) it consisted of a 1.985 m long 50.8 mm internal diameter stainless steel tube of 6.35 mm wall thickness, with a counter-flow cooling jacket for most of its length. The outlet of the combustor was connected to a large silencing chamber - section (4.9). The combustor inlet - see figure (4.2) - was acoustically closed by a constriction to 19 mm diameter with a 16 mm diameter central propane jet with an end nozzle attached. During combustion the combustor produced longitudinal acoustic oscillations of the fundamental and first harmonic - figure (5.1) - the mode of oscillation depending on air and fuel flowrate. Twelve sampling ports were provided along the combustors length for the insertion of probes, two in the combustion chamber and ten in the heat transfer section.

4.2 Air Supply

A two stage reciprocating compressor, with a receiver pressure of 10.5 bars gauge, supplied air (model 15T type 30 manufactured by Ingersoll Rand Limited). The supply flowrate was measured by a Gapmeter (Type IGU/15F) manufactured by G.A. Platon Limited). The range covered was from 0.1×10^{-2} - 0.9×10^{-2} Kg/S at 7 bar gauge and 15° C.

EXPERIMENTAL SYSTEM Fig (4·1)

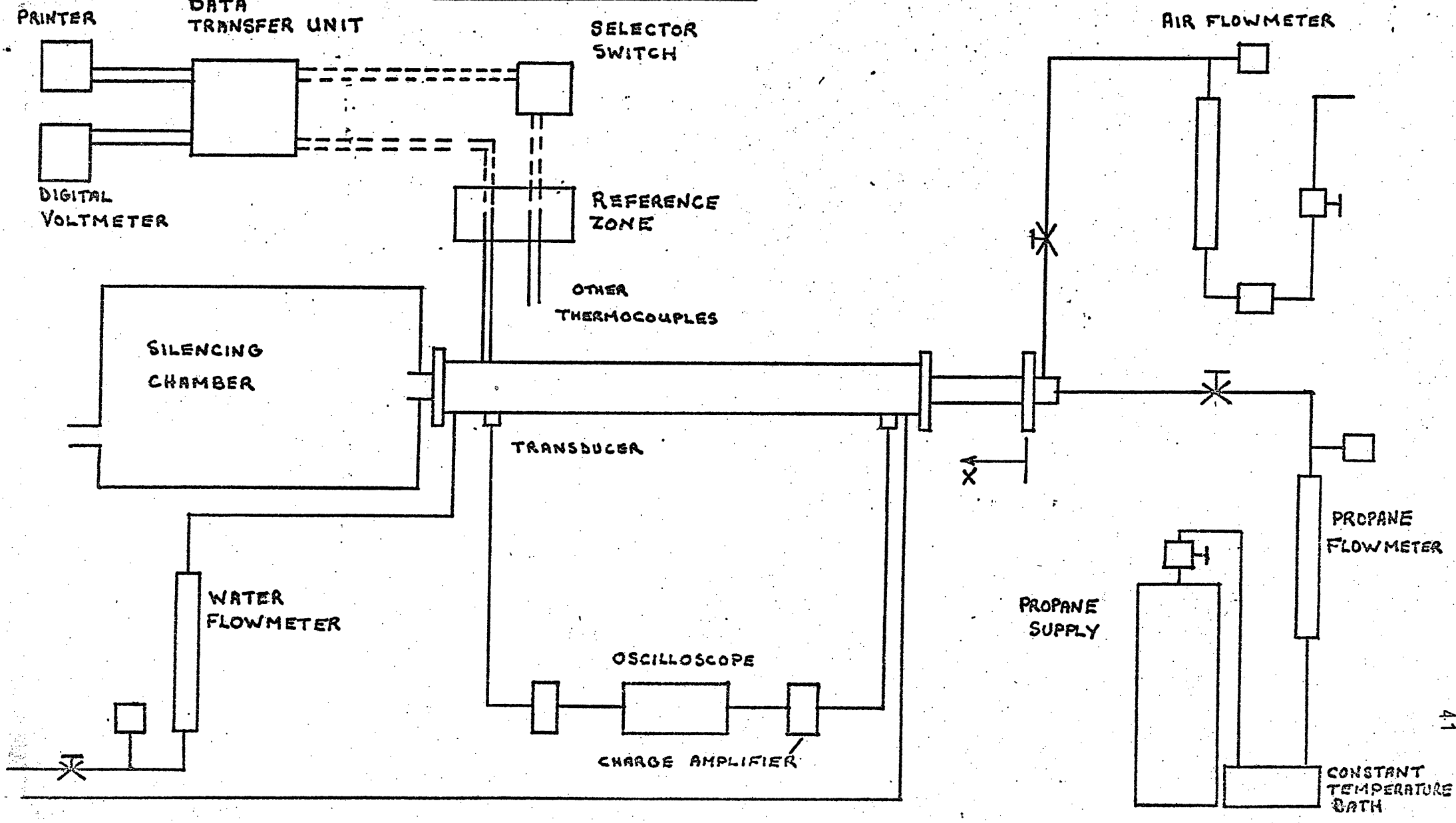

The Gapmeter was calibrated by the manufacturers to an accuracy of ± 1.25% of full scale deflection. The calibration pressure was maintained by a pressure regulator, and any temperature variation was corrected from a measurement of air temperature in the supply line. A large pressure drop was produced in the air supply line at the inlet to the combustion chamber to prevent flow oscillations in the supply line, this was verified by transducer measurement of pressure close to the flowmeter, no variation in pressure was observed - steady flow could be assumed.

4.3 Fuel Supply

In order to simplify as much as possible the mathemetical model a gaseous fuel was used (Commercial Propane from the British Oxygen Company Limited). This choice eliminated the problems associated with predicting vaporization rates and liquid droplet burning rates. The supply flowrate was measured by a high accuracy rotameter (Type 100 manufactured by Rotameter Limited). The range covered was from 0.18 - 1.8 Fm^3/h at 30 psi and 20° C. The rotameter was calibrated by the manufacturers to an accuracy of ± 2.0% of indicated flow. A large pressure drop was produced in the fuel supply line at the inlet to the combustion chamber by flow across a nozzle to prevent flow oscillations in the supply line, transducer measurement of pressure near the flowmeter indicated no variation in pressure - steady flow could be assumed. The temperature of the propane was controlled by passing the propane through a cooling coil immersed in a constant temperature bath. The calibration pressure was maintained by a pressure regulator, and any temperature variation was corrected from a measurement of propane temperature in the supply line.

4.4 Fuel Injection System

The fuel injection system is shown in figure (4·2). Standard Amal nozzles were used, the size of nozzle used was found to affect the pressure smplitude and mode of oscillation, . . many other variables were found to affect these two quantities, that it was decided to use only one nozzle size. Nozzle No.400 was chosen, this produced the fundamental at low fuel flowrates and first harmonic at high fuel flowrates - Figure (5·1).

4.5 Cooling Water Flowrate

The cooling water flowrate was measured by a rotameter (Type Metric 24E manufactured by Rotameter Limited). The rotameter was calibrated by timing the discharge of a quantity of water for set conditions, the error involved was estimated at $\pm$ 2%. The inlet and outlet water temperatures of the cooling jacket were measured by calibrated thermometers $\pm$ 0.2° C over a range of temperature 15°C - 35° C, for a flowrate of 0.15 Kg/s.

4.6 Pressure Measurement

Pressure amplitudes were measured at each of the sampling ports using quartz crystal piezoelectric transducers (Kistler type 601A housed in a cooling adaptor type 728). The measuring range was 0 to 250 bars with a scale linearity of 0.25%. The output from the transducer was displayed on an oscilloscope using a charge amplifier the amplitude was measured from the screen to an accuracy of $\pm$ 3%. The frequency of oscillation was also found from the trace and compared with measurements from a wave analyser (A .F. Analyser type 1461A manufactured by Dawe Limited). A switching adaptor (Kistler type 642) was used for measuring the values of mean pressure in the combustion chamber.

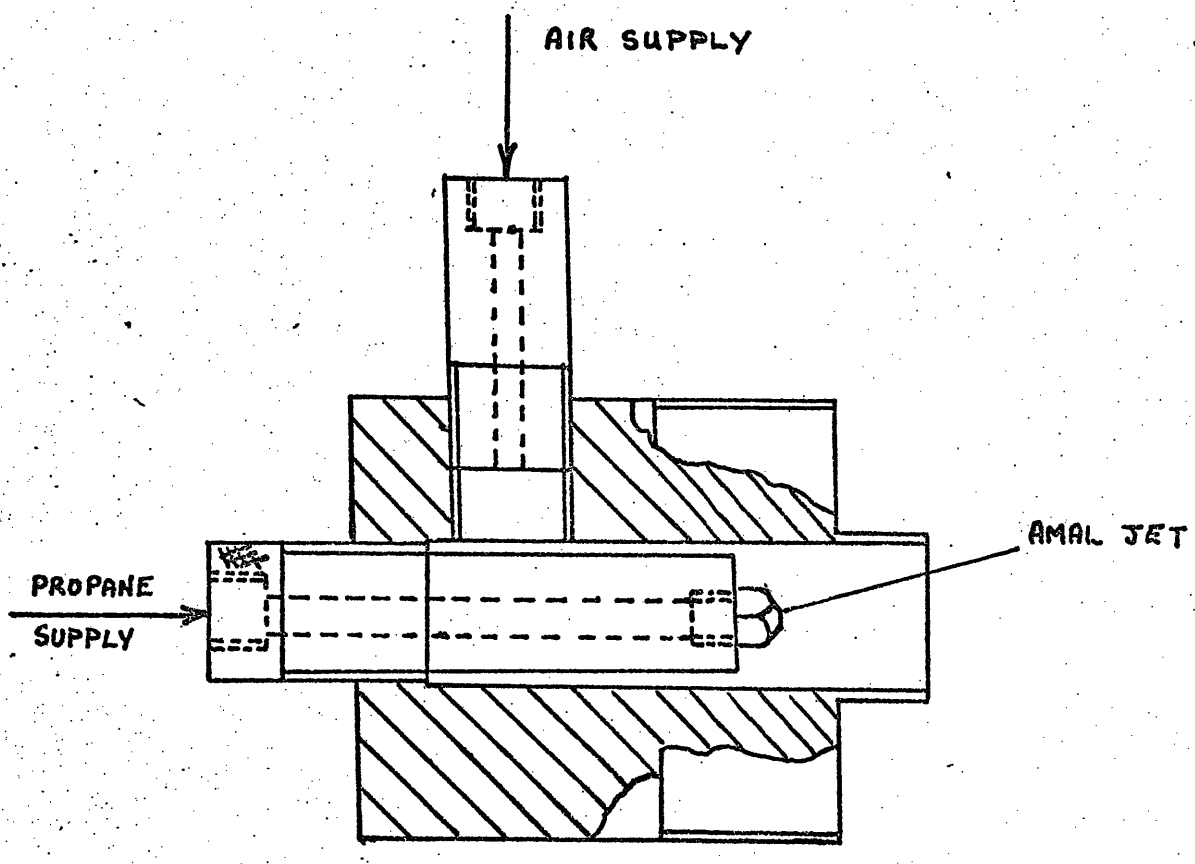

FUEL INJECTION SYSTEM Fig.(4.2)

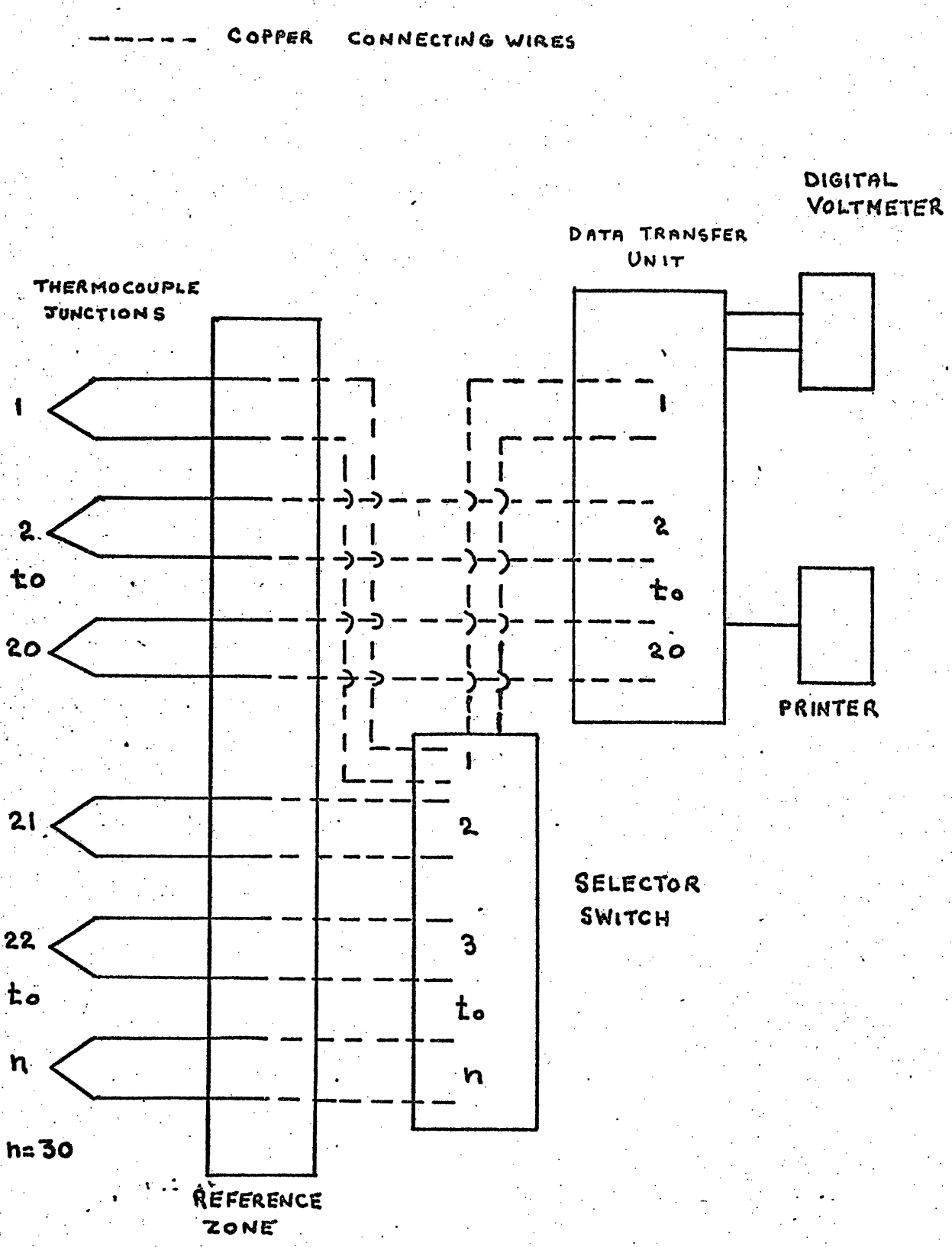

Fig.(4·3) THERMOCOUPLE SYSTEM

4.7 Wall Temperature Measurements

The mathematical model of the combustion system required as input data inside wall temperature measurements of both the heat transfer section and combustion section.

4.7.1 Wall Temperature Measurements of the Heat Transfer Section

The temperature difference across the tube wall had first to be measured this was done by taking temperature measurements at two radial positions for each section corresponding to a sampling port in the heat transfer section.

From measurements of wall temperature it was found that the radial temperature gradient was much greater than the longitudinal temperature gradient. Thus it may be assumed that heat flow is mainly in the radial direction, then it can be shown the temperature T_w at any radius r is given by :-

$$T_w = \frac{(T_1 - T_2)}{\log_e \frac{r_2}{r_1}} \log_e \frac{r_2}{r} + T_2$$

where $T_w = T_1$ at $r = r_1$ and $T_w = T_2$ at $r = r_2$

This equation enabling the inside wall temperature, Tw, to be determined.

The wall temperatures were measured by copper/constantan thermocouples. The junctions were spot welded and electrically insulated by applying a thin covering of araldite. The measuring system for the thermocouples is shown in Figure (4.3). The thermocouples were calibrated against N.P.L. calibrated thermometers ($\pm$ 0.1°C) using a constant temperature oil bath. The bath was controlled with a maximum temperature of 200° C. The results agreed with the standard calibration curves (36) to within 0.5 %

The reference zone was an insulated box containing the junctions of the thermocouple wires and the copper connecting wires - the temperature of the zone was measured with a calibrated thermometer ± 0.2° C . The generated voltages were measured by a digital voltmeter (type LM1604, manufactured by Solatron Limited). The output was printed on a paper tape (Addmaster type 35 manufactured by Addmaster Co. Ltd.) A selector swich had to be incorporated in the design, due to limited input channels to the transfer unit. The arrangement enabled all wall temperatures to be measured relative to a reference temperature, and the equivalent voltage recorded on a paper tape print out.

4.7.2 Wall Temperature Measurements of the Combustion Chamber

It was found that the temperature drop across the wall thickness was quite small, and so only one radial temperature position was needed. Ten equally spaced holes were drilled along the length of the combustor wall, which allowed a thermocouple probe to be inserted to measure the temperature 1.5 mm from the inside surface of the combustion chamber. The thermocouple probe was a nickel/chromium V nickel/aluminium (manufactured by Protenax Type BJ). The thermocouple was calibrated by the manufacturers and agreed with the standard calibration curves (37) to within 0.75%

4.8 Time-independent gas temperature measurements

The axial temperature gradient in the combustion zone was measured by an axial thermocouple probe. The thermocouple probe was made from twin bore ceramic tubing down which the thermocouple leads were fed. The thermocouple was Platinum/10% Rhodium V Platinum and of diameter 0.01 inches the junction formed by spot welding. The thermocouple was calibrated in an electrically heated furnace which was calibrated to within 0.75% of the standard calibration curves (38), the overall calibration of the thermocouple agreed with the standard calibration curves to within

1.5%

The axial gas temperature at each sampling port in the heat transfer section was measured by the same type of thermocouple probe, more details of the method used is described in Appendix II. The transverse temperature profiles in the heat transfer section were found to approximate very closely to the temperature distribution of the form :

$$T = T_a \left(\frac{Y}{F}\right)^{1/7}$$

Where T is the absolute temperature at distance Y from the tube wall, Ta is the absolute temperature at the axis. When testing, Ta was measured by a thermocouple probe situated on the axis and calculating the mean temperature by integration of the above expression to give :

$$\bar{T} = 0.875\, T_a$$

The maximum error was estimated to be 5%

4.9 Silencing Chamber

A chamber was constructed to give a volume of approximately $3m^3$, it exhausted directly to the atmosphere. The sides were lined with fibre - glass insulation and acoustic tiles. An average decrease of 50% in room sound level was measured. The temperature of the gases in the chamber was measured by a calibrated thermometer $\pm$ 0.2° C, this was needed as a requirement for a boundary condition in the mathematical model.

4.10 Experimental Procedure

To obtain the characteristics of the combustor a series of runs were made over the range of air/fuel ratios 14-21:1 and Reynolds numbers of 3400-10900.

A standing wave was produced in the combustor with a pressure antinode at the closed end and a pressure node at the outlet. The combustor could oscillate at either the fundamental or first harmonic depending on the fuel and air flowrates. The oscillation regions were determined by keeping the fuel flowrate constant and varying the air flowrate for various fuel flowrates, figure (5.1). The oscillations could be prevented by removal of a port plug at a position corresponding to the maximum pressure antinode, which enabled non-pulsating conditions to be achieved for the same conditions as for pulsating conditions.

The effectiveness of the heat exchanger was determined for fixed values of fuel flowrate while varying the air flowrate, the effectiveness η_E being defined as :

$$\eta_E = \frac{\text{Energy removed by coolant}}{\text{Energy released by fuel for 100\% combustion}}$$

The variation of pressure amplitude of the pressure antinode at the closed end for variation in air/Fuel ratio, was determined for fixed fuel flows - figure (5.3).

Having obtained the overall characteristics of the combustor, test were carried out for the following conditions :

Details of Test Conditions

Test	M_f	A/F	Mode of Oscillation
1	0.30	15.75	Fundamental
2	0.30	18.89	Fundamental
3a	0.50	18.89	Fundamental
3b	0.50	18.89	First Harmonic
4	0.60	15.75	First Harmonic
5	0.60	18.89	First Harmonic

Equilibrium conditions were defined as constant wall and coolant temperatures. The time to reach equilibrium conditions was approximately 30 minutes.

For each test the following measurements were taken.

Mean Air Flowrate

- Gapmeter
- Air supply line temperature

Mean Fuel Flowrate

- Rotameter
- Fuel supply line temperature

Mean Water Flowrate

- Rotameter
- Coolants Inlet and Outlet temperatures

Wall Temperatures

- Thermocouple readings
- Reference Zone temperatures

Readings at sample ports

- Pressure amplitude
- Frequency of Oscillation
- Gas temperatures

Silencing Chamber

- Temperature

4.11 Error Analysis

The maximum possible experimental errors in the investigation are considered. The errors are derived from the possible errors in the measuring instruments.

The relevant instrument accuracies can be defined :

Air flowrate

Gapmeter accuracy $\pm$ 1.25% full scale deflection

Propane flowrate

Rotameter accuracy accuracy $\pm$ 2.0% indicated flow

Water flowrate

Rotameter accuracy $\pm$ 3.0% indicated flow

Wall temperature

Calibration error of thermocouple wire $\pm$ 0.1°C.

Resolution of digital voltmeter $\pm$ 0.25°C

Gas temperature

Calibration error of thermocouple wire $\pm$ 10°C.

Resolution of digital voltmeter $\pm$ 0.3°C.

Pulsation Parameters

Pressure amplitude measurement oscilloscope resolution $\pm$ 3%
- it is assumed that possible errors of the transducers and charge amplifiers are negligible compared with the oscilloscope resolution.

Frequency Measurement

Oscilloscope resolution $\pm$ 3.0%

An estimate of the performance of the experimental system can be found from a comparison of the system under non-pulsating turbulent flow conditions for which a theory is already well developed (40).

CHAPTER 5.

Results and Discussion

5.1 The Combustors Characteristics

5.2 Test Results

5.3 Non-pulsating conditions

5.4 Pulsating Conditions

5.5 Frequency Measurements

5.6 Time-independent Axial Gas Termpature measurements in the combustion chamber

5.0 Results and Discussion

5.1 The Combustors Characteristics

The modal zones of oscillation are shown in figure (5.1). For any fuel mixture occurring in region 'A' the fundamental mode of oscillation was obtained, in region 'C' the first harmonic and in region 'B' either the fundamental or first harmonic. The fundamental was obtained in region 'B' by operating the combustor in region 'A' then moving into region 'B'. If the combustor was operated in region 'C' then moved to region 'B' the first harmonic was obtained .

A possible explanation for a change in the mode of oscillation, could be the higher flowrate associated with the first harmonic producing in the broadband noises, caused by the flame, a narrow frequency band more closely coupled to the first harmonic than fundamental.

Figure (5.2) shows the comparison of the effectiveness of the heat exchanger η_E for pulsating and non pulsating conditions.

The higher values of η_E were obtained for the fundamental mode, this being mainly due to the larger pressure aplitudes associated with this mode of oscillation. However, Hirst (29) has suggested lower frequencies produce higher heat transfer rates, but this was not verified in the present investigation.

Pressure amplitudes measured at the closed end of the combustor, against air/fuel ratio for different fuel flowrates are shown in figure (5.3), increases in air/fuel ratio caused corresponding rises in pressure amplitude. These results are similar to those reported by Hanby (28) who suggested that it may be caused by increased heat release in the combustion zone and by the increased Kinetic energy of the flow.

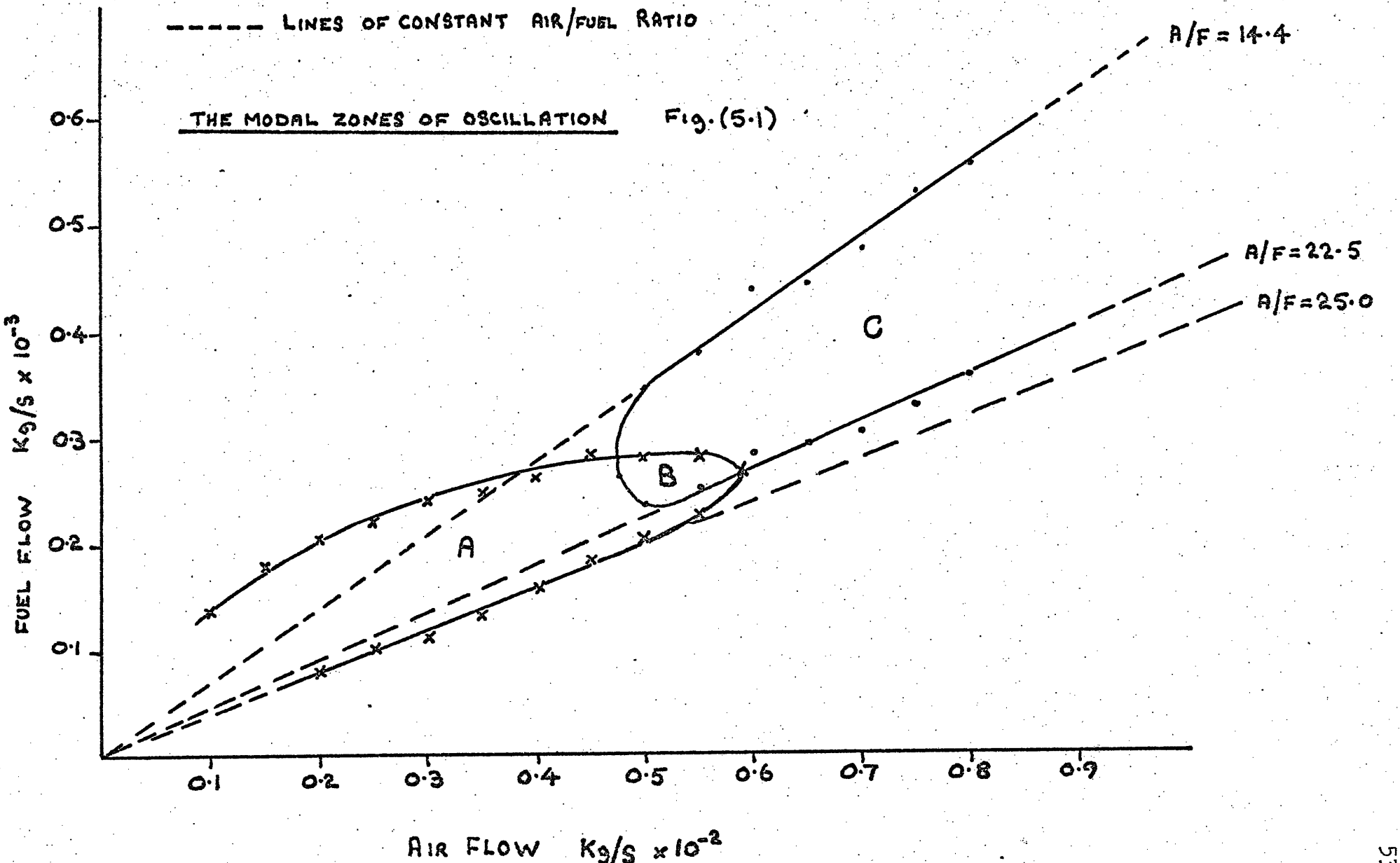
LINES OF CONSTANT AIR/FUEL RATIO
THE MODAL ZONES OF OSCILLATION
Fig.(5.1)
A/F = 14·4
A/F = 22·5
A/F = 25·0
A
B
C
FUEL FLOW Kg/S x 10⁻³
AIR FLOW Kg/S x 10⁻²
0·1
0·2
0·3
0·4
0·5
0·6
0·7
0·8
0·9

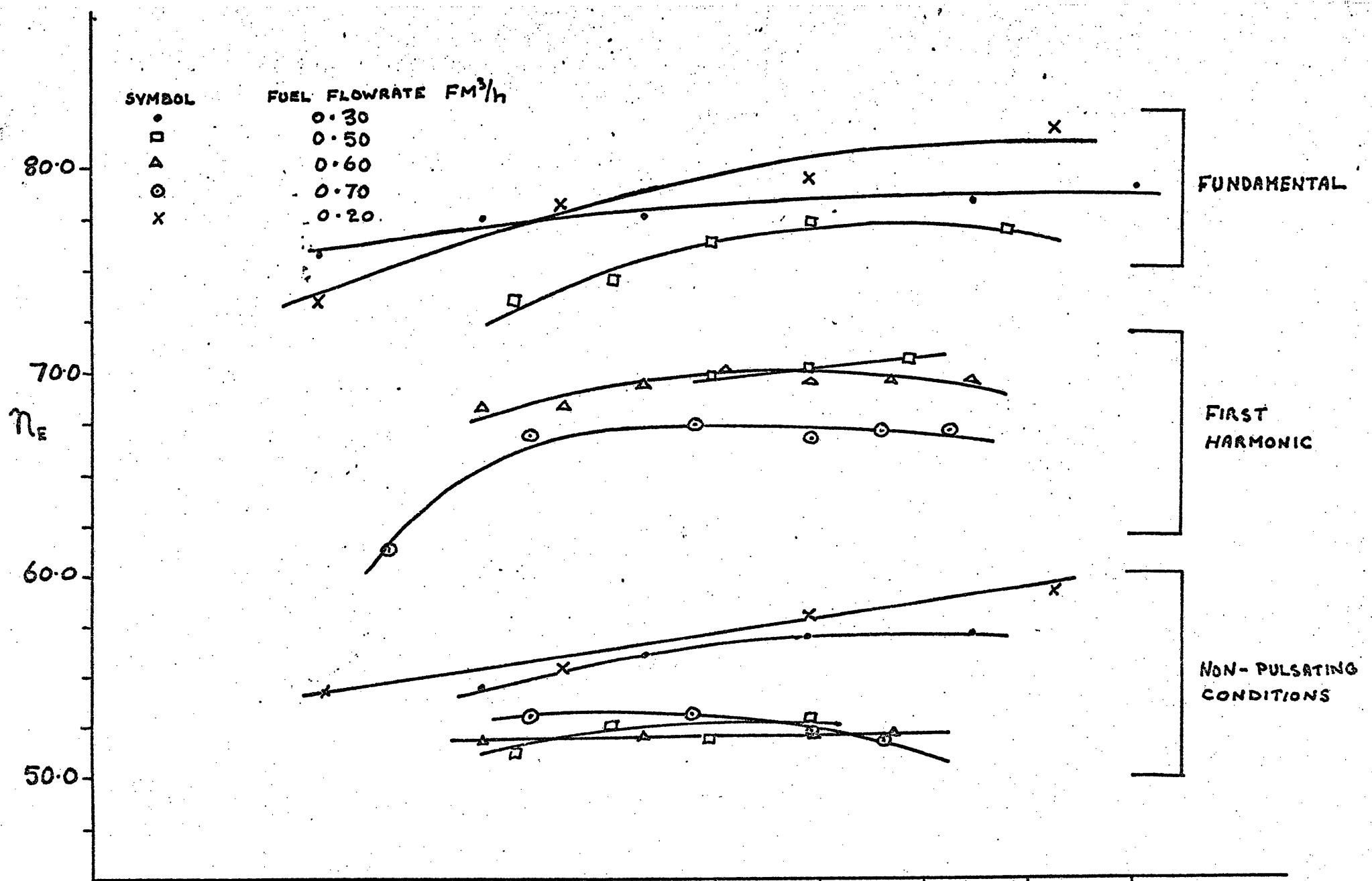
SYMBOL
FUEL FLOWRATE FM³/h
0·30
0·50
0·60
0·70
0·20.
80·0
70·0
60·0
50·0
ηE
FUNDAMENTAL
FIRST HARMONIC
NON-PULSATING CONDITIONS
13
14
15
16
17
18
19
20
21
22
AIR/FUEL RATIO

Fig (5·2)

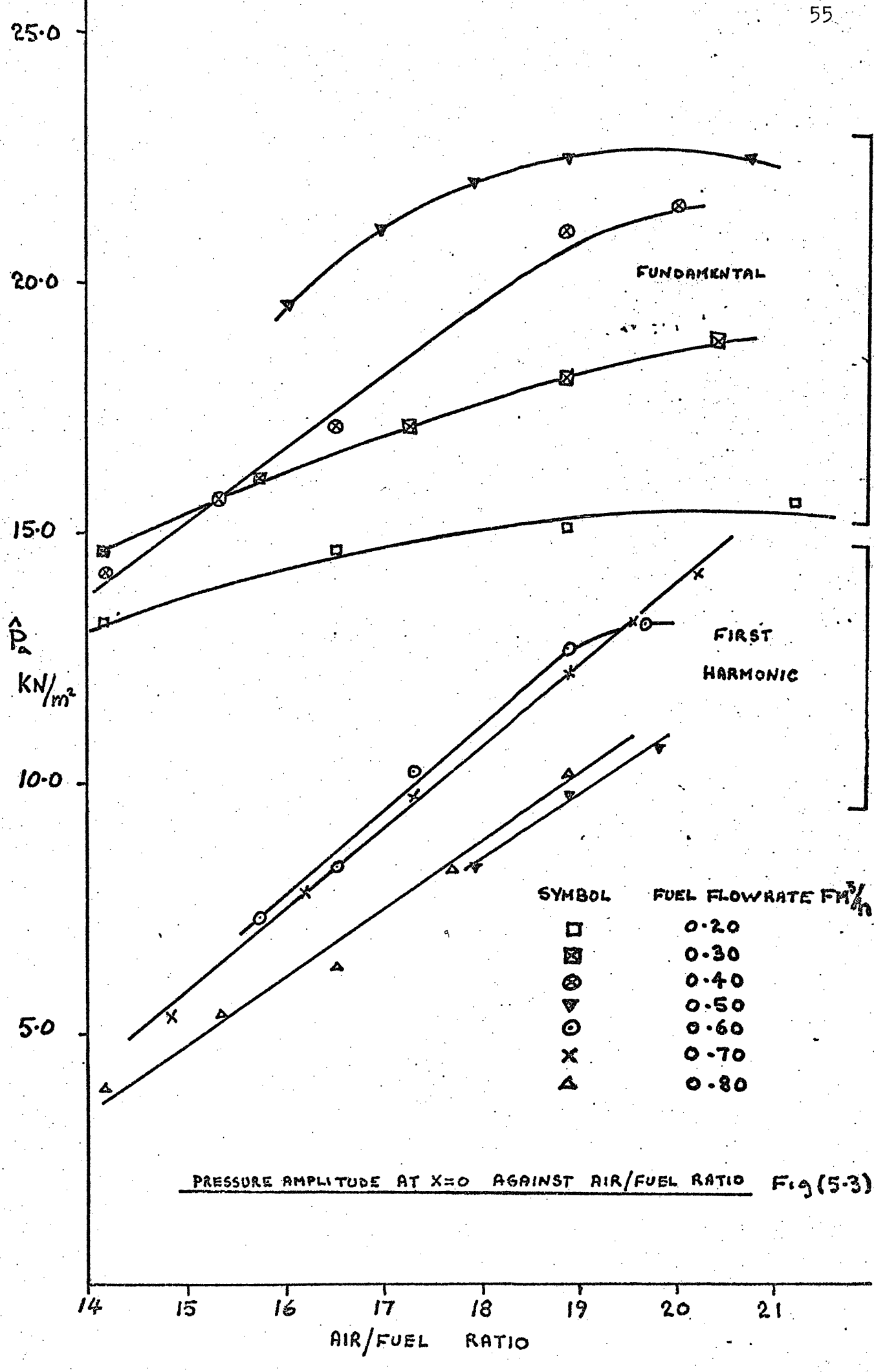

PRESSURE AMPLITUDE AT X=0 AGAINST AIR/FUEL RATIO Fig(5·3)

5.2 Test Results

The results for the test conditions shown below, are recorded graphically in terms of the distribution of the standing pressure waves for pulsating conditions and the time-independent mean gas temperature gradients, for both pulsating and non-pulsating conditions

Details of Test Conditions

Test	Fuel Flow Rate M_f	A/F	Mode of Oscillation
1	0.30	15.75	Fundamental
2	0.30	18.89	Fundamental
3a	0.50	18.89	Fundamental
3b	0.50	18.89	First Harmonic
4	0.60	15.75	First Harmonic
5	0.60	18.89	First Harmonic

5.3 Non Pulsating Conditions

An estimate of the performance of the experimental system was found from a comparison of the system under non-pulsating turbulent flow conditions to those predicted by the already well developed theory (40) on convective heat transfer for fully developed turbulent flow.

The estimate was made by carrying out tests 1 - 5 for non pulsating conditions and a comparison made of predicted and measured gas temperatures in the heat transfer section of the combustor.

Tests 1 and 4 were not considered due to errors of 10% in the predicted inlet gas temperatures to the heat transfer section of the combustor. Test 2 figure (5·18) showed agreement of 3% upto the position X=1.8 m where the difference rises to 10%, which may be explained by a energy loss occurring at the exit of the heat exchanger to the outlet section, which the theory does not take into account.

For tests 3 and 5 an additional plug had to be removed at X = 1.47 m to prevent first harmonic oscillations. Agreement of 2% was obtained up to X = 1.47 m at which position the port plug had been removed. Past this position a marked divergence occurred, the maximum difference of 25% occurring at the exit of the heat exchanger for test 3 figure (5·23). This may be explained by an additional energy loss from the open sampling port at X = 1.47 m.

5.4 Pulsating Conditions

For pulsating conditions a similar analysis was used with an additional comparison being made, that of distribution of pressure standing waves. The measured and predicted gas temperature gradients showed the marked effect pulsationshad on the energy transfer from the exhaust gases. The maximum divergence of 22% between predicted and measured values occurring in test 5figure (5·37).

In trying to make an estimate of the percentage difference between predicted and measured values of pressure distribution, the absolute values were used, as a small error in the predicted position of a pressure node would produce a meaningless error if the difference was based on pressure amplitude alone. The maximum difference of 10% occurred in test 3b figure (5·25).

The measured pressure oxcillations could be assumed sinusoidal - maximum distorition of 5%. The measured mean pressure in the combustion chamber was found to be atmospheric compared to a predicted value of approximately 1500N/m^2 above atmospheric pressure for all test conditions ie an increase of 1.5% above atmospheric pressure.

5.5 Frequency Measurements

The table below shows the measured frequencies compared to the predicted values using the method proposed by Hanby (Section 3·5)

A Comparison of Measured and Predicted Frequencies

Test	Measured Frequency	Predicted Frequency	% Difference
1	48.0	63.0	31.0
2	48.0	63.0	31.0
3a	53.0	70.0	33.0
3b	200.0	220.0	10.0
4	218.0	231.0	6.0
5	202.0	227.0	12.0

Reasonable agreement was found for oscillation of the first harmonic (tests 3b - 5). However, large differences are found in the fundamental mode of oscillation (tests 1 - 3a). The predicted frequencies being based on measured time-independent mean gas temperature gradients. Figure (5.4) shows typical predicted gas temperature amplitudes in the heat transfer section of the combustor, for both the fundamental and first harmonic. It can be seen that the temperature amplitudes are far larger in the fundamental than in the first harmonic. This could be a possible explanation for the large differences found in the frequencies for the fundamental mode of oscillation, since the basic frequency equation uses only the time-independent mean gas temperatures.

5.6 Time-Independent Axial Gas Temperature Measurements in the Combustion Chamber

As it was not possible to take transverse temperature measurements at various cross-sections in the combustion chamber, the measured time-independent axial gas temperatures are shown plotted on the graphs of gas temperature gradients. Vertical transverse temperature measurements were possible at X = 0.229 m a typical distribution is shown in figure (5.5). The percentage difference between axial and mean gas temperature measurements at this section of the combustion chamber are shown below for all test conditions

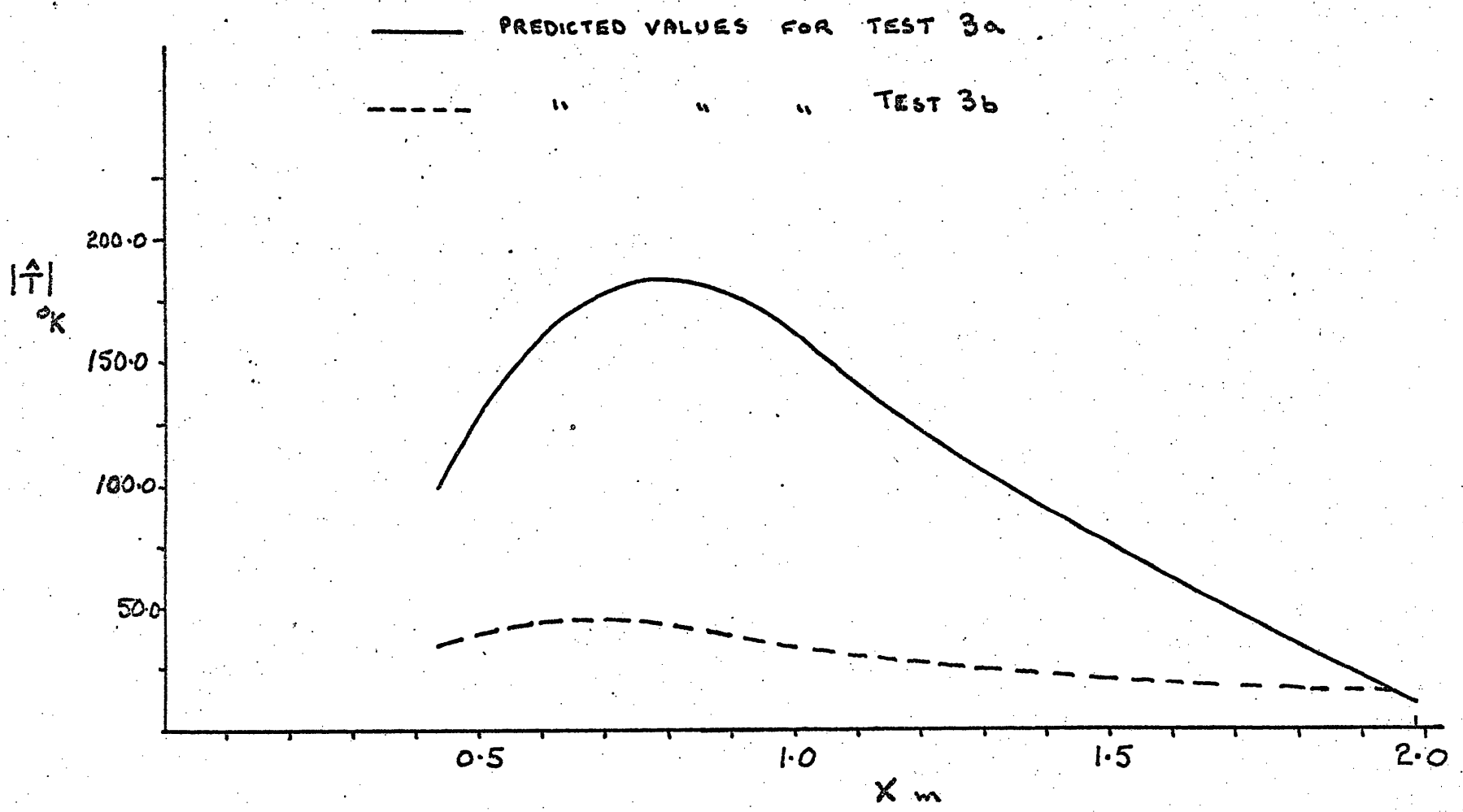

Fig.(5·4) MODULUS OF TEMPERATURE AMPLITUDE AGAINST POSITION ALONG LENGTH OF COMBUSTOR

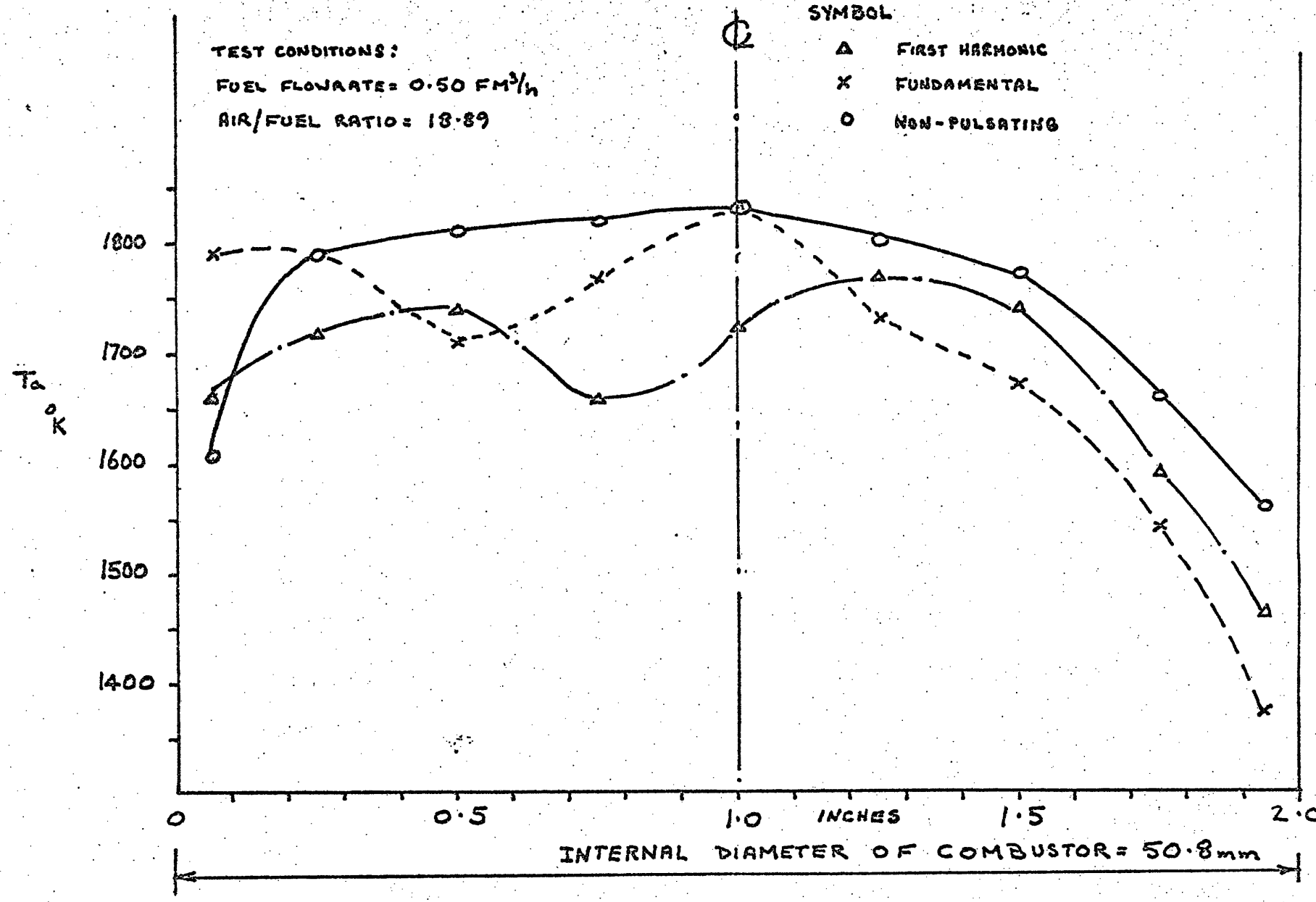

Fig.(5·5) TRANSVERSE TEMPERATURE MEASUREMENTS OF COMBUSTION CHAMBER AT X=0·229 m

Test	Percentage difference between mean and axial gas temperature at X = 0.229 m	
	Non pulsating	Pulsating
1	2.5	2.0
2	3.0	3.0
3a	3.0	7.0
3b	3.0	3.0
4	6.0	2.0
5	6.0	4.0

In making a comparison of predicted and measured time - independent gas temperatures in the combustion chamber, the percentage difference was based on the difference of the maximum temperatures rather than on gas temperatures at corresponding positions. A maximum difference of 22% occurred in test 3a figure (5·24).

The predicted instantaneous gas temperatures for pulsating conditions showed large temperature oscillations. Figure (5·7) shows for the conditions of test 3a temperature variations of various particles passing through the combustion chamber (path line characteristics) for different instances in time. Figure (5·9) shows the pressure variation each path line experienced on its path through the combustion chamber, and figure (5·8) shows the consumption of propane in terms of propane mass fraction XCH for each path line. These were typical of all tests considered, the following table showing the predicted maximum temperature amplitude for each test condition.

Test	1	2	3a	3b	4	5
Maximum gas temperature amplitude ^{o}C	300	315	425	90	145	195

Also shown in figure (5·8) is the consumption of propane XCH for non pulsating conditions the comparison suggesting no marked overall increase in combustion intensity being achieved.

SYMBOLS CORRESPOND TO PRESSURE VARIATIONS OF Fig.(5·9a)

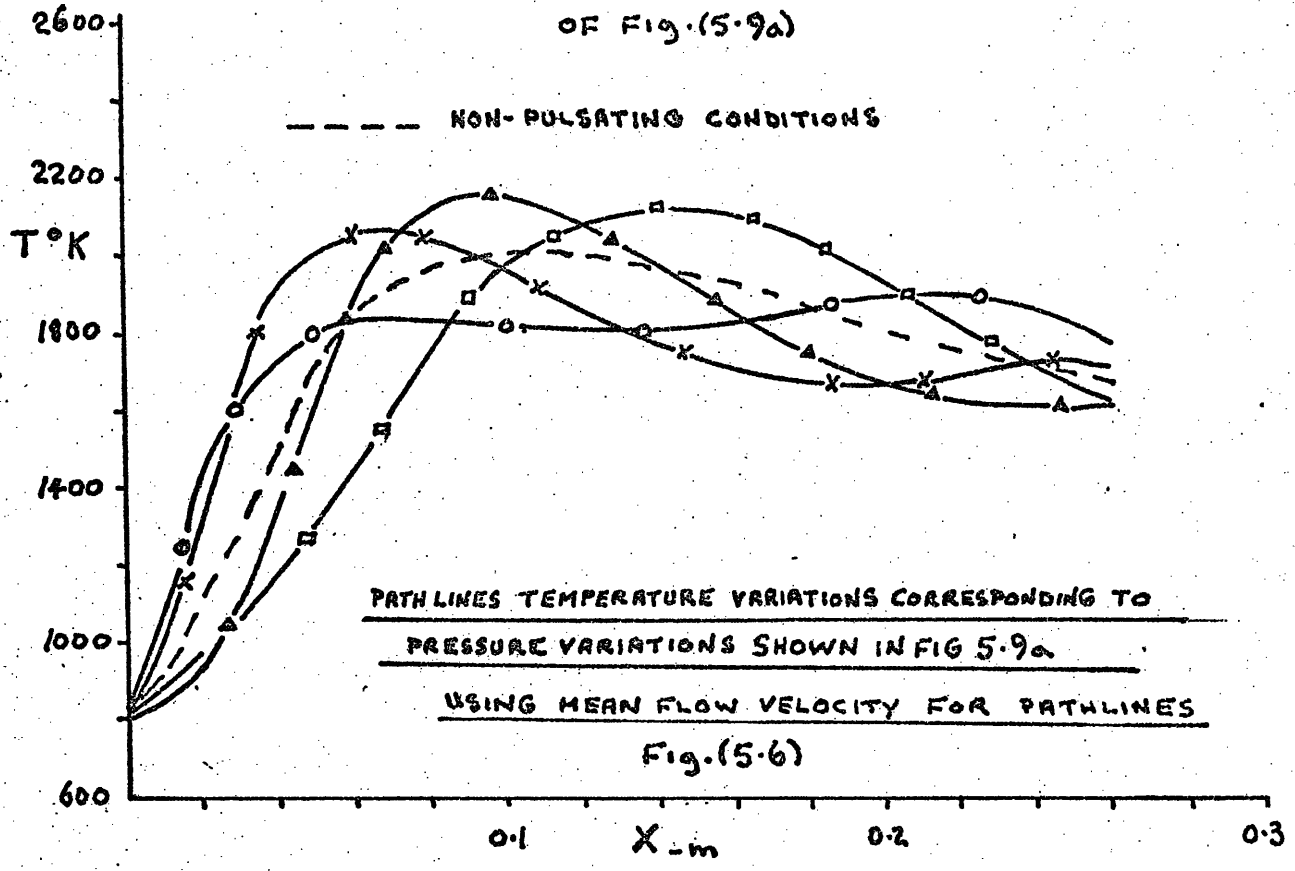

PATH LINES TEMPERATURE VARIATIONS CORRESPONDING TO PRESSURE VARIATIONS SHOWN IN FIG 5·9a USING MEAN FLOW VELOCITY FOR PATHLINES

Fig.(5·6)

SYMBOLS CORRESPOND TO PRESSURE VARIATIONS OF Fig (5·9)

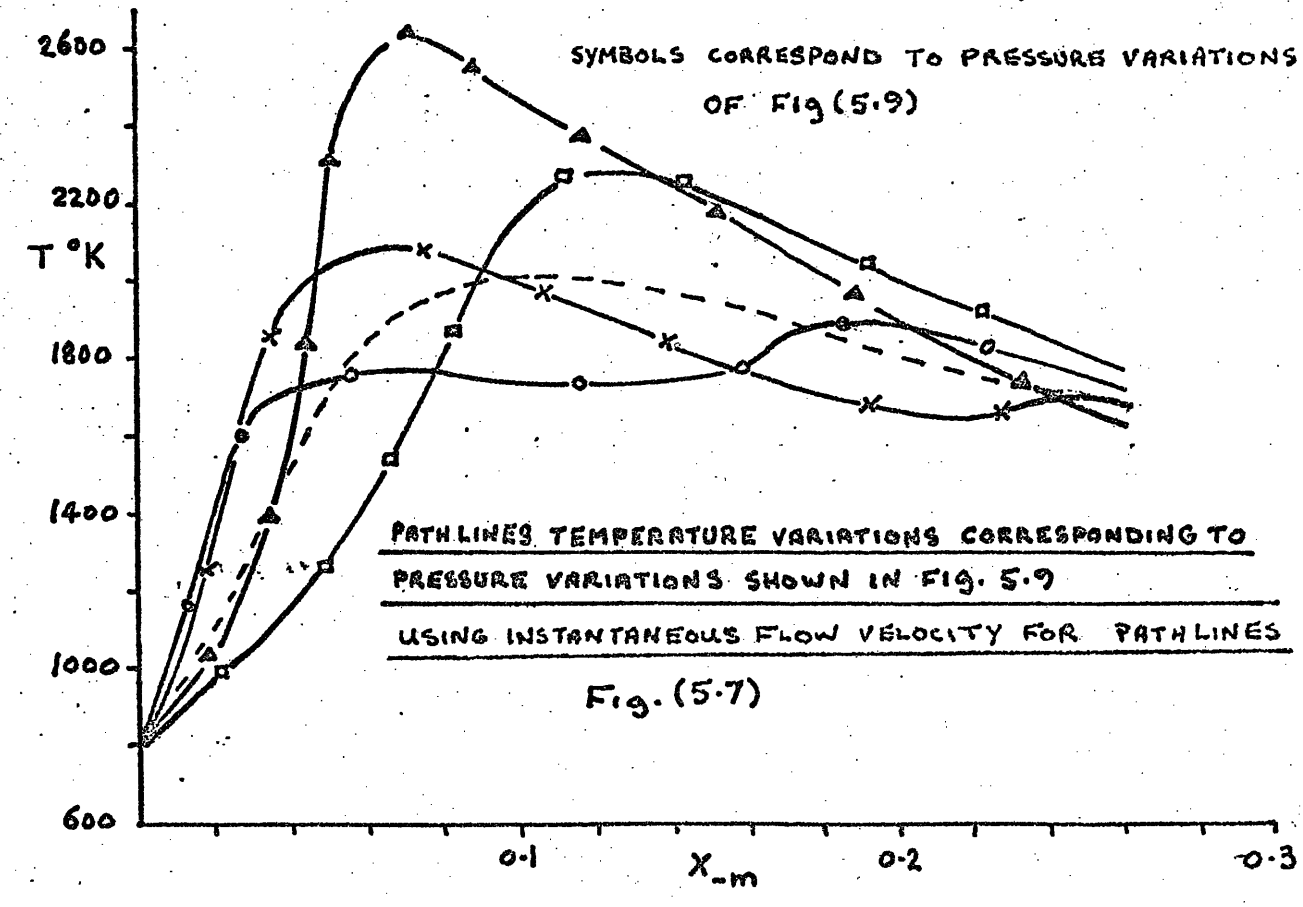

PATH LINES TEMPERATURE VARIATIONS CORRESPONDING TO PRESSURE VARIATIONS SHOWN IN Fig. 5·9 USING INSTANTANEOUS FLOW VELOCITY FOR PATH LINES

Fig. (5·7)

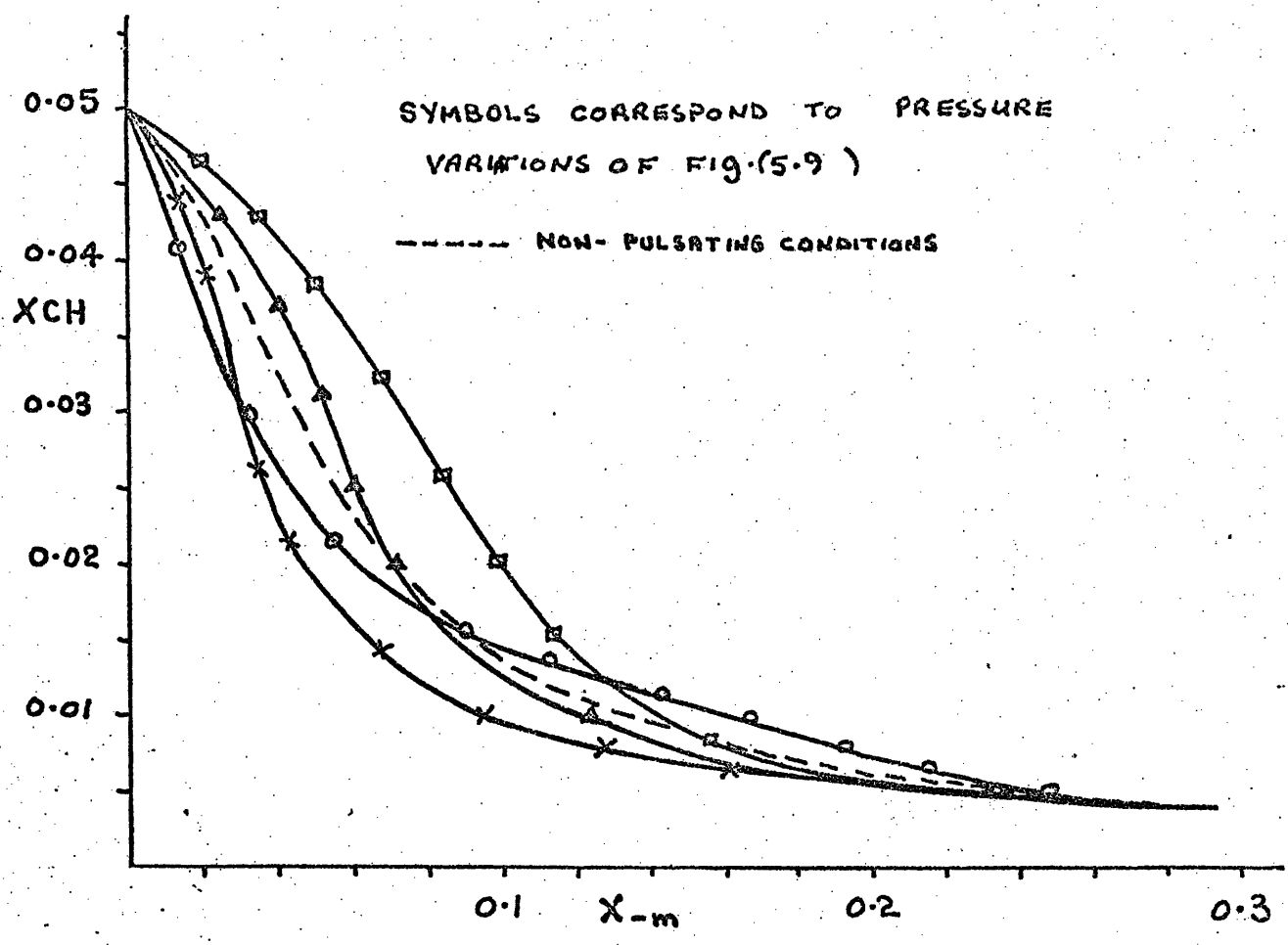

Fig·(5·8) PATH LINES VARIATIONS OF XCH FOR VARYING FLOW CONDITIONS

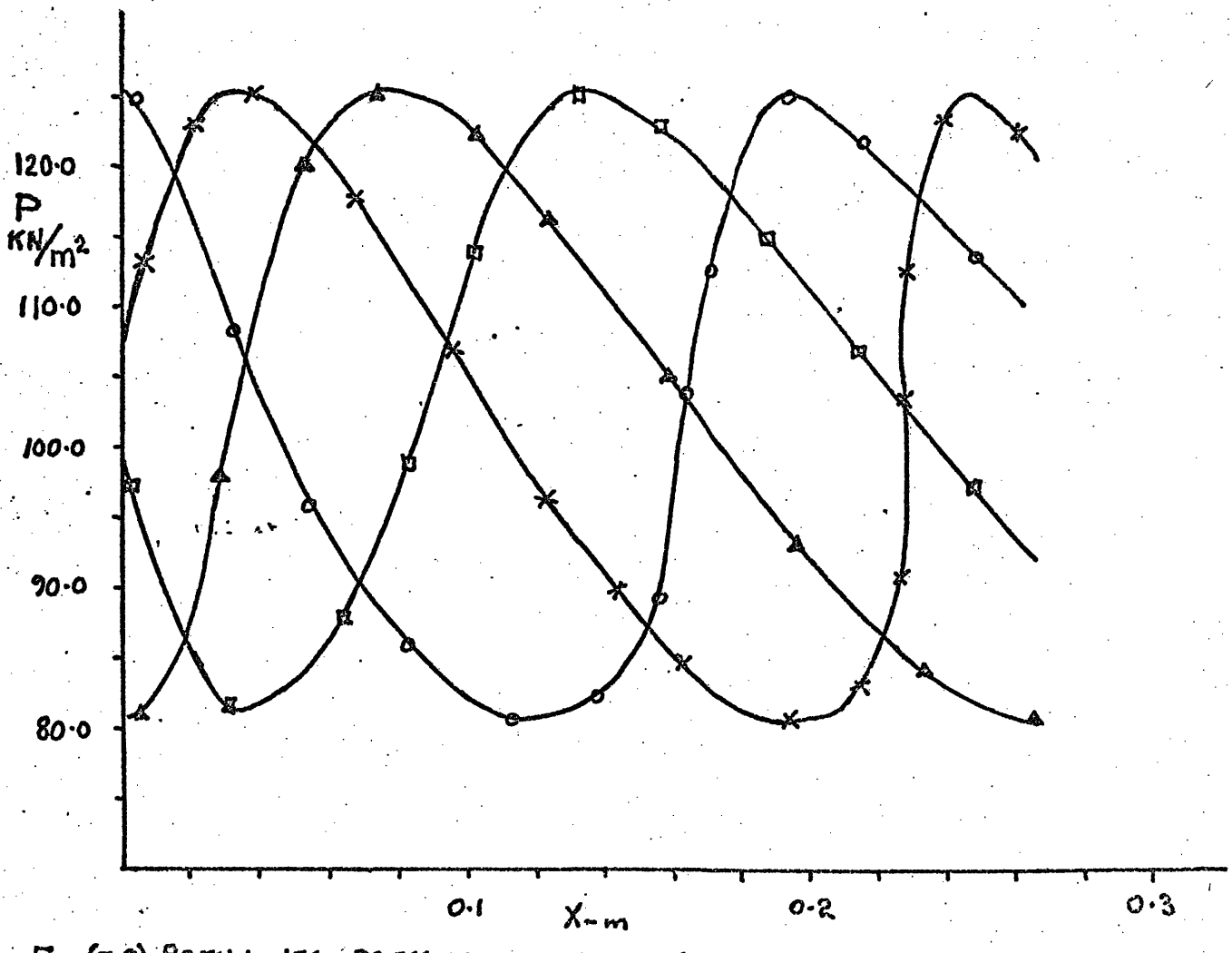

Fig(5·9) PATH LINES PRESSURE VARIATIONS FOR DIFFERENT INSTANCES IN TIME

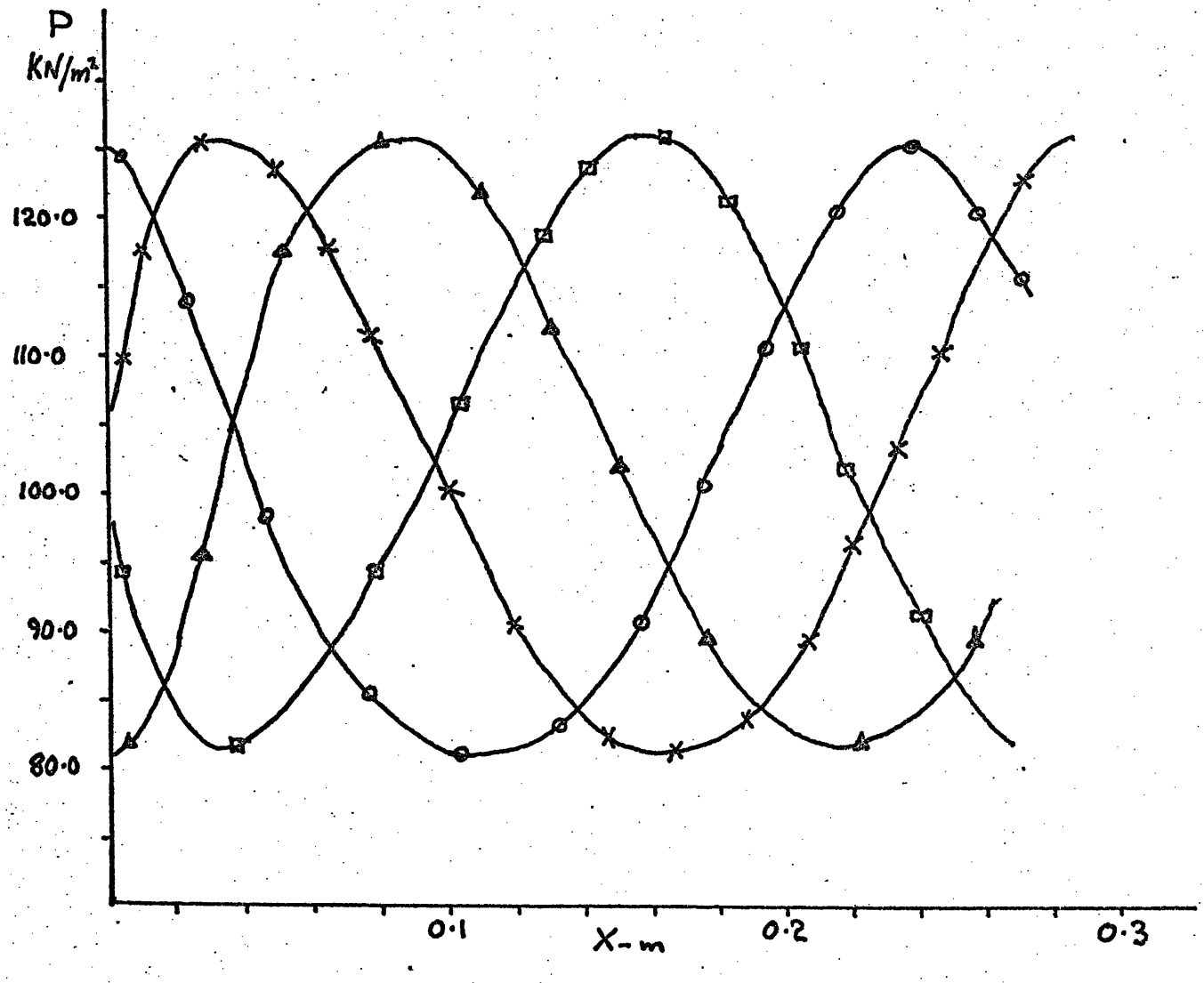

PATH LINES PRESSURE VARIATIONS FOR DIFFERENT INSTANCES IN TIME USING MEAN VELOCITY FOR PATH LINES

Fig 5.9a

The measurement of temperature oscillations of the kind quoted above require very elaborate techniques, measurements of this nature were not attempted in this investigation. However, Brown (39) has reported temperature oscillations associated with the pressure oscillations in a pulsating combustor which are of interest. At a time-mean gas temperature of 975°C, the instaneous maximum and minimum temperature measured were 1400°C and 470°C, the temperature peaks were 0-20° out of phase with the pressure.

TEST 1

Fuel Flowrate 0.30 Fm^3/h

Air/Fuel Ratio 15.75:1

Fundamental Mode of Oscillation

Fig.5·10 MEASURED TIME-INDEPENDENT MEAN GAS TEMPERATURE GRADIENT

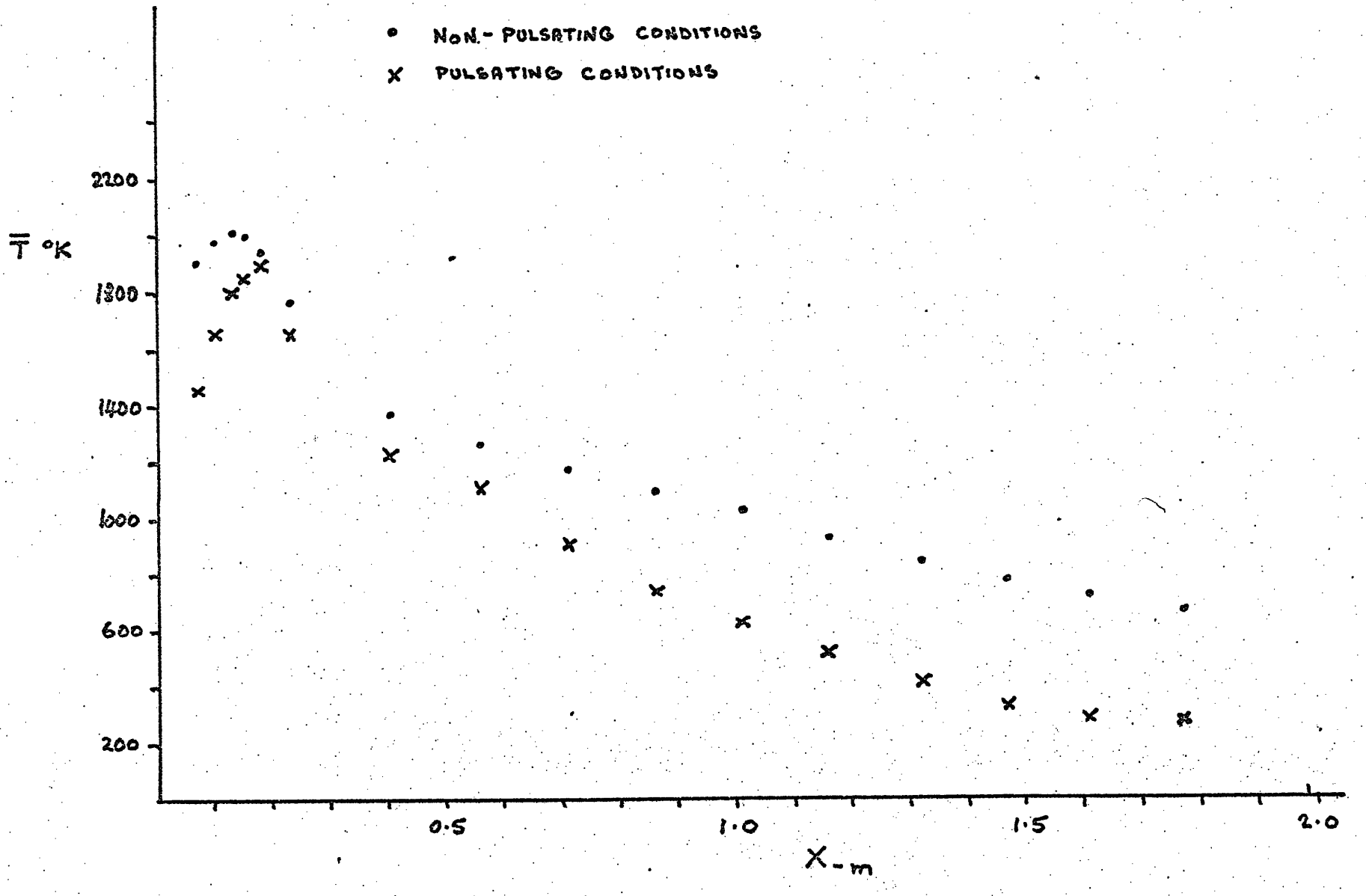

Fig·5·11 MODULUS OF PRESSURE AMPLITUDE AGAINST DISTANCE ALONG COMBUSTOR

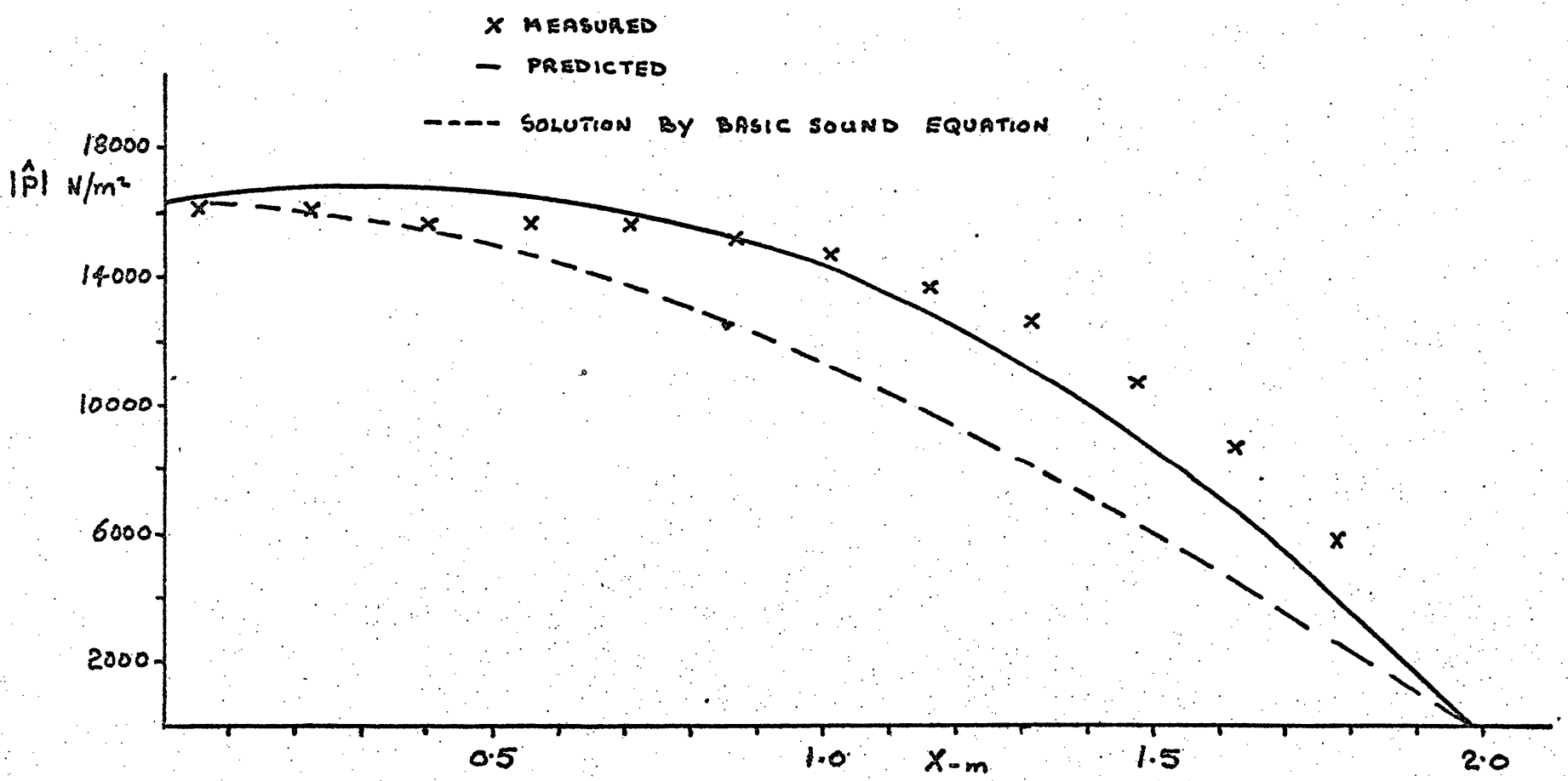

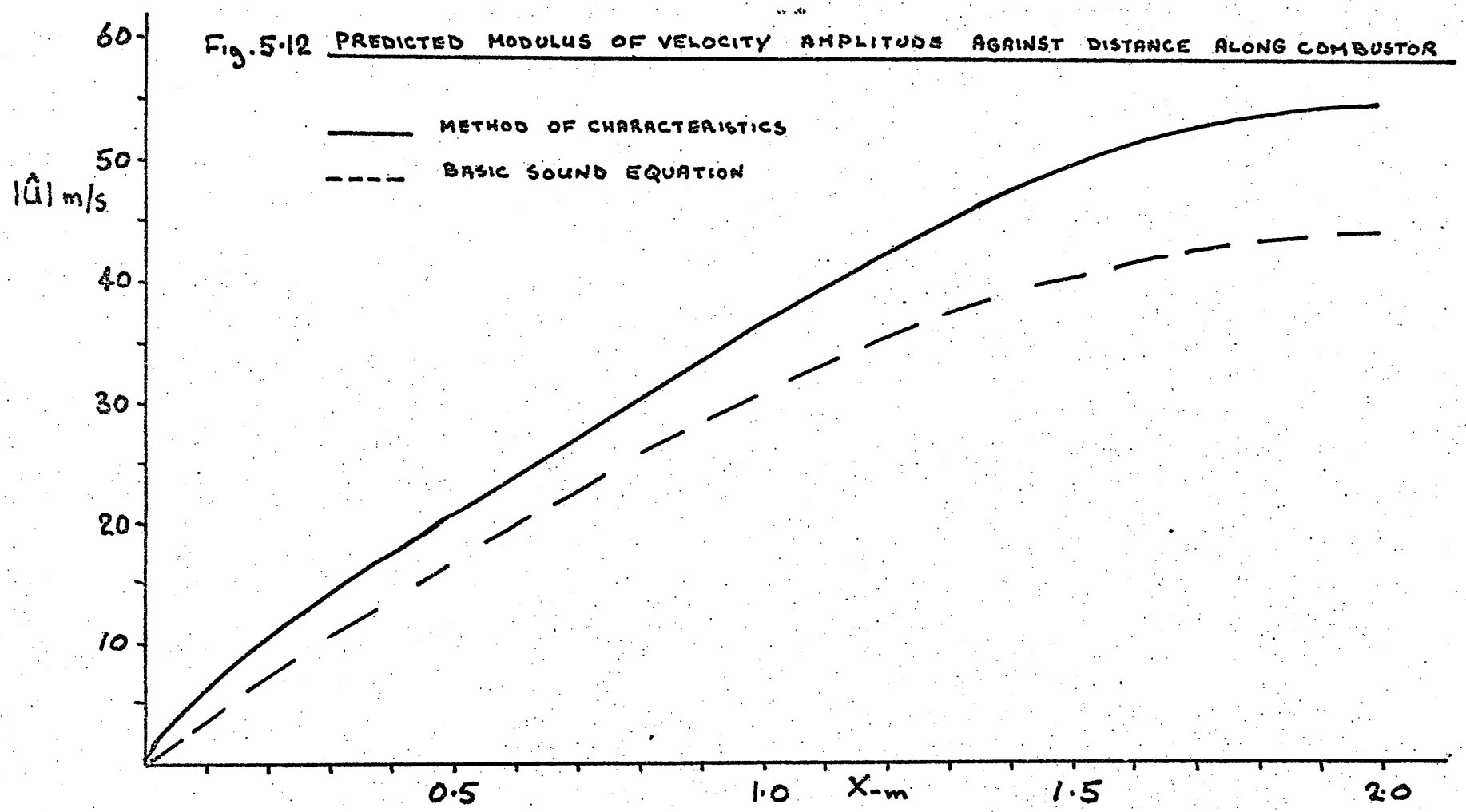

Fig. 5·12 PREDICTED MODULUS OF VELOCITY AMPLITUDE AGAINST DISTANCE ALONG COMBUSTOR

Fig. 5·13 COMPARISON OF MEASURED AND PREDICTED TEMPERATURE GRADIENT FOR NON-PULSATING CONDITIONS

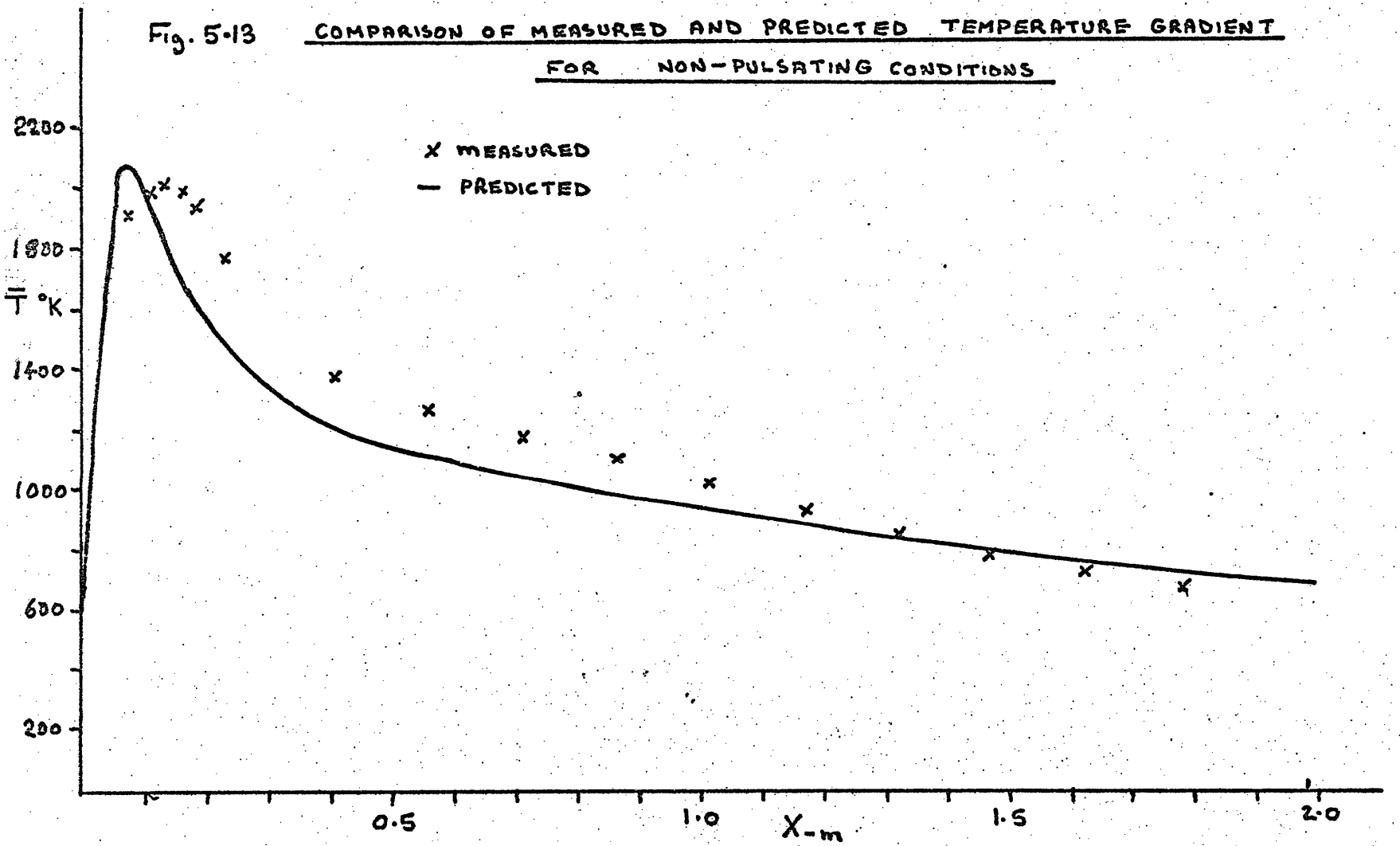

Fig. 5·14 COMPARISON OF MEASURED AND PREDICTED TEMPERATURE GRADIENT FOR PULSATING CONDITIONS

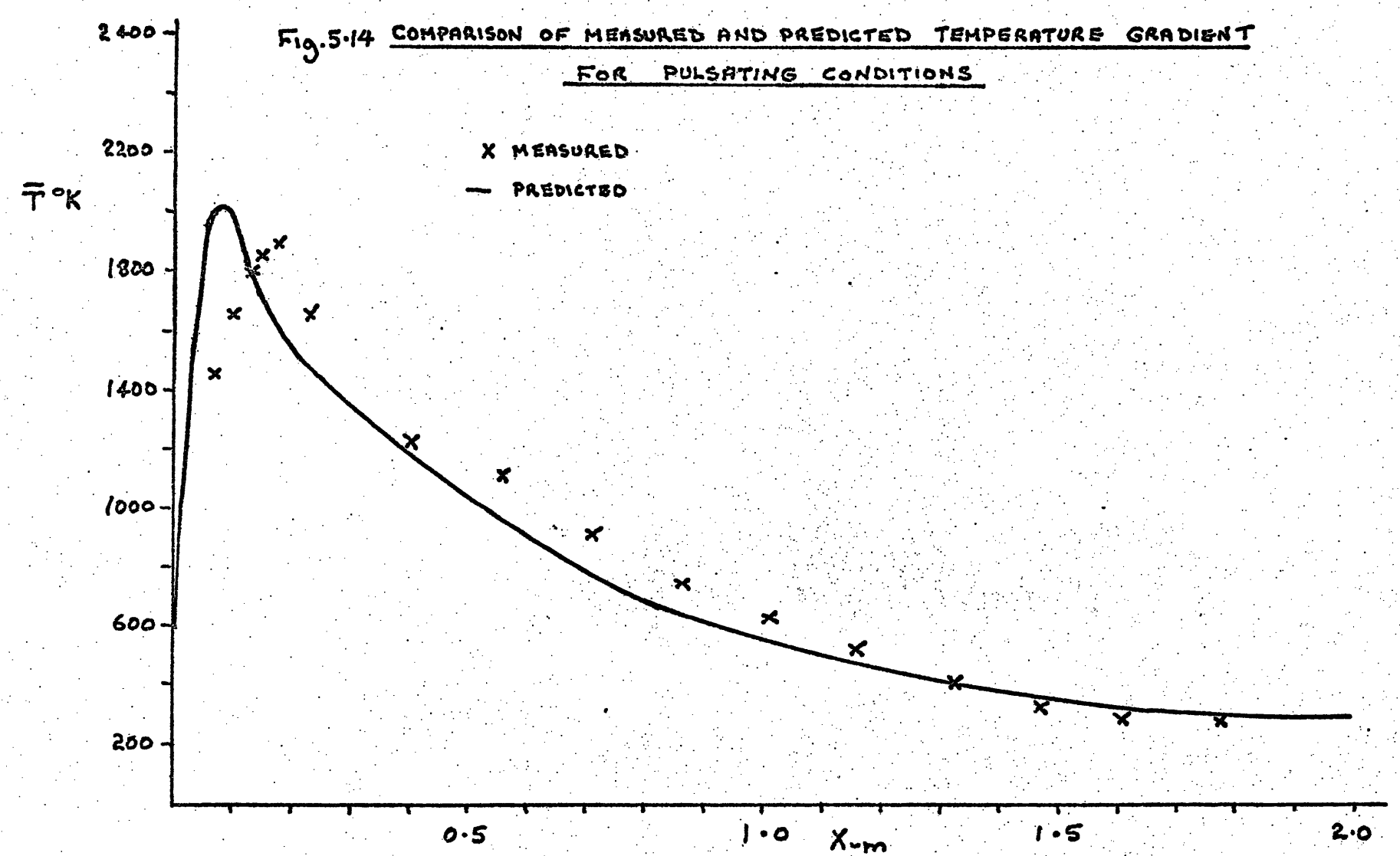

TEST 2

Fuel Flowrate 0.30 Fm^3/h

Air/Fuel Ratio 18.89:1

Fundamental Mode of Oscillation

Fig. 5·15 MEASURED TIME-INDEPENDENT MEAN GAS TEMPERATURE GRADIENT

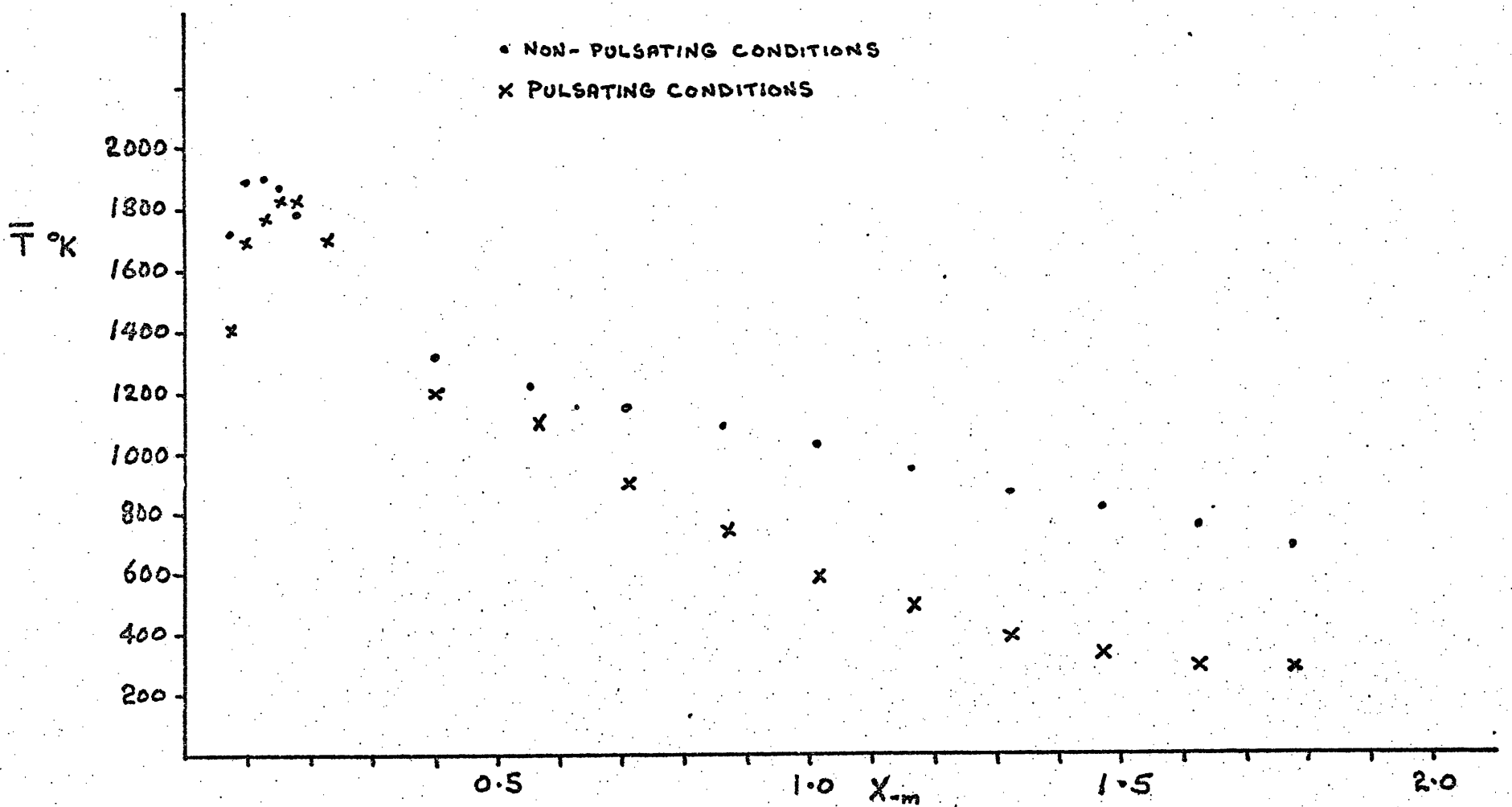

Fig. 5·16 MODULUS OF PRESSURE AMPLITUDE AGAINST DISTANCE ALONG COMBUSTOR

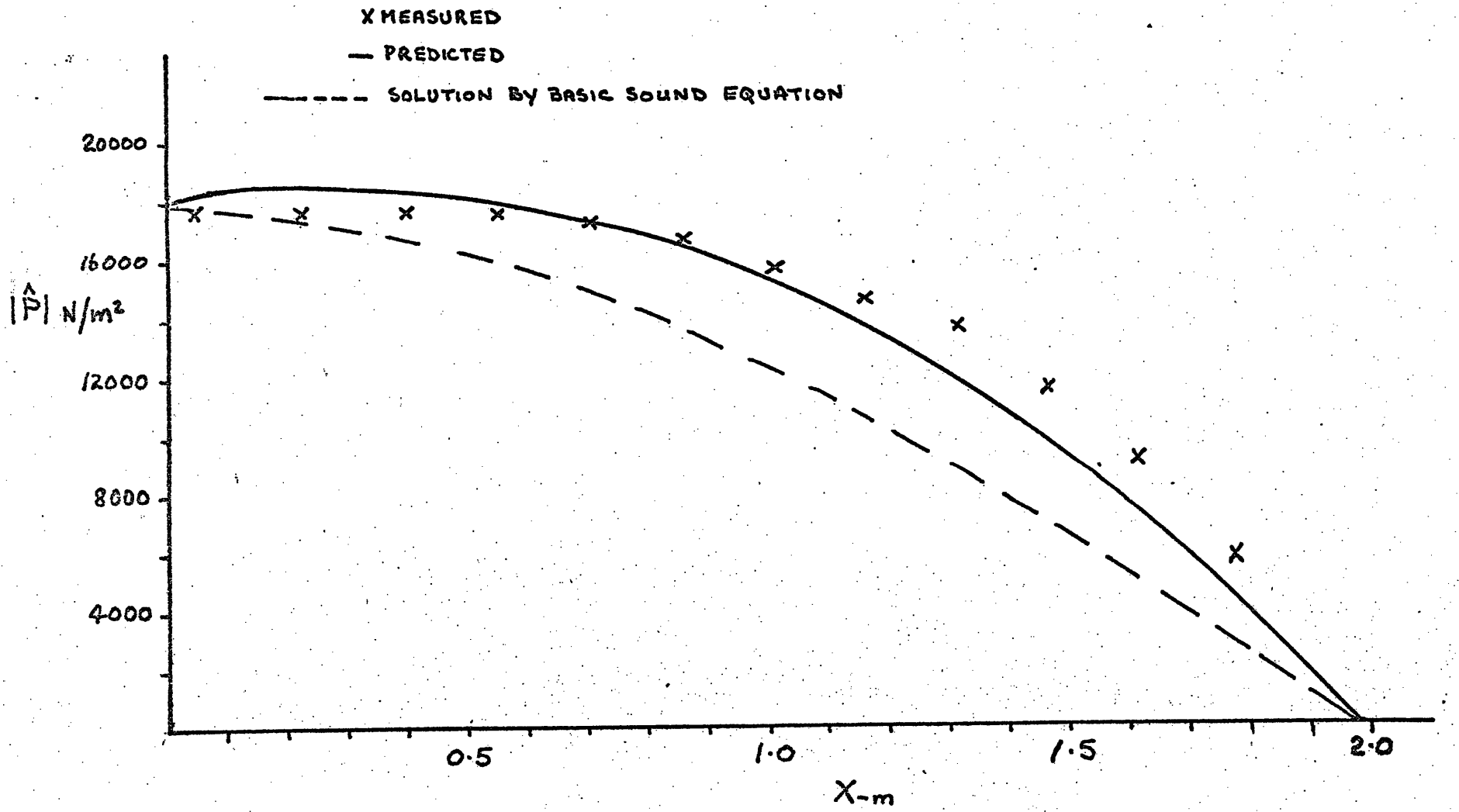

Fig. 5·17 PREDICTED MODULUS OF VELOCITY AMPLITUDE AGAINST DISTANCE ALONG COMBUSTOR

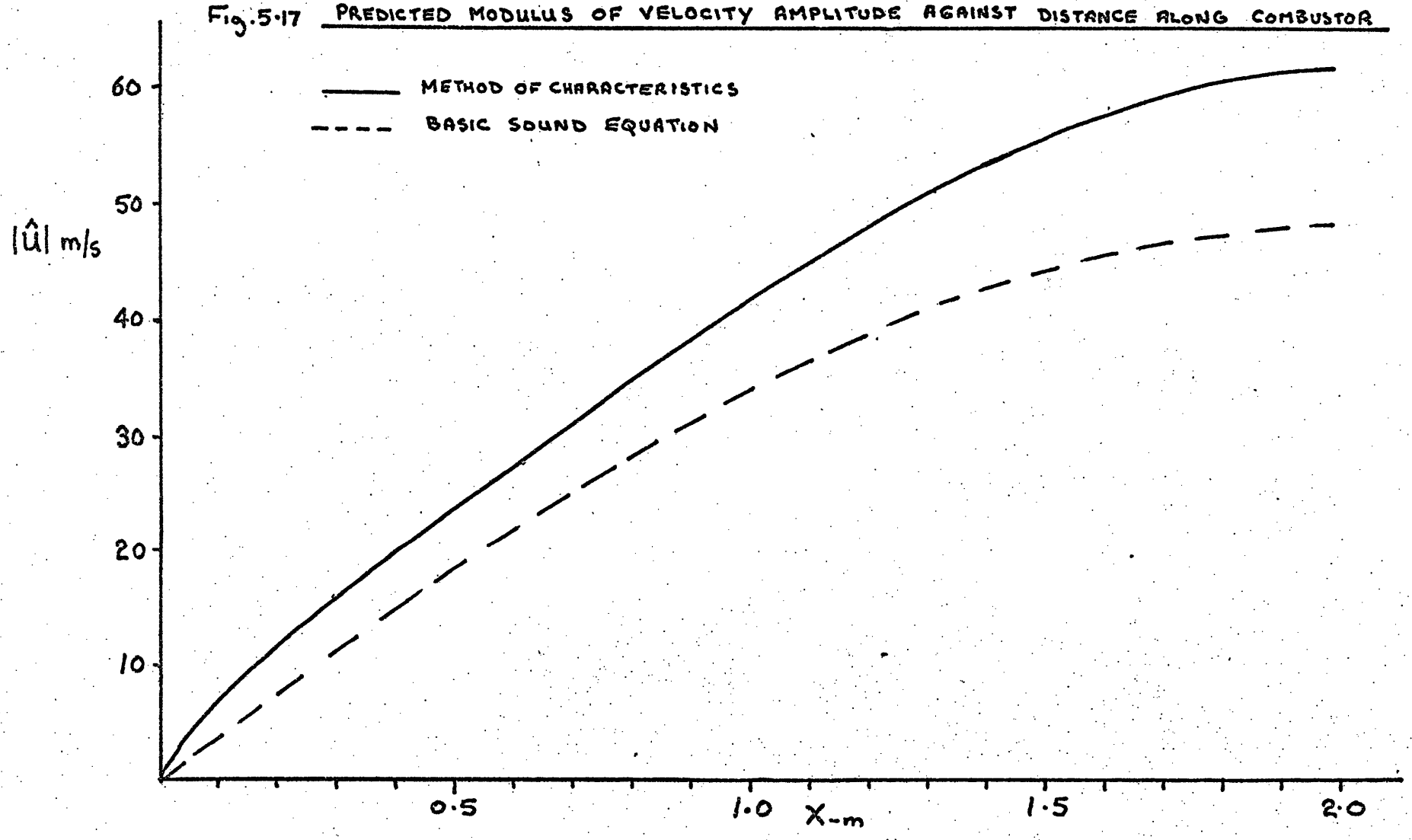

Fig 5.18 TEMPERATURE GRADIENT FOR NON-PULSATING CONDITIONS

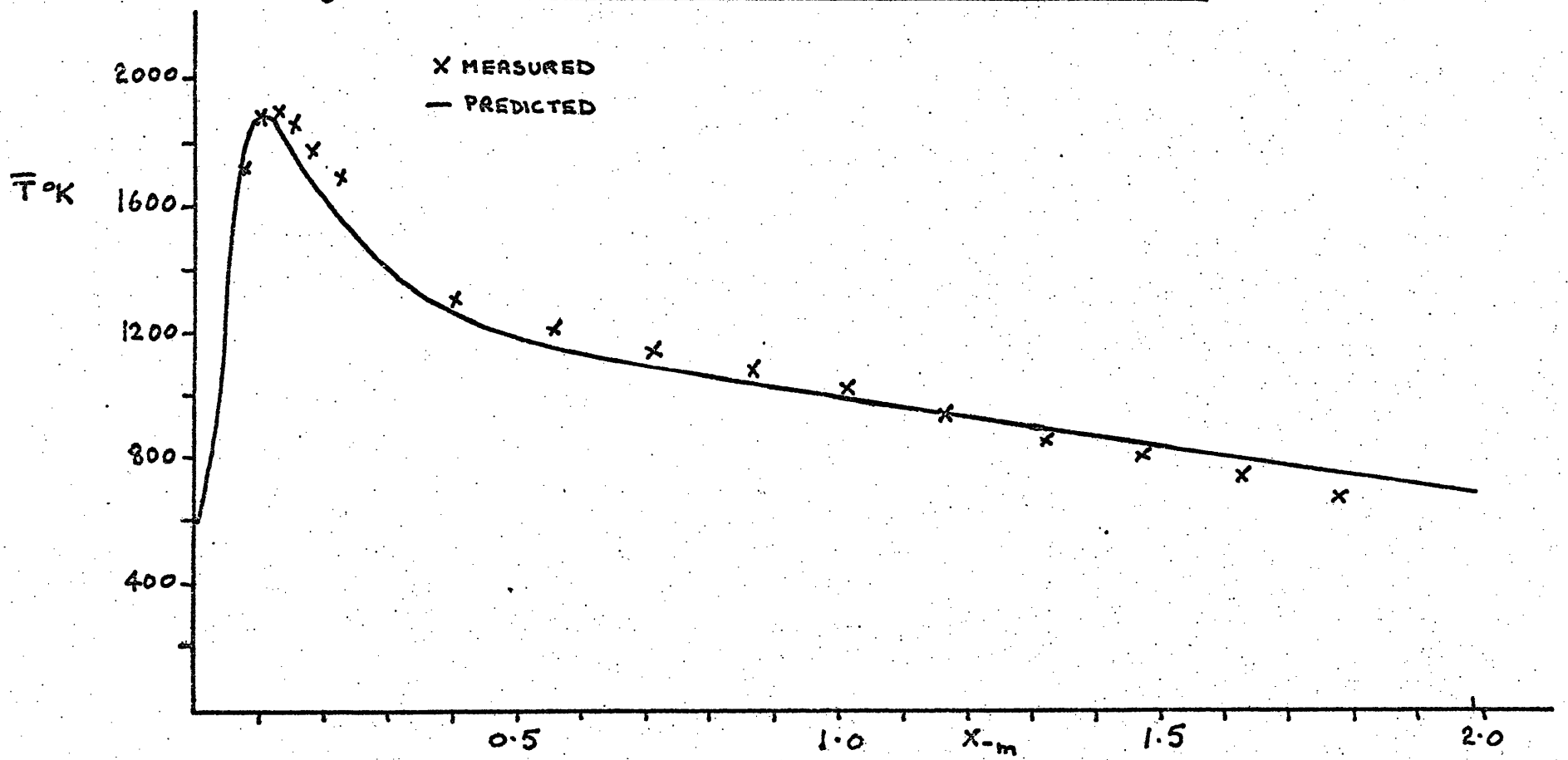

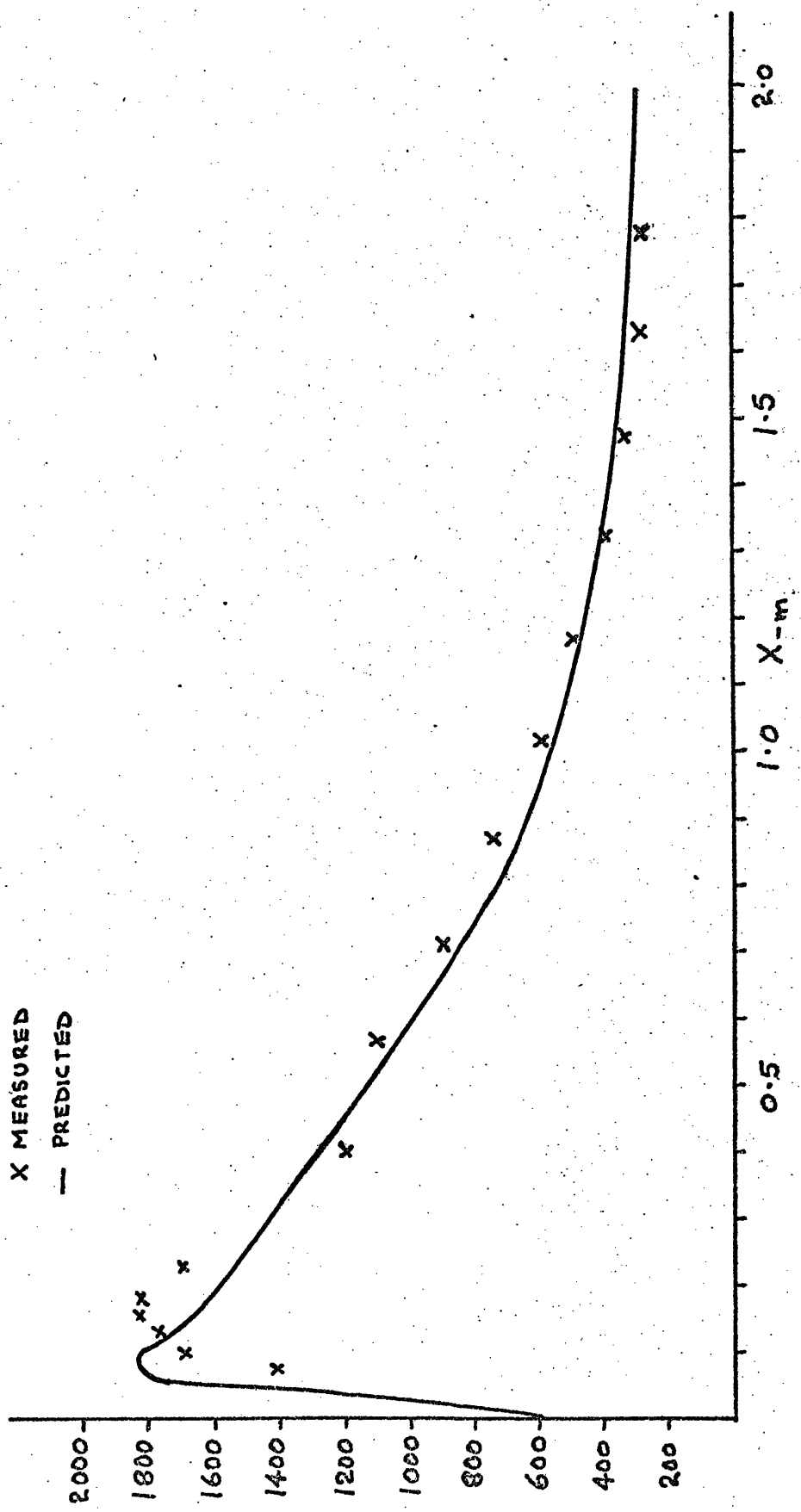

Fig. 5.19 TEMPERATURE GRADIENT FOR PULSATING CONDITIONS

TEST 3

Fuel Flowrate 0.50 Fm^3/h

Air/Fuel Ratio 18.89:1

Test 3a Fundamental Mode of Oscillation

Test 3b First Harmonic

Fig. 5.20 MEASURED TIME-INDEPENDENT MEAN GAS TEMPERATURE GRADIENT

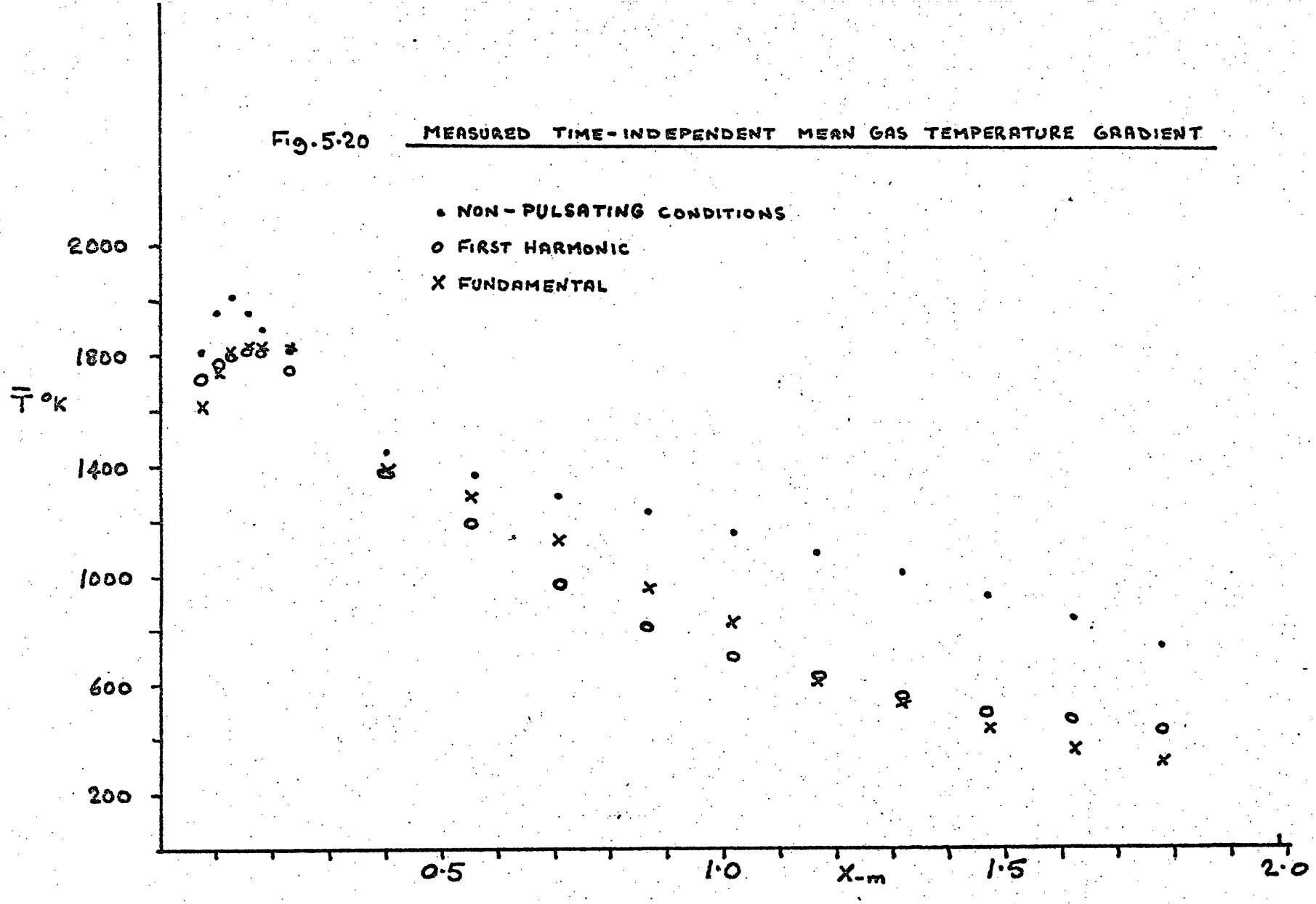

Fig. 5·21 MODULUS OF PRESSURE AMPLITUDE AGAINST DISTANCE ALONG COMBUSTOR

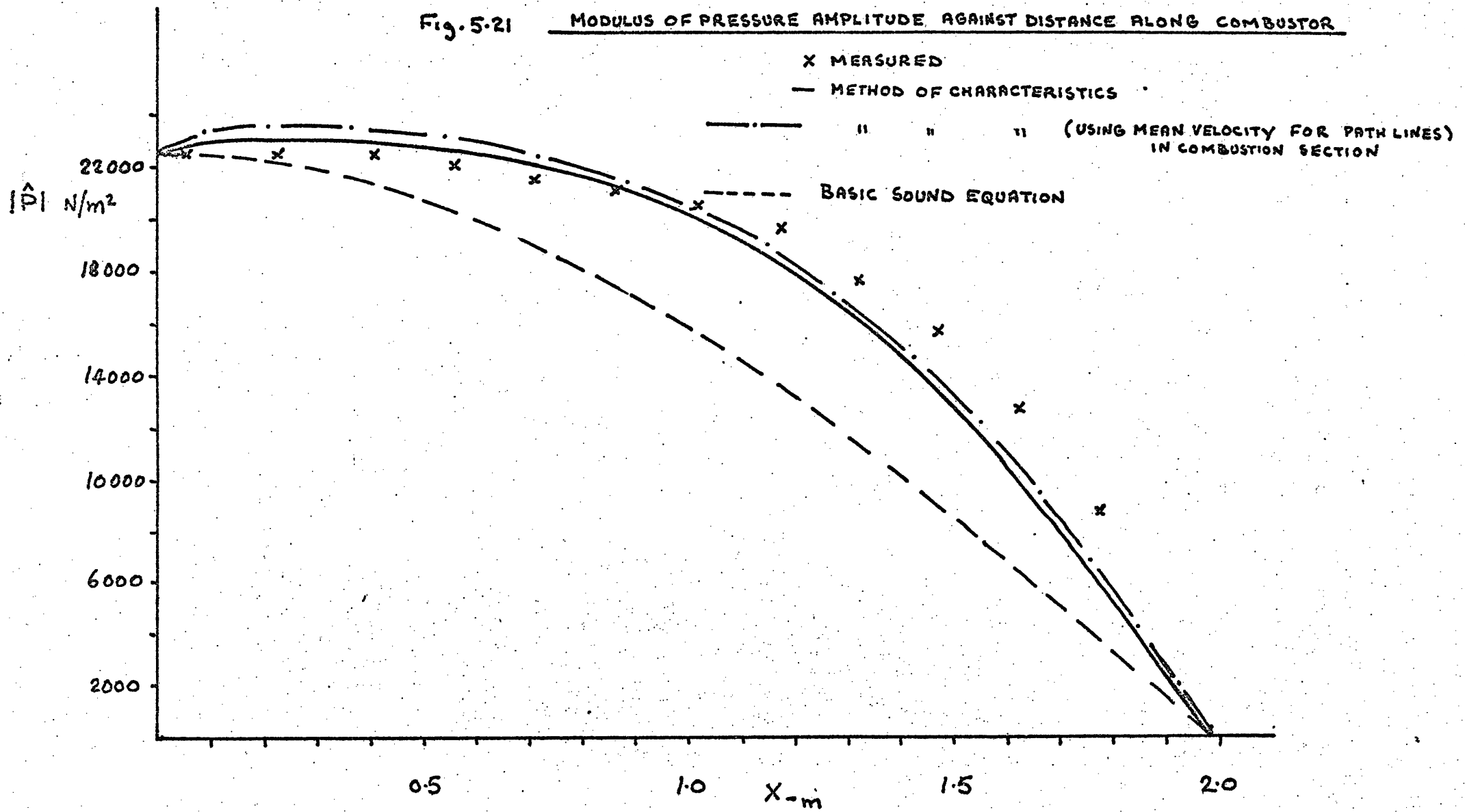

Fig. 5·22 PREDICTED MODULUS OF VELOCITY AMPLITUDE AGAINST DISTANCE ALONG COMBUSTOR

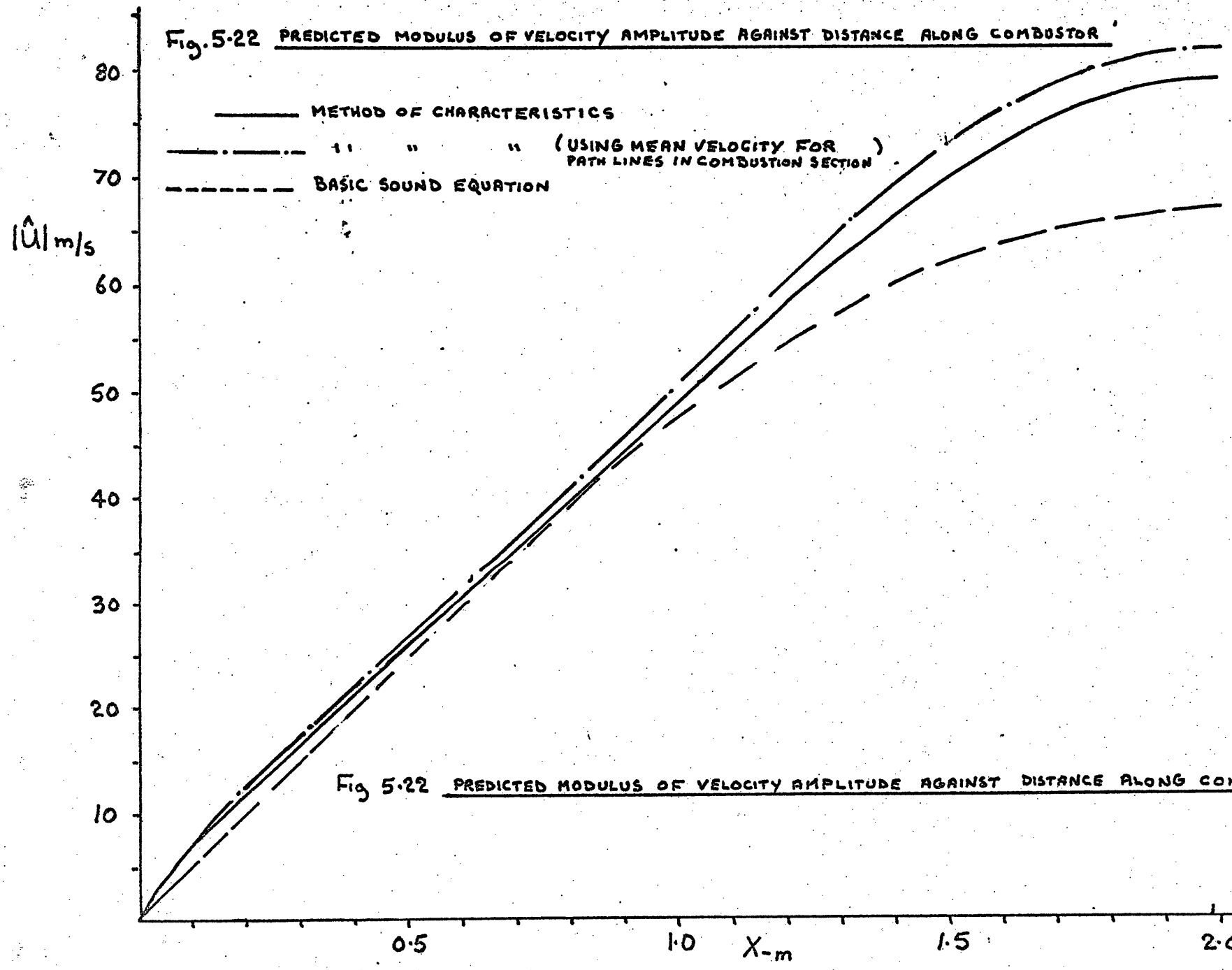

Fig 5·22 PREDICTED MODULUS OF VELOCITY AMPLITUDE AGAINST DISTANCE ALONG COMBUSTOR

Fig. 5·23 TEMPERATURE GRADIENT FOR NON-PULSATING CONDITIONS

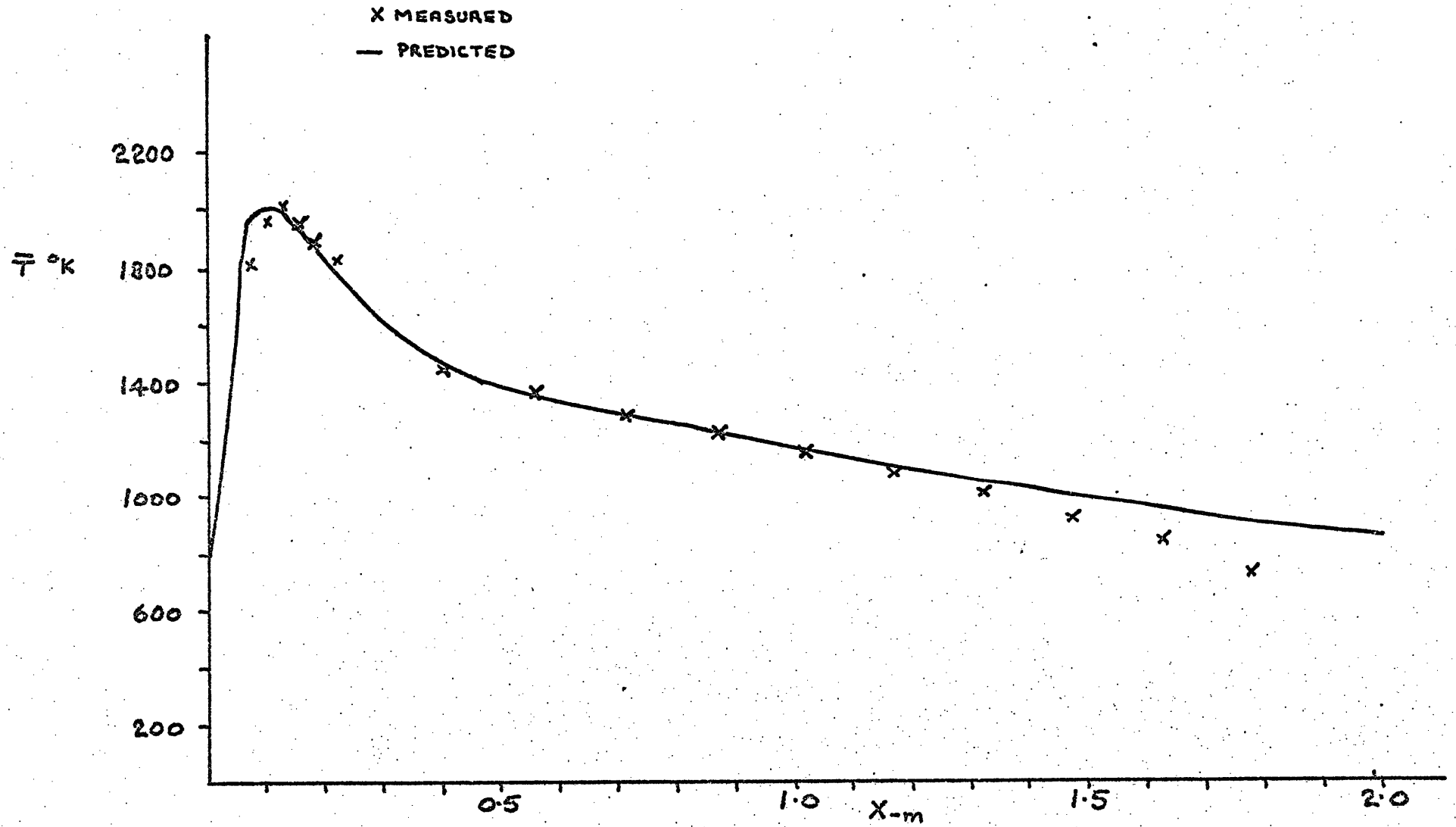

Fig. 5·24 TEMPERATURE GRADIENT FOR THE FUNDAMENTAL MODE

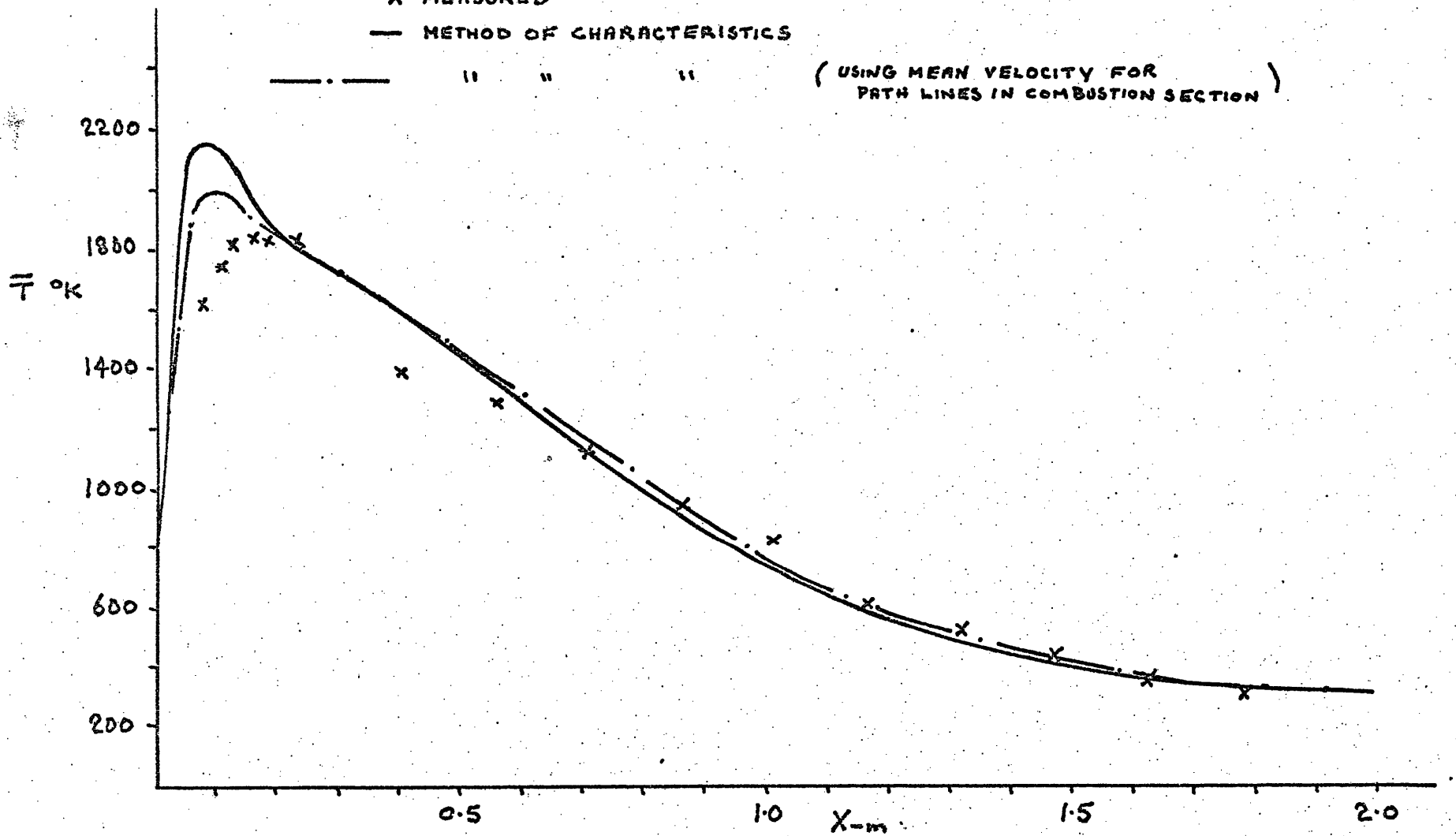

Fig.5·25 MODULUS OF PRESSURE AMPLITUDE AGAINST DISTANCE ALONG COMBUSTOR

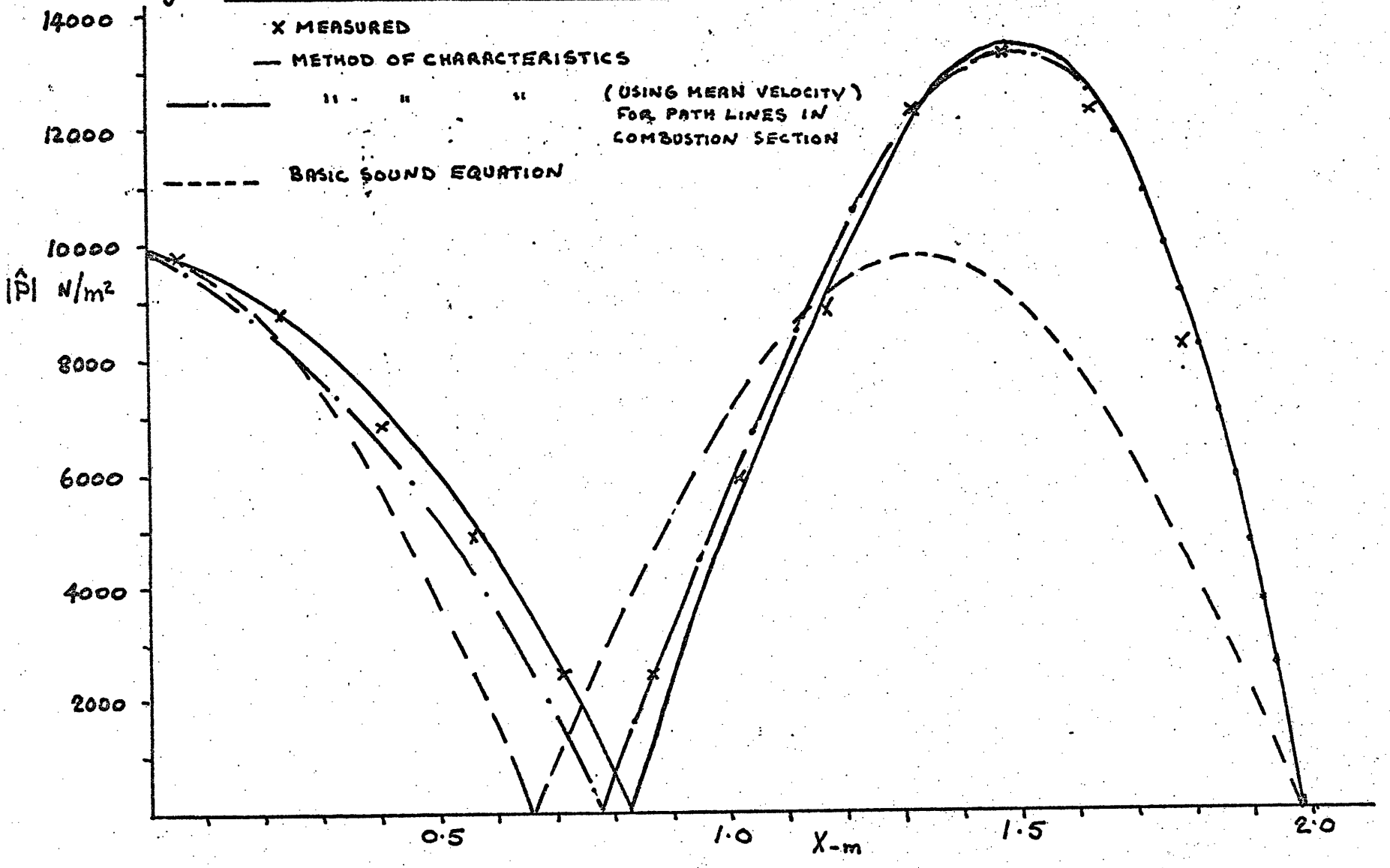

Fig 5·25 MODULUS OF PRESSURE AMPLITUDE AGAINST DISTANCE ALONG COMBUSTOR

Fig. 5·26 PREDICTED MODULUS OF VELOCITY AMPLITUDE AGAINST DISTANCE ALONG COMBUSTOR

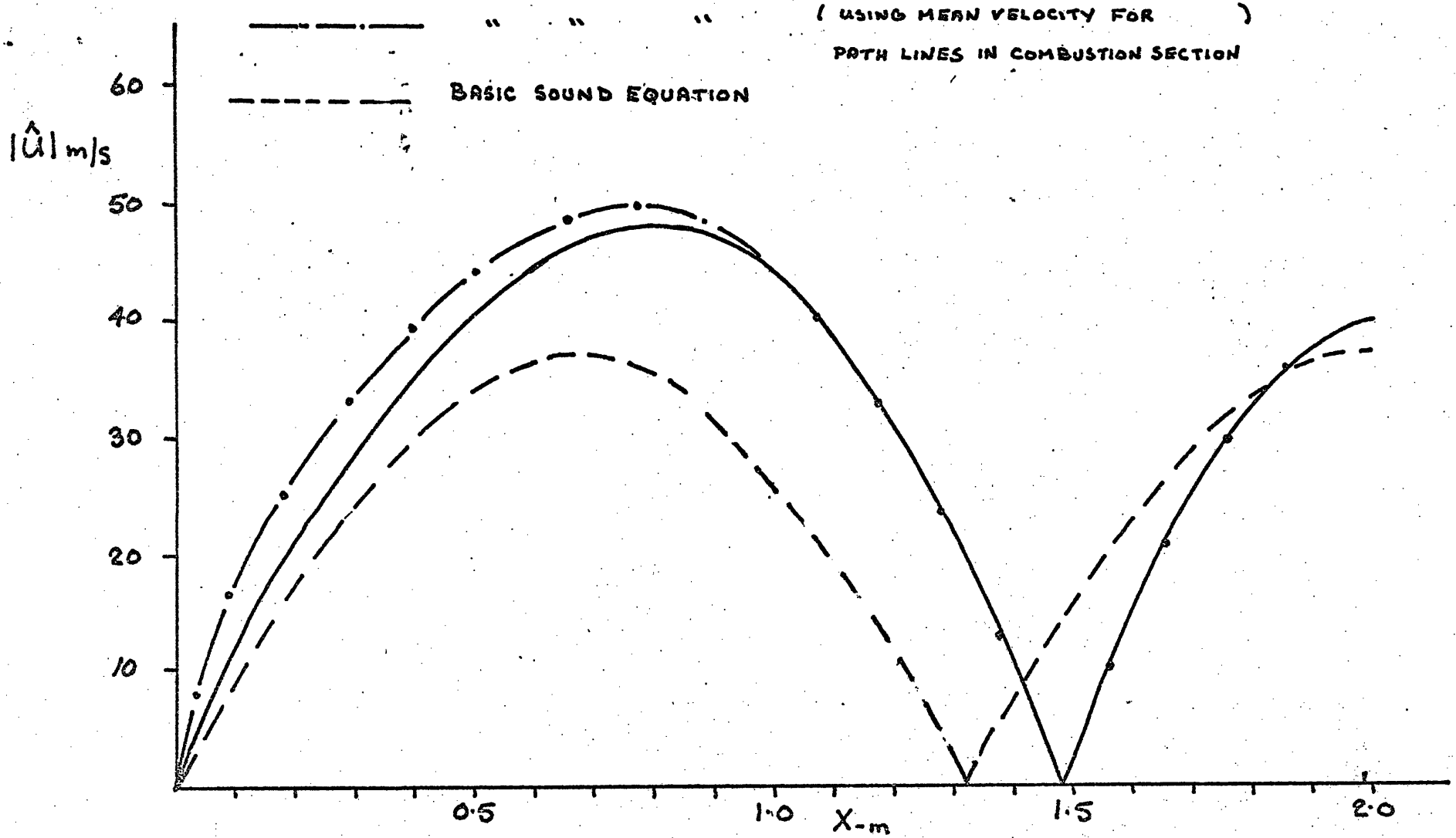

Fig 5·26 PREDICTED MODULUS OF VELOCITY AMPLITUDE AGAINST LENGTH OF COMBUSTOR

Fig. 5.27 TEMPERATURE GRADIENT FOR THE FIRST HARMONIC

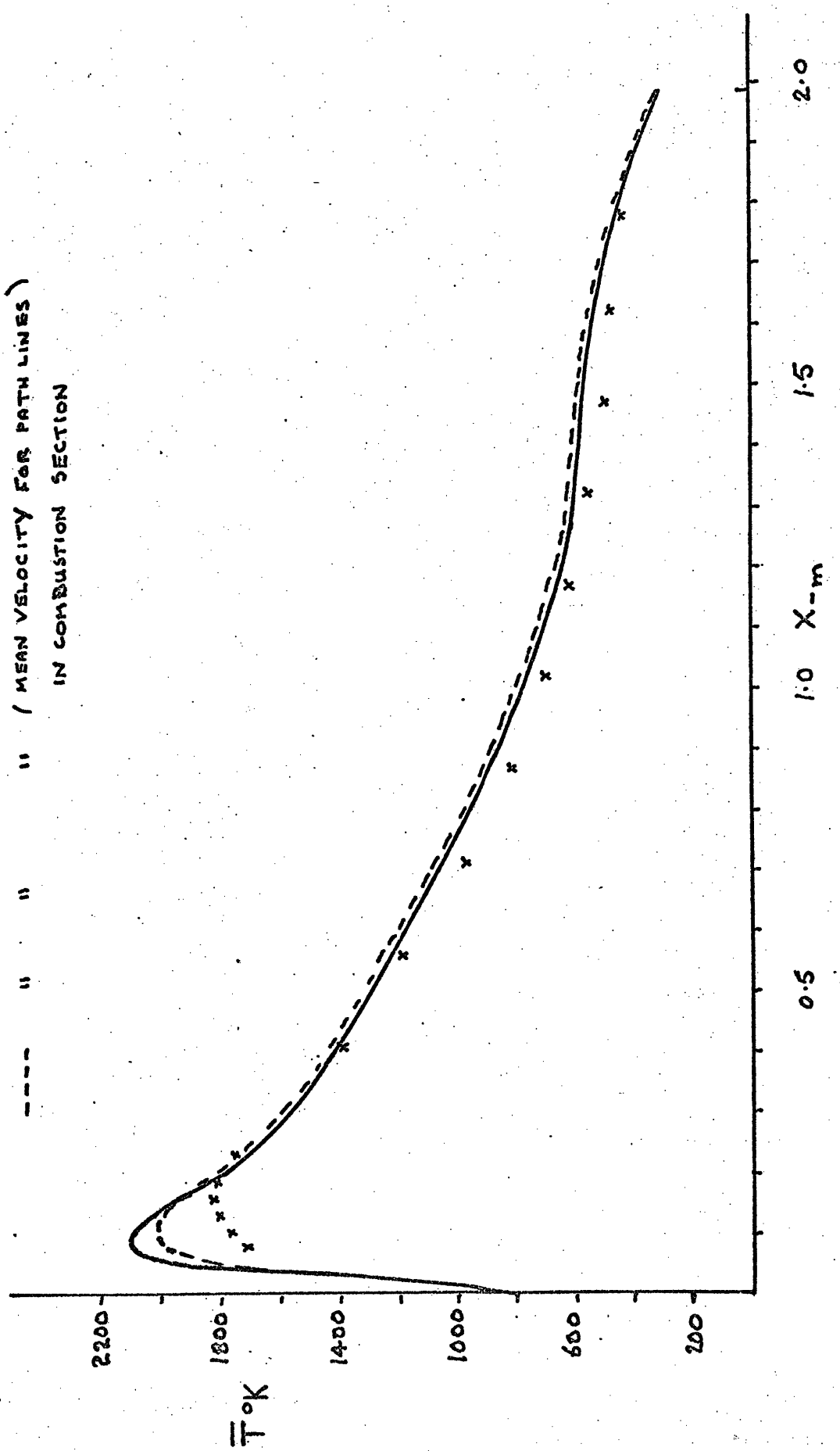

TEST 4

Fuel Flowrate 0.60 Fm^3/h

Air/Fuel Ratio 15.75:1

First Harmonic

Fig. 5.28 MEASURED TIME-INDEPENDENT MEAN GAS TEMPERATURE GRADIENT

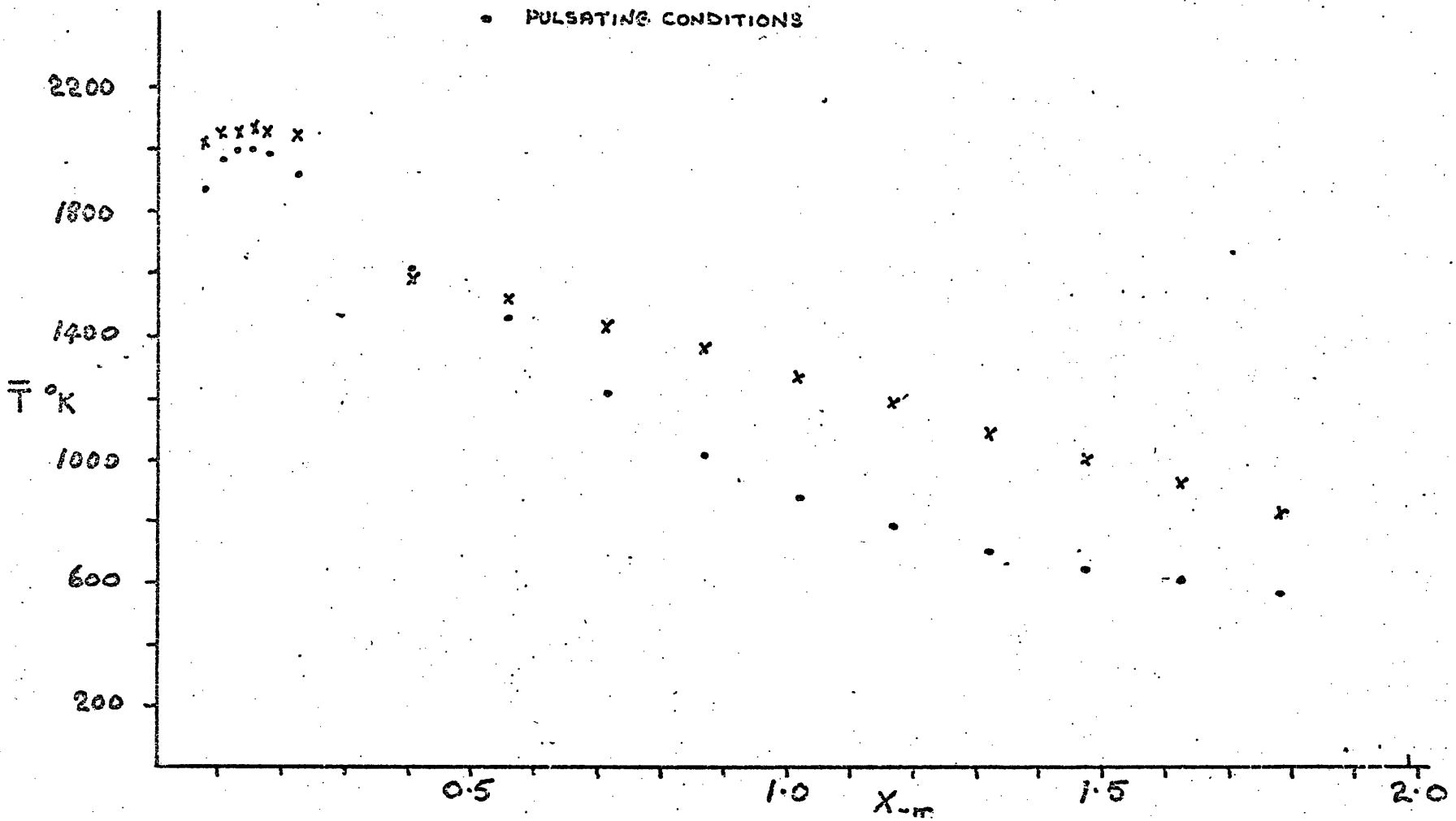

Fig. 5·29 MODULUS OF PRESSURE AMPLITUDE AGAINST DISTANCE ALONG COMBUSTOR

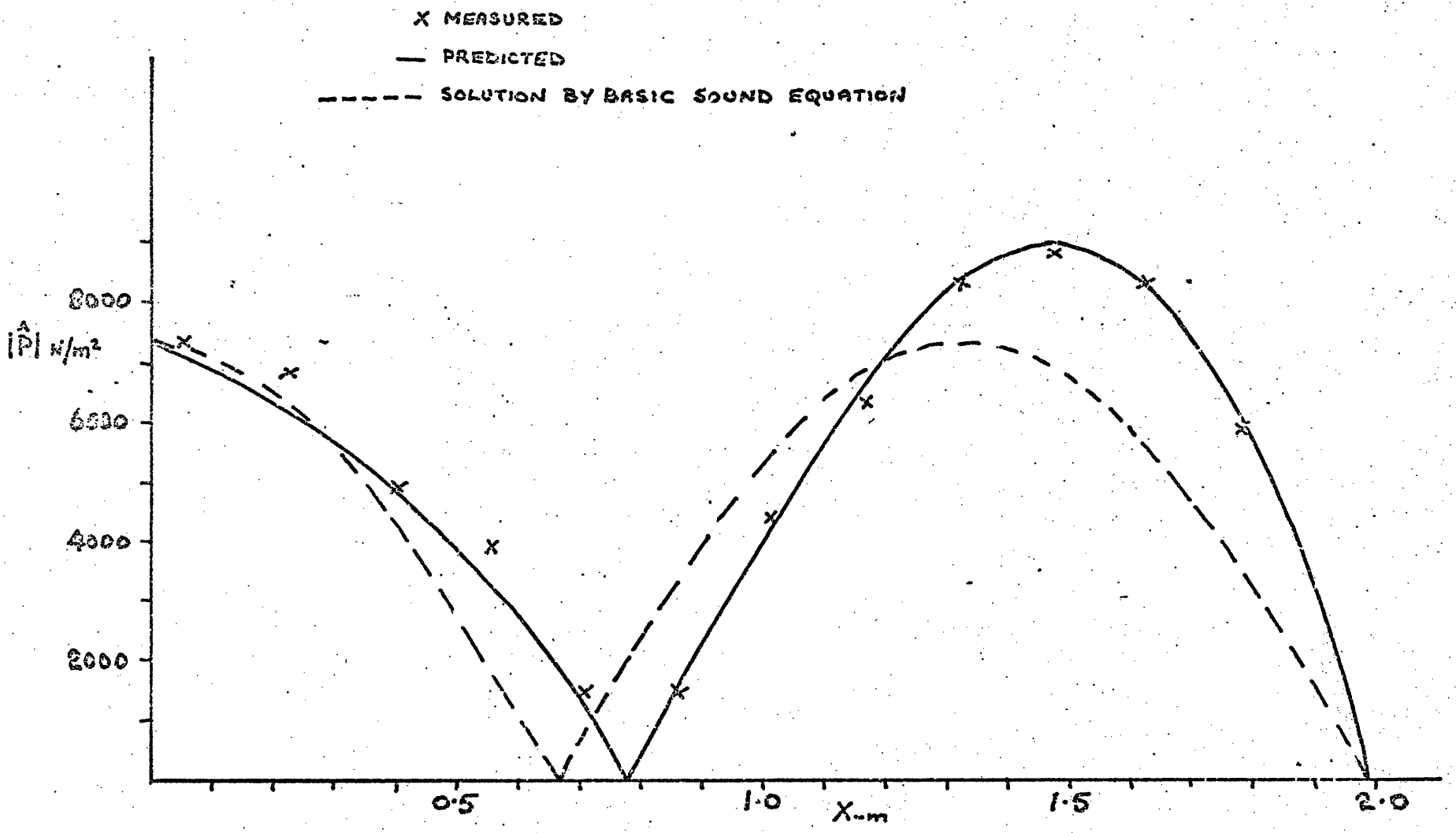

Fig·5·30 PREDICTED MODULUS OF VELOCITY AMPLITUDE AGAINST DISTANCE ALONG COMBUSTOR

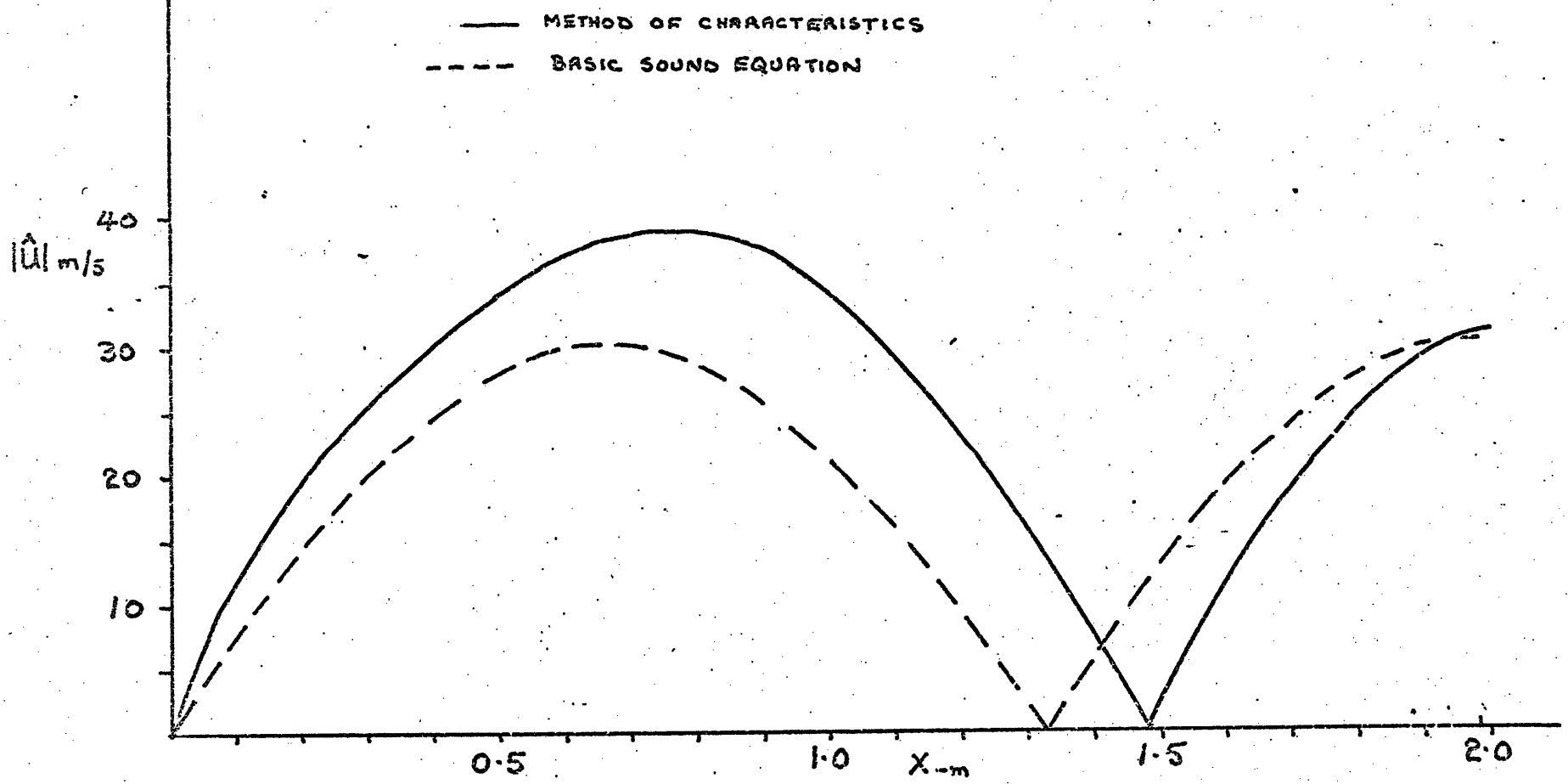

Fig. 5.31 TEMPERATURE GRADIENT FOR NON-PULSATING CONDITIONS

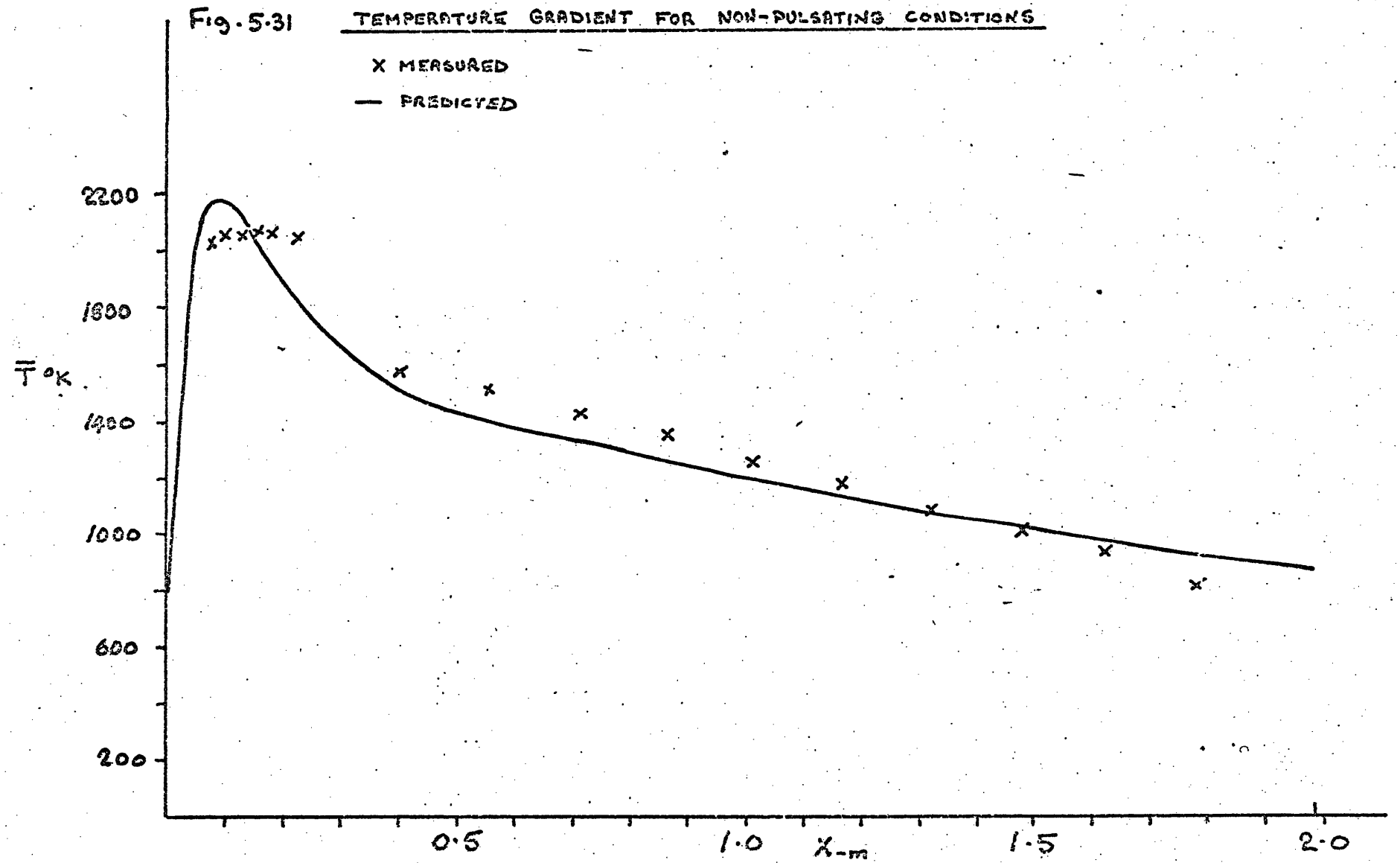

Fig. 5·32 TEMPERATURE GRADIENT FOR PULSATING CONDITIONS

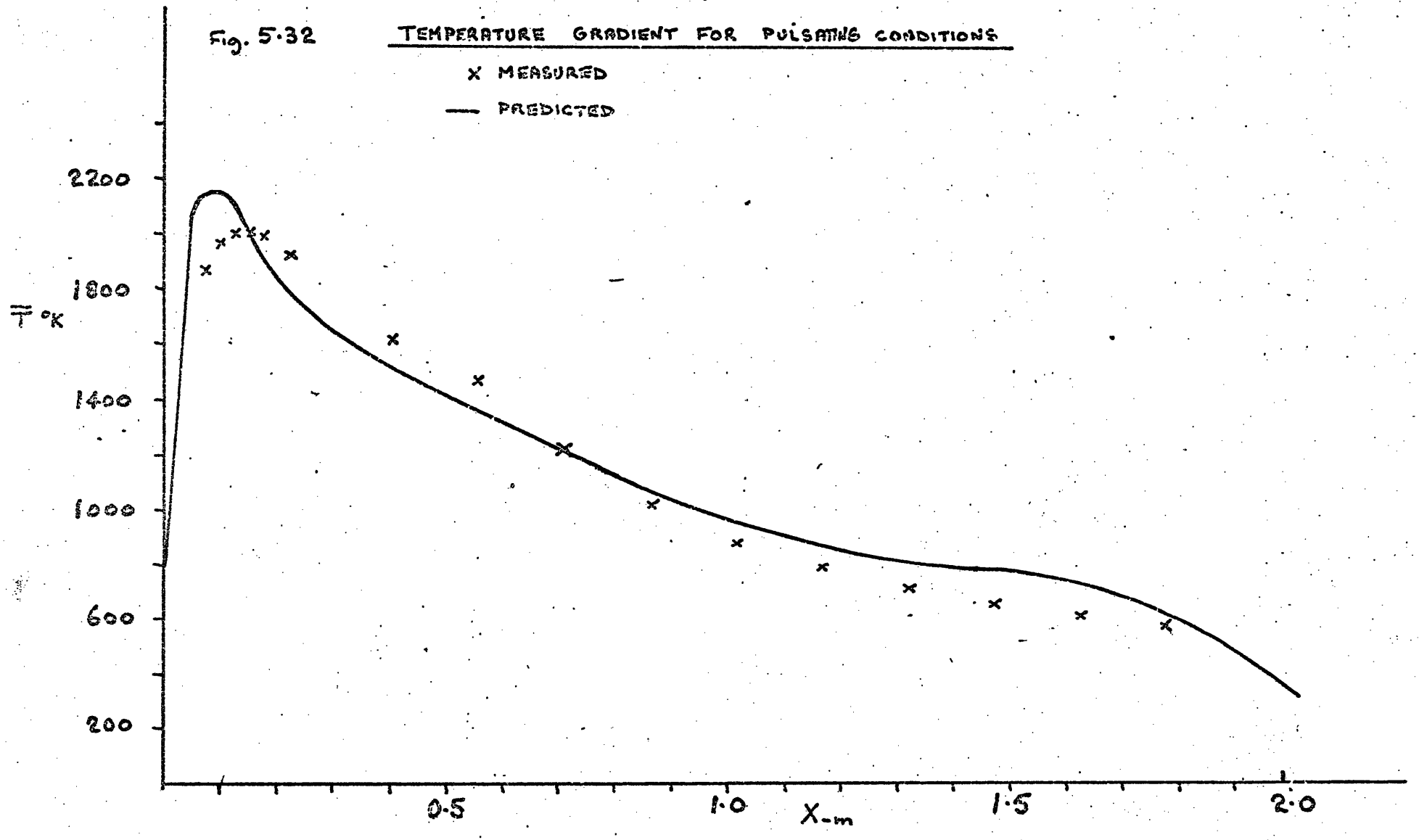

TEST 5

Fuel Flowrate 0.60 Fm^3/h

Air/Fuel Ratio 18.89:1

First Harmonic

Fig. 5·33 MEASURED TIME-INDEPENDENT MEAN GAS TEMPERATURE GRADIENT

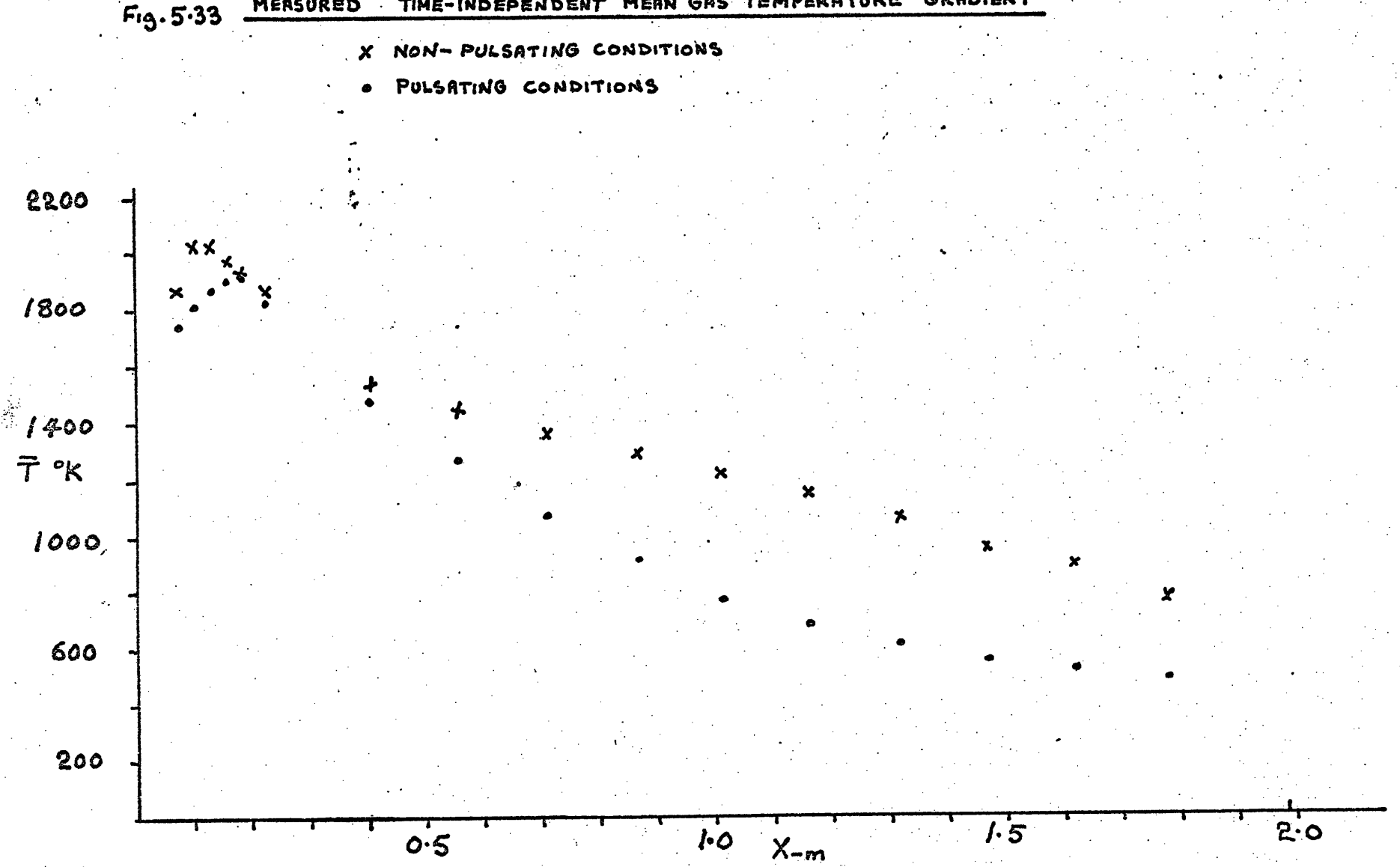

Fig 5·33 MEASURED TIME-INDEPENDENT MEAN GAS TEMPERATURE GRADIENT

Fig. 5·34 MODULUS OF PRESSURE AMPLITUDE AGAINST DISTANCE ALONG COMBUSTOR

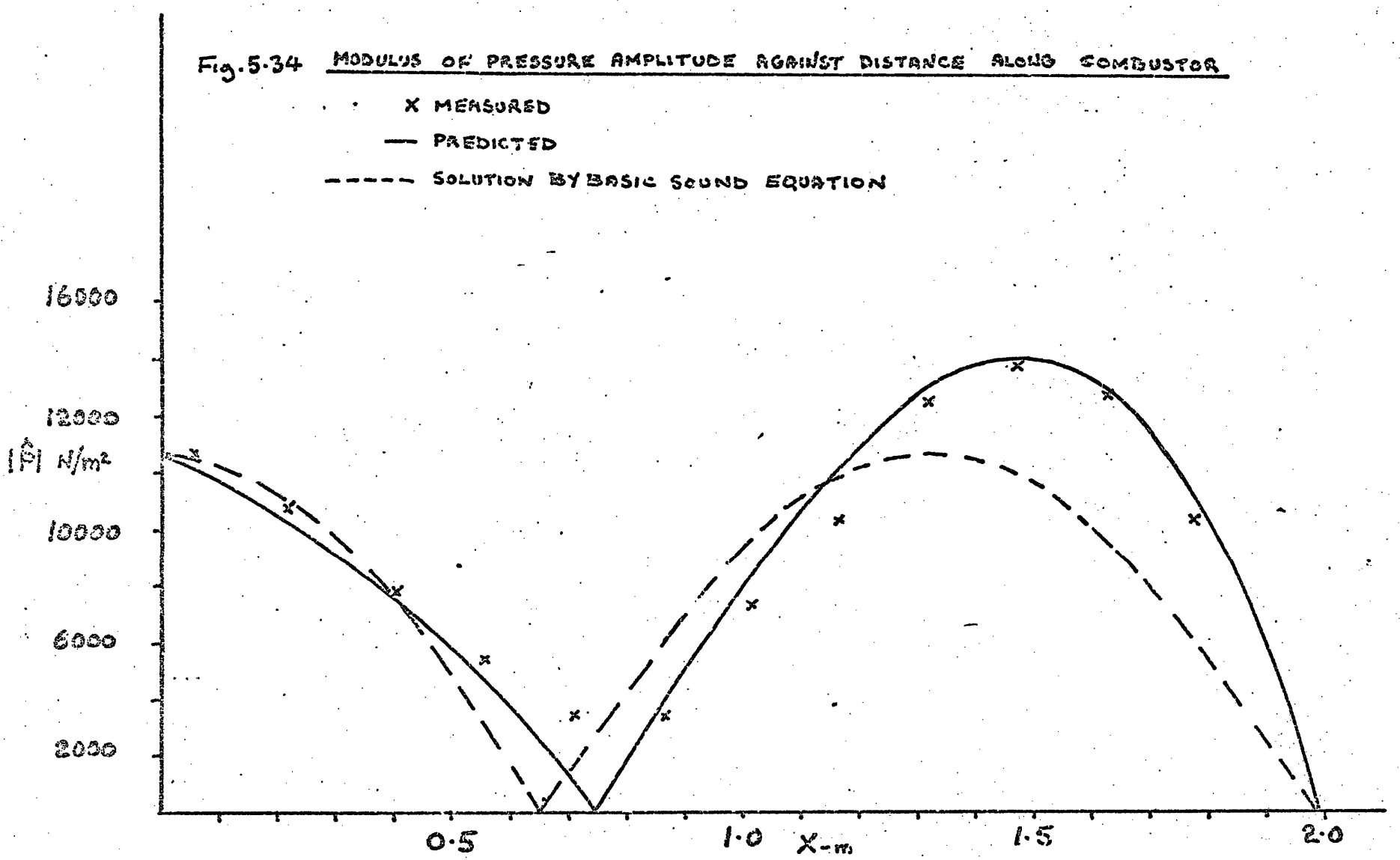

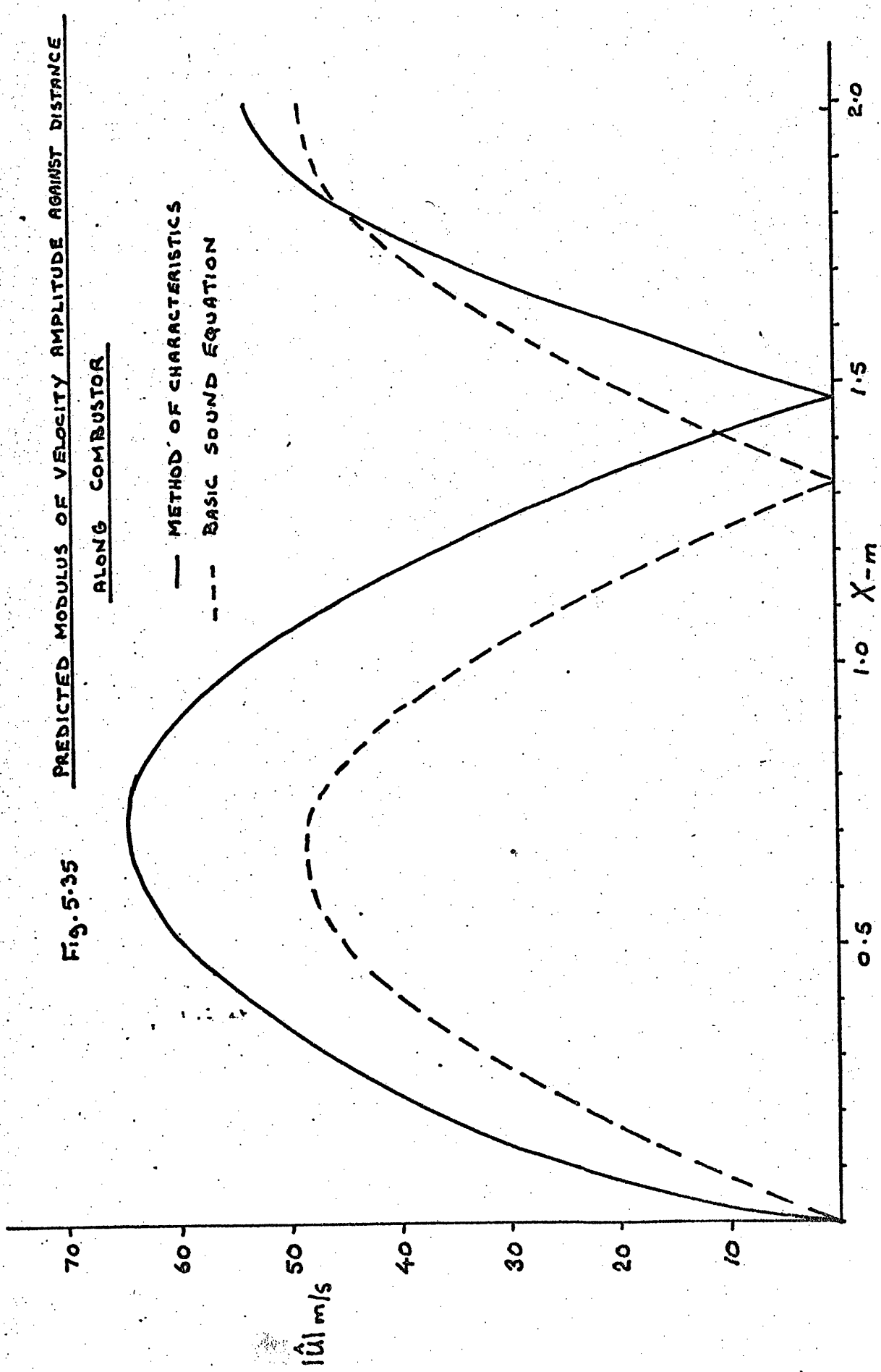

Fig. 5·35 PREDICTED MODULUS OF VELOCITY AMPLITUDE AGAINST DISTANCE ALONG COMBUSTOR

Fig. 5.36 TEMPERATURE GRADIENT FOR NON-PULSATING CONDITIONS

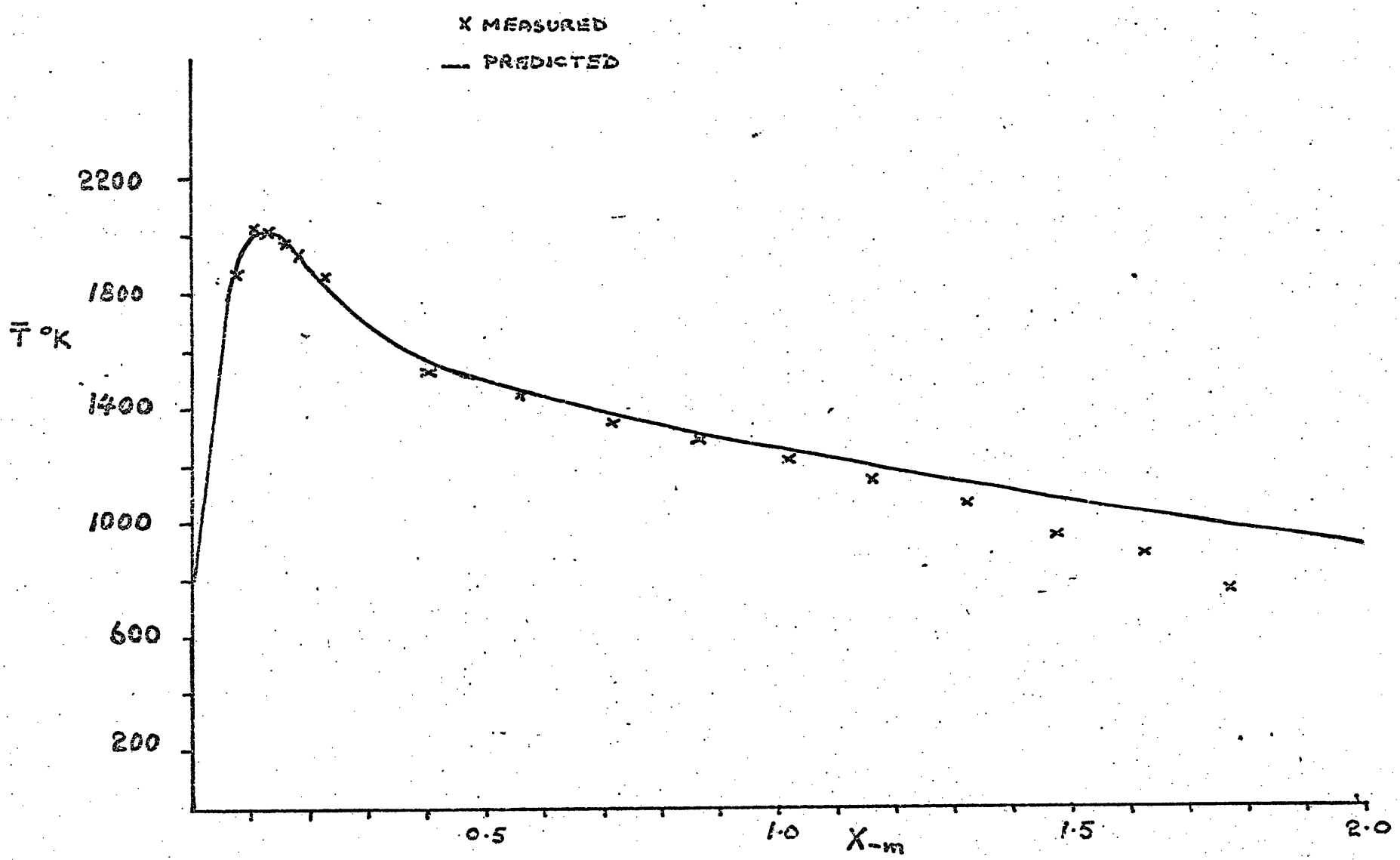

Fig. 5·37 TEMPERATURE GRADIENT FOR PULSATING CONDITIONS

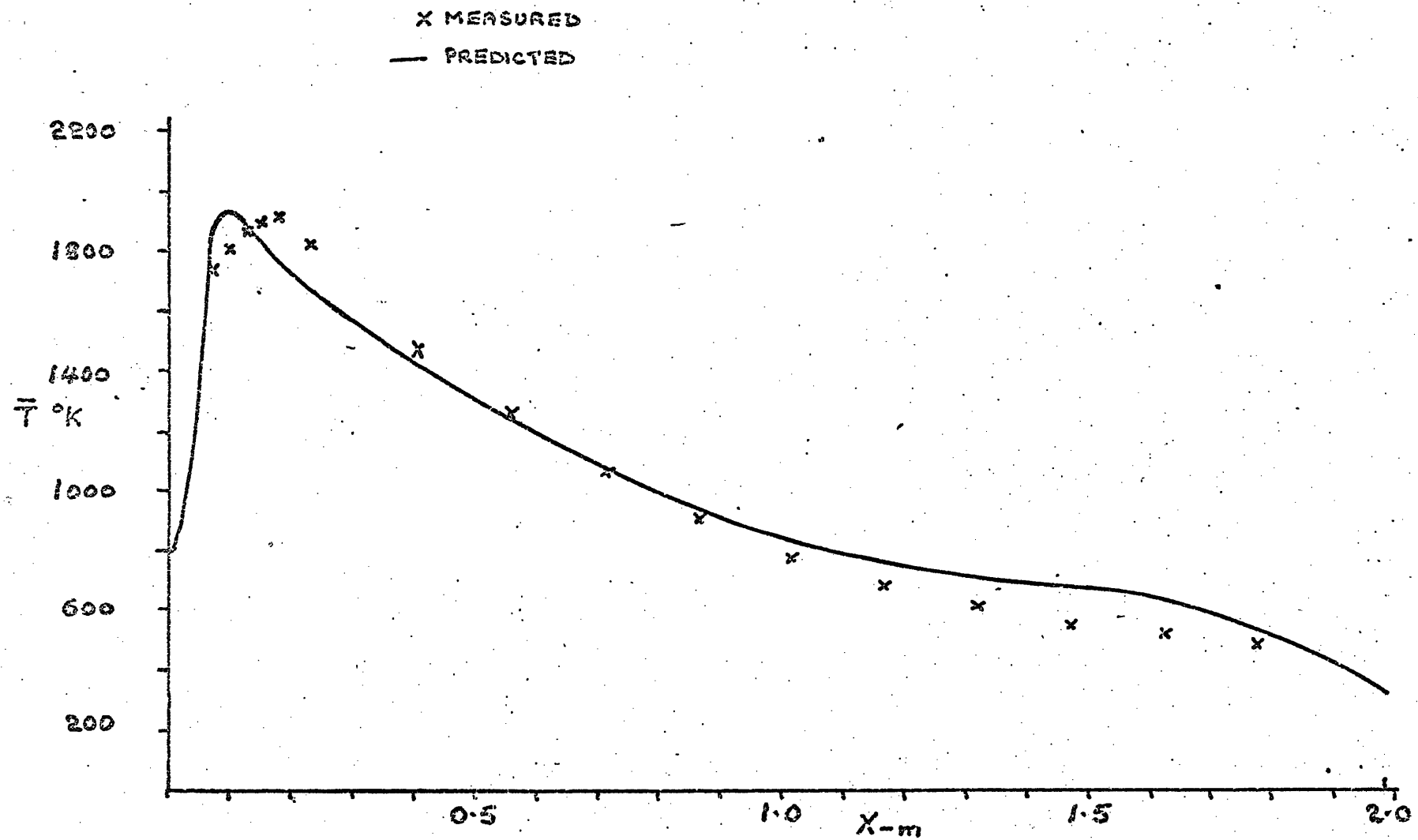

CHAPTER 6

Conclusion

6.0 Conclusion

A pulsating combustor producing longitudinal acoustic oscillations was constructed and a mathematical model of the system developed. The mathematical model predicted with reasonable accuracy the gas temperature gradients and distribution of the pressure and velocity standing waves. It was unable to predict the acoustic energy required to determine the amplitude and frequency of oscillation due to the use of a much simplified combustion model. The combustion model although greatly simplified served well as a prediction of inlet gas temperatures to the heat transfer section of the combustor.

The quasi-steady state theory gave a satisfactory description of the effects of longitudinal convective heat transfer rates in the heat transfer section of the mathematical model.

The measured and predicted results showed the effect large temperature gradients have on the distribution of standing waves, the effects are summarised below :

a) Wavelength of the standing wave decreases with decrease in temperature.

b) Nodes and antinodes are displaced in the same direction as temperature fall.

c) Pressure amplitude at pressure antinodes increase in the direction of temperature fall.

d) Velocity amplitude at velocity antinodes decrease in the direction of temperature fall.

e) Resonant frequencies are increased relative to ambient conditions

Using the simple method proposed by Hanby (28) for predicting the frequency of operation, reasonable agreement was found for frequencies of the first harmonic, where predicted gas temperature oscillations were of small amplitude. However, large differences in frequency were encountered with the fundamental mode of oscillation, where large temperature oscillations were predicted.

When using the basic equation of sound, to predict the standing wave distributions, large errors were obtained. This method having been used by Hanby (28) who reported satisfactory agreement with experimental results.

The following suggestions are made for future work. In attempting to predict the amplitude of oscillation it will be necessary to isolate such variables as : fuel injection system, Air/Fuel ratio, mode of oscillation and heat release rate, so as to understand what part each plays in the driving mechanism of combustion driven oscillations. To develop a more advanced combustion model it will be necessary to have more knowledge on how properties such as activation energy and flame emissivity vary with temperature and flow conditions.

REFERENCES

1. General survey of pulse combustion.

   A.A. Putman
   1st Int. Symposium on Pulsating Combustion,
   University of Sheffield. September, 1971

2. The pulsations and energy transfers in a double-orifice pulsating combuster.

   C.K. Beale
   Ph.d Thesis, University of Durham 1974
   (To be published).

3. Pulsating combustion - The collected works of

   F.H. Reynst
   ed. M. Thring
   Pergamon Press 1961

4. Non-steady Flame propagation

   ed. G.H. Markstein
   Pergamon Press 1964

5. Combustion - driven oscillations in industry

   A.A. Putman
   American Elsevier 1971

6. Vibrational Combustion

   transl FTD-TT-62-942/1+2, April, 1963.
   B.V. Raushenbakh.

7. Supersonic Flow and Shock Waves

R. Courant and K.O. Friedrichs
Interscience Publishers, New York, 1948.

8. An Introduction to the Method of Characteristics

M.B. Abbott
American Elsevier, New York 1966

9. Gasdymnamic investigation of the pulsejet tube

F. Schultz - Grunow
NACA TM1131, Parts I & II February, 1947

10. Nonsteady Duct Flow : Wave Diagram Analysis

G. Rudinger
Dover Publications , Inc. 1969

11. A Numerical Solution of Unsteady Flow Problems

R.S. Benson R.D.GARG and D. Woollatt
Int. J. Mech. Sci. 1964 Vol.6. pp 117-144

12. The Dynamics and Thermodynamics of Compressible Fluid Flow.

A.H. Shapiro Vol. I and II
Ronald Press Co., 1954

13. Effects of Variable Specific Heats and Gas Composition on Unsteady Flow Calculations

R.S. Benson, A. Wild and D. Woollatt
Proc. Instu. Mech. Engrs. 1969-70
Vol. 184 Pt 3G(1)

14. Influence of pipe friction and heat transfer on pressure waves in gases ; Effects in a Shock tube.

F.K. Bannister
Journal Mechanical Engineering Science
Vol.6. No.3. 1964.

15. Numerical soluation on One-Dimensional Non-steady Flow with supersonic and subsonic flows and heat transfer.

R.S. Benson
Int. J. Mech. Sci. 1922 Vol. 14, PP 635-642

16. Unsteady One - Dimensional Compressible Frictional Flow with Heat Transfer.

R.I. Issa and D.B. Spalding
Jour. Mech. Eng. Sc. Vol. 14 No.6. 1972

17. A preliminary investigation of gas turbine combustor modelling.

D.C. Hammond and A.M. Mellor
Combustion Science and Technology
1970, Vol.2., pp 67 - 80

18. Combustion Stability in a Spherical Combustor

A.E. Clarke, A.J. Harrison and J. Odgers
7th Symposium (International) on
Combustion, Butterworth, London, 1959.

19. Convective heat transfer in a gas fired pulsating combustor.

V. Hanby
Trans. A.S.M.E. 1968. Paper No. 68-WA
/FU-1 Page 1 - 5

20. Heat transfer in the cylinder of reciprocating internal combustion engines.

W.J.D. Annand
Proc. Instn. Mech. Engrs.
Vol. 172 No.36 1963

21. Heat transfer in compression ignition engines.

N.D. Whitehouse, W.J.D. Annand and T.H. Ma
Proc. Instn. Mech. Engrs. 1970-71

22. Numerical analysis

D.R. Hartree.
Oxford University Press 1958

23. Theory of Sound Vol. I and II

Lord Rayleigh
MacMillan and Co. 1896

24. Comparison of combustion instabilities found in various types of combustion chambers.

M. Barrere and F.A. Williams
12th Symposium (Int) on Combustion.

25. Combustion Noise

F.E.J. Briffa and G.T. Williams
Journal of the Institute of Fuel May, 1973.

26. A Study of Heat Driven Pressure Oscillations in a Gas

K.T. Feldman and R.L. Carter
August, 1970 - Journal of Heat Transfer A.S.M.E.

27. Combustion Oscillations in Gas-Fired Appliances

P.K. Baade
Conference on Natural Gas Research and Technology, Atlanta, Georgia - June, 1972.

28. Basic Considerations on the operation of a simple pulse combustor.

V. Hanby
Journal of the Institue of Fuel - Nov. 1971

29. Heat Transfer to a resonant pulsating air stream in a pipe

S.L. Hirst
Ph.d Thesis, University of Durham, 1974.

30. Theoretical study of pulsating combustion.

D. Bhaduri
Indian Journal of Technology 1968, 6 , 245

31. A theoretical model for stable combustion inside a refractory tube.

J.L. Chen and S.W. Churchill
Combustion and Flame
18, 27-36 (1972)

32. Activation Energies in a Baffle Stabilized Flame

P.G. Walburn
Combustion and Flame
12, De c ember, 1968, Pg 550 - 556

33. Measurement of High Gas Temperatures with Fine Wire Thermocouples

D. Bradley and K.J. Mathews
Jour Mech Eng. Sc. Vol.10 No.4.1968

34. The relation between the total thermal emissive power of a metal and its electrical resistivity

C. Davisson and J.R. Weeks
J.Opt. Soc. Amer.1924 8, 581

35. The Platinum metals and their alloys

E.M. Wise and R.F. Vines
1941 (International Nickel Co.,New York)

36. Calibration graphs - Copper/Constantan Thermocouples
B.S. 1828 : 1961

37. Calibration graphs - Nickel/Chromium V Nickel/ Aluminium
B.S.1827 : 1952

38. Calibration graphs - Platinum/Rhodium V Platinum
B.S. 1826 : 1952

39. Combustion Oscillation in industrial combustion chambers
M.W. Thring comment by T.D. Brown pg 168
12th Symposium (Int) on combustion

40. Heat Transmission
W.H. McAdams
McGraw-Hill Book Company Limited

Appendices

I The determination of step length Δx

II Measurement of High Gas Temperature

Appendix I

The determination of Step Length ΔX

The accuracy of the numerical solution is dependent on the value of ΔX. For a high order of accuracy ΔX should be as small as possible, for speed of calculation it should be as large as possible.

To determine the optimum conditions for the calculation, a simple problem was considered .

Consider an adiabatic flow of gas in the following system. It is assumed the gas can be considered perfect. Assume a sinusoidal pressure oscillation of angular frequency W is generated at X = 0 . At resonance a standing wave is produced in the pipe due to wave reflection from the open end.

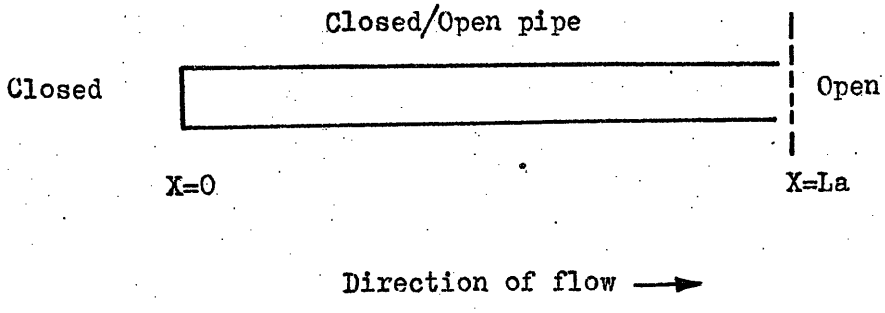

where La = acoustic length

If the motion can be considered as steady, having mean properties $\bar{u}$, $\bar{\rho}$ and $\bar{P}$ on which is superimposed incremental time-varying properties u_1, ρ_1, P_1

i.e. Velocity, $u = \bar{u} + u_1$

Density, $\rho = \bar{\rho} + \rho_1$

Pressure, $P = \bar{P} + P_1$

The incremental properties are such that their square and products can be considered negligible, By applying the small pertubation theory it can be shown (12) that such a system can be respresented by the one - dimenstional wave equation.

$$\frac{\partial^2 P_1}{\partial t^2} = \bar{c}^2 \frac{\partial^2 P_1}{\partial x^2}$$

which describes the propagation of plane sound waves, assuming

$$\bar{u} << \bar{c}$$

Applying this equation to the above problem, using the boundary conditions,

$$u_1 = 0 \quad \text{at} \quad x = 0$$

$$P_1 = 0 \quad \text{at} \quad x = La$$

for perfect reflection

$$P_1 = \hat{P}_a \cos\left(\frac{wx}{\bar{c}}\right) \sin(wt)$$

$$u_1 = \frac{\hat{P}_a}{\bar{\rho}\bar{c}} \sin\left(\frac{wx}{\bar{c}}\right) \cos(wt)$$

where Pa is the pressure amplitude at the closed end of the duct, and $\bar{C}$ the velocity of sound.

To obtain coressponding values of pressure and velocity from the numerical solution it was necessary to make :

$$\Delta X = \frac{L\lambda}{24}$$

Δt being obtained from the Courant - Fredrichs stability criterion as quoted in (11).

i.e. $$\frac{\Delta t}{\Delta x} \leq \frac{1}{(\bar{c} + |u|)_{max}}$$

In such problems ΔX is kept constant for all step lengths along the duct.

If a system with a large temperature gradient is considered, it will be seen from figure (I) that ΔX will have to vary along the length of the duct.

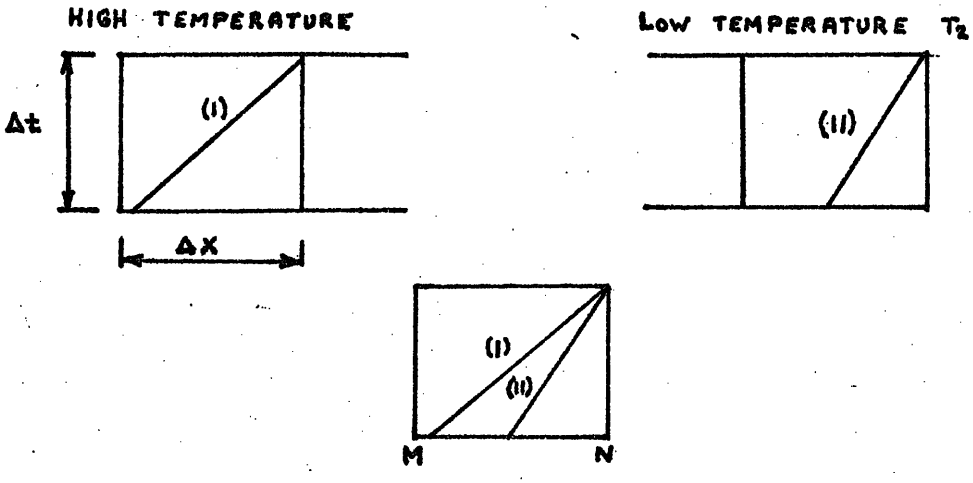

Fig (1)

(1) and (11) represent characteristic directions whose gradients are $\frac{1}{(\bar{C}_1 + |u_1|)}$ and $\frac{1}{(\bar{C}_2 + |u_2|)}$ respectively where $\bar{C}_1 > \bar{C}_2$

The accuracy of the solution is increased the closer the intersect of a characteristic approaches M. Thus in figure (I) it can be seen inaccuracies will be introduced into the calculation at the low temperature end of the grid due to characteristic (11) intersecting MN at quite a distance from M.

This effect was investigated by considering a similar problem as the first, this time considering an energy transfer to the system which produces a large temperature gradient in the system.

Hirst (29) has shown such a system can be represented by :-

$$\frac{\partial^2 P_1}{\partial t^2} = \bar{C}^2 \frac{\partial^2 P_1}{\partial x^2}$$

where $\bar{C}$ is a $f(x)$

The analytical solution to such an equation becomes rather complex depending on the form $\bar{C}$ takes. Hirst has produced an analytical solution to the problem for a system with an axial temperature gradient such that the change in the velocity of sound is linear.

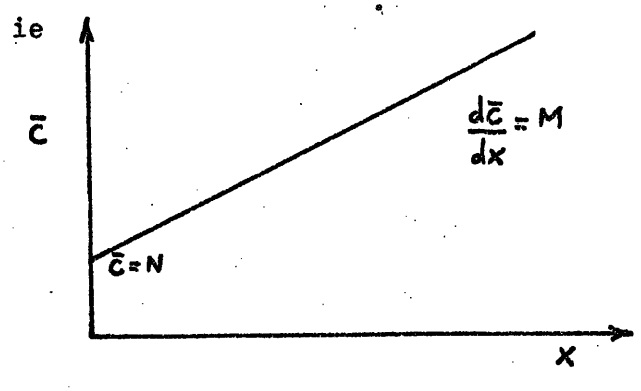

Fig 2

where N = velocity of sound at X = 0

M = rate of change of velocity of sound along the pipe.

The system can be represented by the equation

$$\frac{\partial^2 P_1}{\partial t^2} = (MX+N)^2 \frac{\partial^2 P_1}{\partial x^2}$$

applying the same boundary conditions as for the adiabatic case

$$U_1 = 0 \quad at \quad X=0$$
$$P_1 = 0 \quad at \quad X=La$$

for perfect reflection

then

$$P_1 = \frac{N}{b(MX+N)} \hat{P}_a e^{Mz/2} \left(\frac{M}{2} \sin(bz) + b\cos(bz) \right) \sin(wt)$$

$$U_1 = -\frac{WN}{b\gamma\bar{P}} \hat{P}_a e^{Mz/2} \sin(bz)\cos(wt)$$

where

$$b = \frac{1}{2}\sqrt{(4w^2 - M^2)}$$

$$z = \frac{1}{M} \log_e \left(\frac{MX}{N} + 1 \right)$$

$\hat{P}_a$ is the pressure amplitude at X = 0

The resonant frequencies are given by solving the following equation by the Newton - Raphson iteration technique

$$\frac{M}{2} \sin(bZ_L) + b\cos(bZ_L) = 0$$

Figures (1a-2a) shows the comparison of results produced by the numerical solution to those produced by Hirst for the conditions shown.

The ΔX used in the adiabatic case was used in determining Δt from

$$\frac{\Delta t}{\Delta X} \leq \frac{1}{(\bar{c} + |u|)_{max}}$$

ΔX was found from

$$\Delta X = (\bar{c} + u_N)\,\Delta t$$

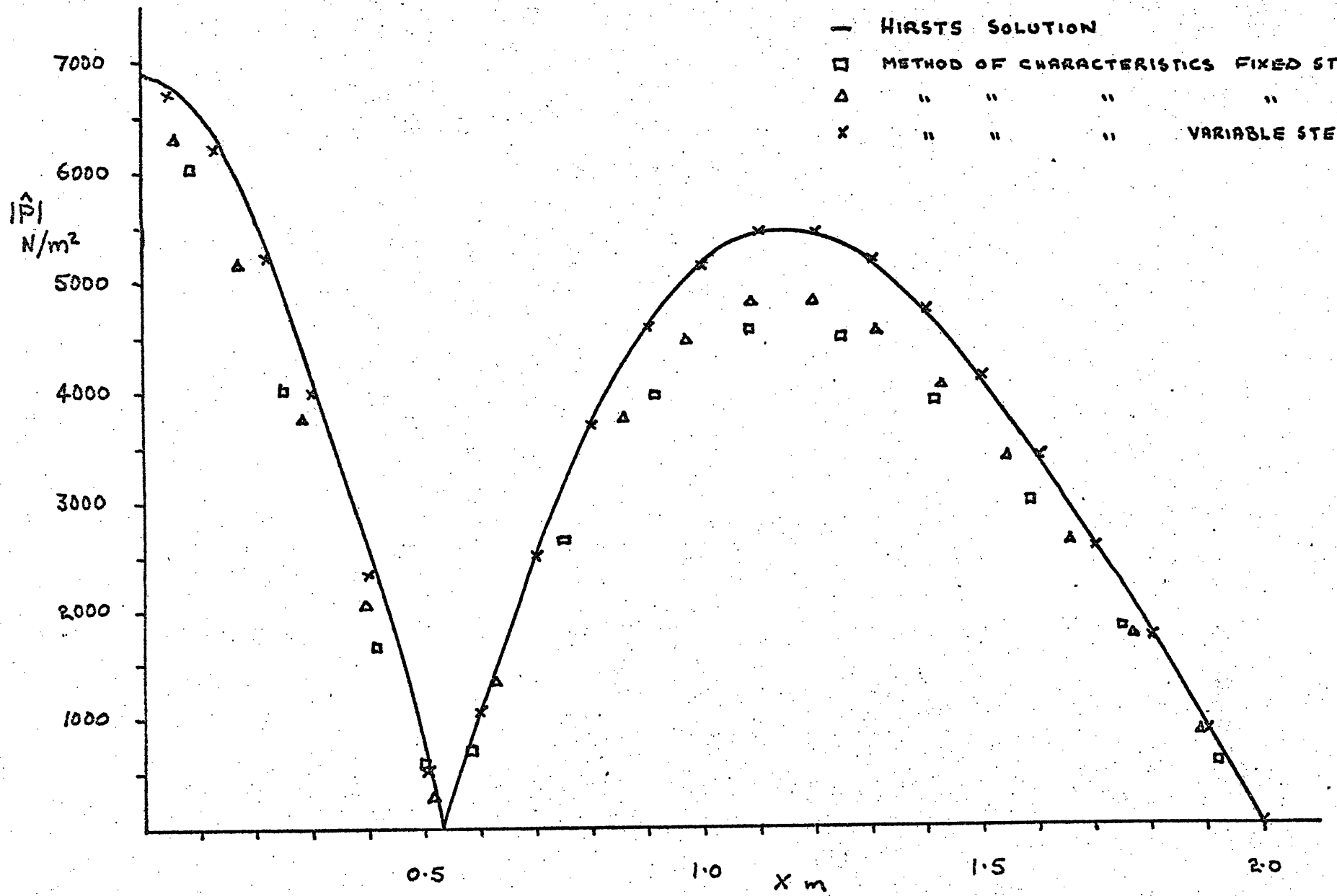

T = 288°K

FIG. 1a' MODULUS OF PRESSURE AMPLITUDE AGAINST POSITION FOR 1000°C TEMPERATURE RISE

T = 1288°K

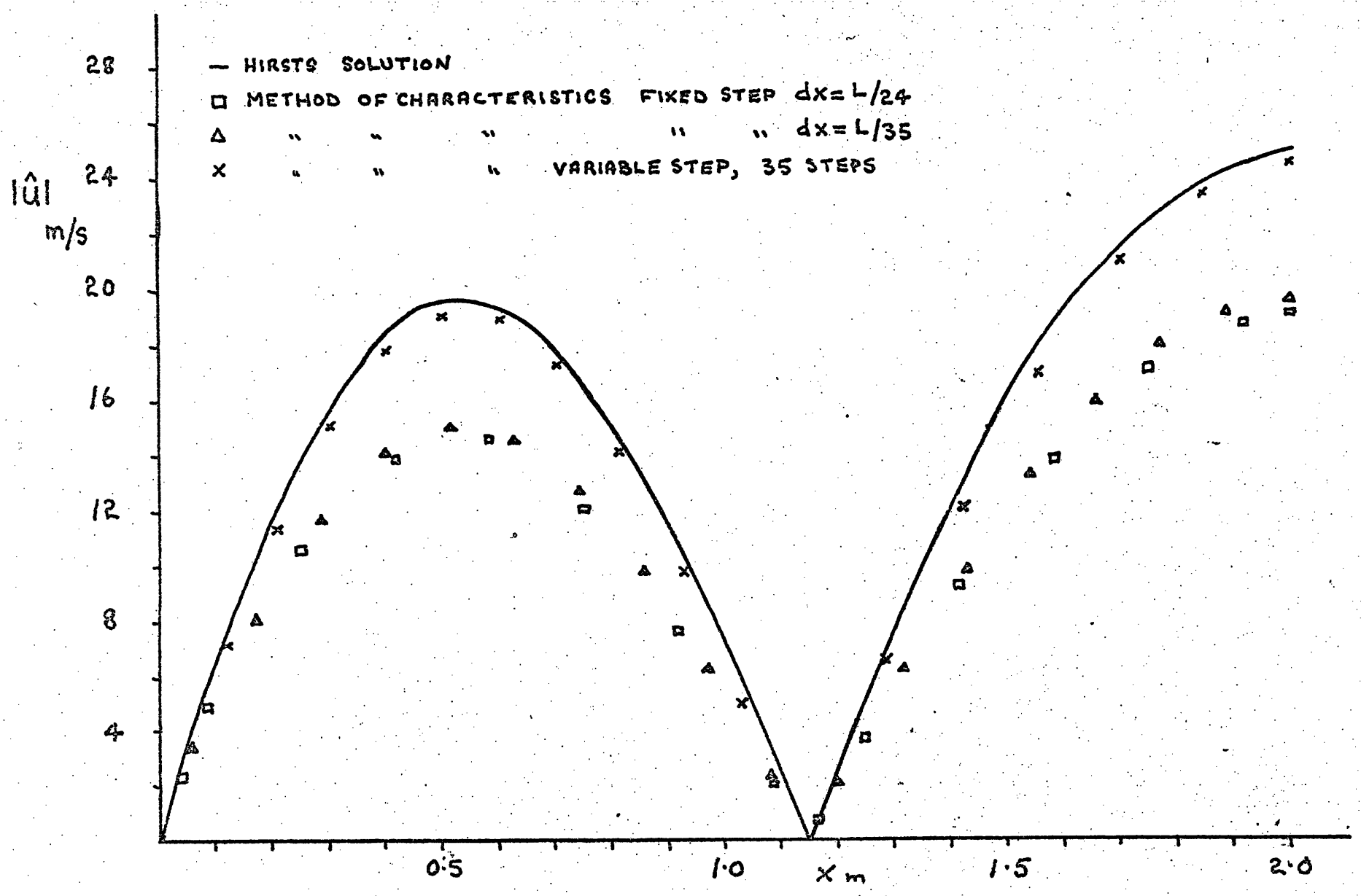

T=288°K

Fig. 2a MODULUS OF VELOCITY AMPLITUDE AGAINST POSITION FOR 1000°C TEMPERATURE RISE

T=1288°K

where u_N is an estimate of the maximum velocity amplitude. u_N may be varied slightly to allow a whole number of step lengths to be accommodated in the characteristic length of the tube.

For the combustion system it was decided to use the measured temperature gradient in determining ΔX. However, the predicted steady state temperature gradient could equally well have been used.

APPENDIX II

Measurement of High Gas Temperatures

In general the thermocouple probe does not attain the same temperature as the hot gas. The gas is contained by solid walls and there is a radiative energy exchange between these and the probe. The probe usually radiates energy to cooler walls and in the steady state this is balanced by convective energy transfer from the gas to the probe, this means that the wire is at a lower temperature than the gas. The value of the temperature difference is called the radiation correction. Because the radiation from the probe increases as the fourth power of the probe temperature, this correction increases very sharply with temperature. Consideration of the energy balance for the probe also shows that the magnitude of the correction decreases with the size of the probe.

Assuming that the surrounding walls are black to radiation from the wire and that radiant exchange between the wire and the gases is negligible, the steady state energy equation can be written as follows :

$$\frac{d}{dx}\left(K\frac{dT_s}{dx}\right) + \frac{4h}{d}(T-T_s) - \frac{4\sigma}{d}(\varepsilon T_s^4 - \alpha T_w^4) = 0 \qquad (1)$$

where T is the gas temperature, Ts the probe temperature and Tw the wall temperature, Bradley et al (33) have produced a generalised temperature profile associated with a simply supported fine wire thermocouple figure (1 b). The support at A, because of radiative and conductive energy losses, will be at a temperature below that of the gas and the fine thermocouple wire. The profile at ABC shows the cooling effect of the support by the conduction of heat along the wire, which becomes negligible at C. The profile CD shows the wire at a steady temperature, such that radiative energy loss to the cooling surrounding walls is balanced by convective energy gain from the gas.

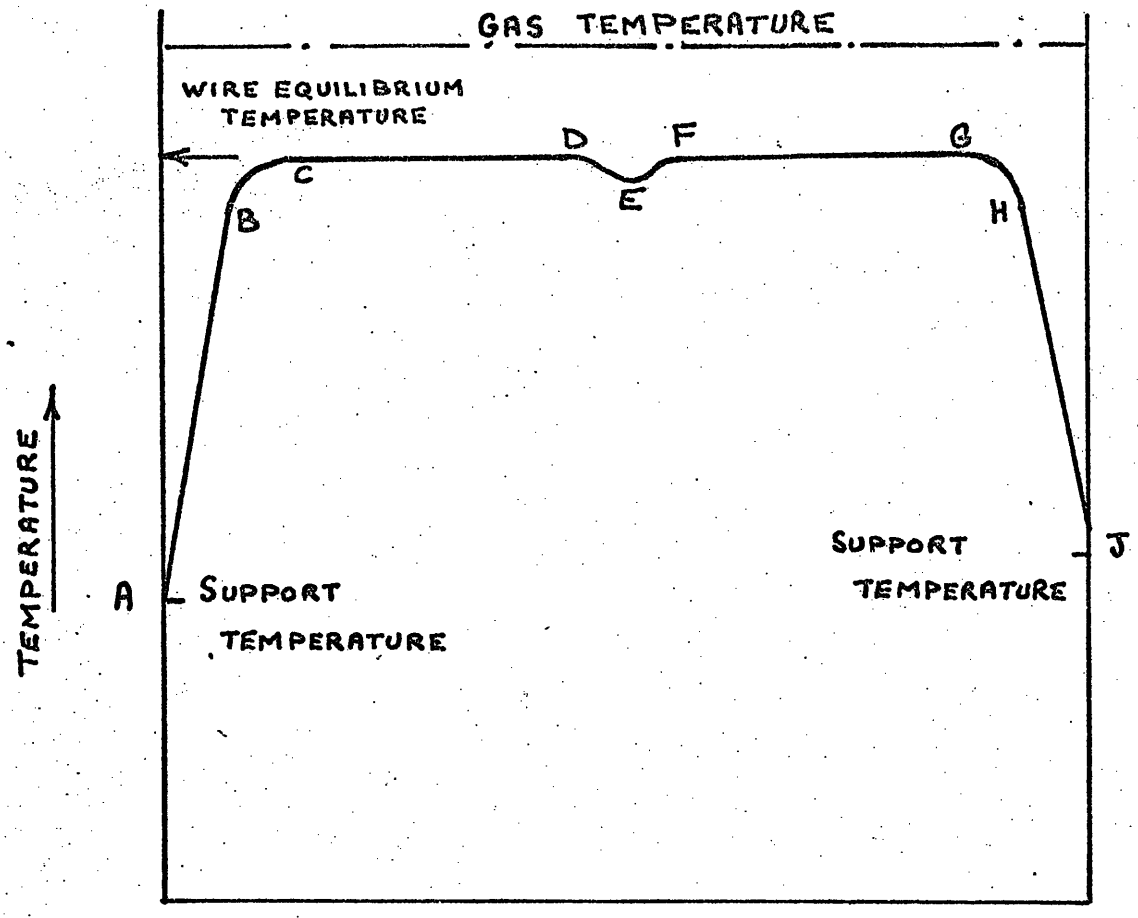

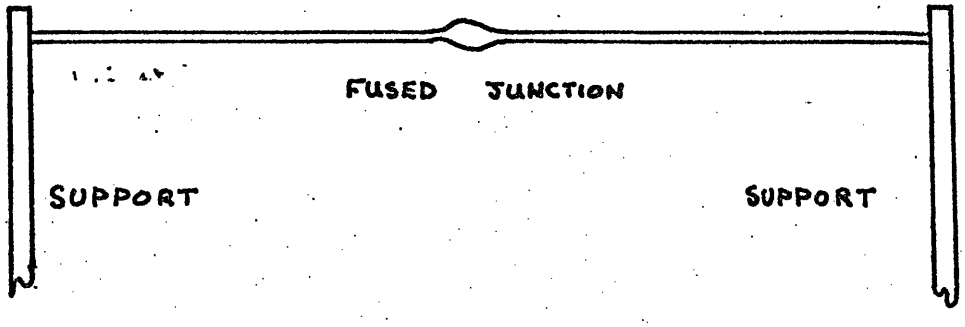

Fig. 1b WIRE TEMPERATURE DISTRIBUTION

The hot junction of the thermocouple formed by fusing the two component wires together, has slightly a larger diameter than the two component wires. The increase in diameter creates a relatively larger energy loss by radiation than energy gain by convection and the junction temperature is lower than that of the adjoining component wires. This is shown by point E, Bradley (33) has shown this effect to be negligible. The curve FGHJ represents the temperature for the other component wire.

When their is no thermal conduction along the wire it may be said to be at its semi-infinite equilibrium temperature T_∞ . The difference between this temperature and the gas temperature is the radiation correction. In this case the first term in equation (1) is zero, hence :

$$\frac{4h}{d}(T-T_\infty) - \frac{4\sigma}{d}(\epsilon T_\infty^4 - \alpha T_w^4) = 0$$

for low wall temperature the αT_w^4 term is negligible and so

$$T = T_\infty + \frac{\sigma \epsilon T_\infty^4}{h} \qquad \text{——————} \quad 2$$

Bradley has found the junction will only be cooled a few degrees by conduction along the fine wire thermocouple. However, if the fine wires are too short serious cooling of the hot junction can result. For this investigation it was found that increasing the length of the wire past 22mm had no effect on temperature readings and so this length was considered to be the correct value to eliminate conduction errors.

The importance of reliable values of emissivity now becomes apparent. Unfortunately, there is a dearth of experimental data for thermocouple materials at high temperatures. Another approach is to derive values of emissivity from electrical resistivity on the basis of electromagnetic theory.

Davisson and Weeks (34) give a theroetical expression for the emissivity :

$$\varepsilon = 0{\cdot}751(T\,Re)^{1/2} - 0{\cdot}632(T\,Re) + 0{\cdot}67(T\,Re)^{3/2} - 0{\cdot}607(T\,Re)^{2}$$

Resistivities for the platinum - rhodium alloys can be estimated from the data presented by Wise and Vines (35).

The heat transfer coefficient in equation (2) is determined from the expression from Kromer quoted by Bradley (33).

$$Nu = 0{\cdot}42\,Pr^{0{\cdot}2} + 0{\cdot}57\,Pr\,Rn^{0{\cdot}5}$$

It is frequently used in anemometry for cross flow to a wire.

Figure (2b) shows typical radiation correction data for the thermocouple probe used in this investigation.

GAS TEMPERATURE RADIATION CORRECTION DATA

Fig. 2b